2020-01-01

Formulation Strategies To Enhance Solubility And Permeability Of Small Molecules For Drug Delivery Applications

Pradeep Kumar Bolla
University of Texas at El Paso

FORMULATION STRATEGIES TO ENHANCE SOLUBILITY AND PERMEABILITY OF SMALL MOLECULES FOR DRUG DELIVERY APPLICATIONS

PRADEEP KUMAR BOLLA

Doctoral Program in Biomedical Engineering

APPROVED:

Jwala Renukuntla, Ph.D., Chair

Thomas Boland, Ph.D.

Thenral Mangadu, M.D, M.P.H, Ph.D.

Ian Mendez, Ph.D.

Stephen L. Crites, Jr., Ph.D.
Dean of the Graduate School

Dedication

For my father and mother who were hardworking and encouraging all my life. My brother who has supported, guided, and mentored throughout my journey. This dissertation is dedicated to my family, guide, Dr. Devaraj Sambalingam, friends, and all the people who have always been there for me in every way.

FORMULATION STRATEGIES TO ENHANCE SOLUBILITY AND PERMEABILITY OF SMALL MOLECULES FOR DRUG DELIVERY APPLICATIONS

by

PRADEEP KUMAR BOLLA, M.S (Pharm), B. Pharmacy

DISSERTATION

Presented to the Faculty of the Graduate School of

The University of Texas at El Paso

in Partial Fulfillment

of the Requirements

for the Degree of

DOCTOR OF PHILOSOPHY

Department of Metallurgical, Materials, and Biomedical Engineering

THE UNIVERSITY OF TEXAS AT EL PASO

May 2020

Acknowledgements

First and foremost, I offer my sincerest thankfulness to my supervisor, mentor and advisor, Dr. Jwala Renukuntla, who has supported me throughout my work with her patience, motivation and immense knowledge whilst allowing me the room to work in my own way. It gives me an immense pleasure and pride to express my deep sense of gratitude and respect for her expertise and inspiring guidance throughout the period of my Ph.D. I am indebted to her for enlightening me on the finer skills of dealing with research problems. I attribute the level of my Ph.D. degree to her encouragement, effort, critical remarks, and valuable suggestions and without her, this dissertation, too, would not have been completed or written. She is the one behind giving me a decisive turn and significant boost to my career. I consider myself one of the fortunate people to be associated with her.

I would like to express special thanks to Dr. Devaraj Sambalingam his help, kind suggestions, untiring cooperativeness, and valuable support without which I would not have successfully completed my dissertation.

I also avail this privilege to express my deep sense of gratitude to my committee members Dr. Thomas Boland, Dr. Thenral Mangadu, and Dr. Ian Mendez for their kind help and valuable suggestions. Their benevolent attitude and unending motivation have helped me immensely in completing my work well.

I would like to express my heartfelt thanks to Dr. Bradley A. Clark, Dr. Sai Hanuman Sagar Boddu, Dr. Venkata Kashyap Yellepeddi, Vrinda Gote, and Mahima Singh for their kind support, encouragement and help that catalyzed my work. I also sincerely thank Dr. Manohar Katakam and Dr. Kumaril Bhargava for giving an opportunity to work on their projects.

I am thankful to my friendly and cheerful lab members Julian Franco, Victor Rodriguez, Carlos Meraz, Maya Ruiz, and David Ramos. I would also like to thank my friends Abhishek Juluri, Abhishek Dodda, Ashrith, Vikas, Pradeep, Azharuddin, Raju, Srikanth, Sandeep, Kamesh, Sunil, Rajesh, Rajinikanth, Sudeep, Jayanth, Teja, Prashanth, Karthik, Rajpal, Rakesh V, Dileep N, Dheeraj P, master's and bachelor's classmates, for their constant encouragement.

I would like to thank the Dean and non-teaching staff members of UTEP School of Pharmacy for their support.

Finally, I take this opportunity to acknowledge my parents Krishna Prakash Bolla and Rama Devi Bolla, my brother Sandeep Kumar Bolla, my sister-in-law Shwetha Bolla, my nephew Advaith Bolla, my grandmother's Saraswathi Bolla and Andamma Ponaganti, my cousins and family, for their sacrifice, unconditional love, moral support and encouragement.

Abstract

All the new chemical entities/drug molecules intended for therapeutic use must be administered using an appropriate delivery system/dosage form to achieve maximum bioavailability. However, designing a drug delivery system is complex as several factors such as lipophilicity, molecular mass, crystallinity, ionic charge, polymorphic forms and hydrogen bonding) affect the solubility and permeability of these molecules. Biopharmaceutics drug classification system (BCS) categorizes the existing drugs into four classes based on the aqueous solubility and membrane permeability and it is reported that >70% of the drugs are poorly soluble and belong to BCS class II and BCS class IV. Several physical, chemical and formulation techniques have been employed to improve the bioavailability. This dissertation delineates several formulation strategies to improve the solubility and permeability of small molecules for drug delivery applications.

Global incidence of superficial fungal infections caused by dermatophytes is high and affects around 40 million people. It is the fourth most common cause of infection. Clotrimazole, a broad-spectrum imidazole antifungal agent is widely used to treat fungal infections. Conventional topical formulations of clotrimazole are intended to treat infections by effective penetration of drugs into the stratum corneum. However, drawbacks such as poor dermal bioavailability, poor penetration, variable drug levels limit the efficiency. The first study was aimed to load clotrimazole into ufosomes and evaluate its topical bioavailability. Clotrimazole loaded ufosomes were prepared using cholesterol and sodium oleate by thin film hydration technique and evaluated for size, poly dispersity index (PDI), and entrapment efficiency to obtain optimized formulation. Optimized formulation was characterized using scanning electron microscopy (SEM), x-ray diffraction (XRD) and differential scanning calorimetry (DSC). Skin diffusion studies and tape-

stripping were performed using human skin to determine the amount of clotrimazole accumulated in different layers of the skin. Results showed that the optimized formulation had vesicle size <250 nm with ~84% entrapment efficiency. XRD and DSC confirmed the entrapment of clotrimazole into ufosomes. No permeation was observed through the skin up to 24 h following the permeation studies. Tape-stripping revealed that ufosomes led to accumulation of more clotrimazole in the skin compared to marketed formulation (Perrigo). Overall, results revealed the capability of ufosomes in improving the skin bioavailability of clotrimazole.

Perinatal asphyxia caused due to hypoxia complicates and causes hypoxic-ischemic encephalopathy (HIE). Therapeutic hypothermia widely used to treat HIE and is successful in 50%-60% patient population. It was reported that lutein supplementation showed neuroprotective properties in rat model of neonatal HIE. Lutein has poor bioavailability owing to poor aqueous solubility. In the second study, lutein was encapsulated into polymeric nanoparticles (PLGA and PLGA-PEG-FOLATE) and evaluated enhanced uptake in human neuroblastoma cells. Lutein loaded polymeric nanoparticles were prepared using O/W emulsion solvent-evaporation technique. Particle diameter and zeta potential (ZP) were measured using dynamic light scattering (DLS). Other characterizations included DSC, FTIR, SEM, and *in vitro* release studies. *In vitro* uptake studies were conducted in neuroblastoma cells using flow cytometry, confocal microscopy and high-performance liquid chromatography analysis. Lutein was successfully encapsulated into PLGA and PLGA-PEG-FOLATE nanoparticles with uniform size distribution of around 200 nm and high ZP. Entrapment efficiency of lutein was ~61% and ~73% for lutein PLGA and PLGA-PEG-FOLATE nanoparticles, respectively. DSC and FTIR confirmed encapsulation of lutein into nanoparticles. Cumulative release of lutein was higher in PLGA nanoparticles with 100% release within 24 hours. In PLGA-PEG-FOLATE nanoparticles, cumulative release was ~80% at

48 hours. Cellular uptake studies in neuroblastoma cells confirmed a significant increase in lutein uptake with PLGA-PEG-FOLATE nanoparticles compared to PLGA nanoparticles and lutein alone. Findings from this study suggest that lutein loaded PLGA-PEG-FOLATE nanoparticles can be potentially used for treatment of HIE.

Overuse and misuse of antibiotics in clinics and poor new antibiotic pipeline in pharmaceutical industries have contributed to antibiotic crisis. Silver complexes are effective as broad-spectrum antibiotics due to chemical nature. Furosemide-silver complex (Ag-FSE) has been recently reported to have antibacterial activity that is, however, limited by its poor solubility in water and majority of organic solvents. Solid lipid nanoparticles (SLNs) offer advantages such as controlled and sustained release, enhanced solubility, scale-up and, biocompatibility. Present study aims to encapsulate Ag-FSE into SLNs and evaluate its sustained and improved antibacterial activity. Ag-FSE SLNs were prepared using hot homogenization and ultrasonication method. Size, PDI and ZP of Ag–FSE SLNs, evaluated using DLS, were 129.8±38.5 nm, 0.114 ± 0.033 and -23.9 ± 3.62 mV, respectively. Ag-FSE SLNs exhibited high encapsulation efficiency (~93%) and drug loading (~9.3%). Shape of Ag-FSE SLNs was roughly spherical with smooth surfaces. *In vitro* release studies confirmed that encapsulation of Ag-FSE into SLNs resulted in sustained release of Ag-FSE over 96 h. Results also confirmed 2-fold and 4-fold enhancement of activity against *Pseudomonas aeruginosa* and *Staphylococcus aureus*, respectively. In conclusion, Ag-FSE SLNs can be considered as promising topical antibacterial agent against bacterial infections.

Table of Contents

List of Tables

List of Figures

List of Illustrations

Chapter 1

Introduction

Development of new chemical entities/drug molecules for clinical use is expensive and time consuming. After discovery, delivery of these drugs to the site of action is equally challenging and is influenced by several factors such as absorption and distribution. Drug delivery is defined as a method/process of administering drugs to achieve desired therapeutic effects. In addition to the therapeutic effect, balancing the safety to efficacy ratio should also be considered (Tiwari et al. 2012). Drug delivery to the site of action is achieved by several routes of drug administration which include oral (by mouth), parenteral (by injection), topical/transdermal (by skin), inhalation (by nose), and rectal (by rectum). Of these, oral route is the most preferred route of administration due to safety and ease of administration. However, first pass effect is a drawback, as majority of the dose administered is eliminated due to the metabolism in the liver. To avoid first pass effect alternative routes such as parenteral, transdermal and others have been employed but each of them are associated with their own advantages and disadvantages (Ruiz and Scioli Montoto 2018).

All the drugs intended for therapeutic use have to be administered using an appropriate delivery system. However, in most cases of therapeutic development, designing of a suitable drug delivery system is complex. Several challenges are faced by the formulation scientists during the design and development of an appropriate drug delivery system to improve the bioavailability. Some of the important factors include physicochemical properties the drug such as lipophilicity (pKa and LogP), molecular mass, crystallinity, ionic charge, polymorphic forms and hydrogen bonding which influence the solubility and permeability of new drugs (S. Gupta, Kesarla, and Omri 2013; Christopher A Lipinski et al. 1997; *No Title* 2014).

1.1. SOLUBILITY AND PERMEABILITY

Solubility is a property of a specific solvent-solute combination, defined as the maximum amount of solute that is dissolved in a given amount of solvent at constant temperature and pressure (C A Lipinski et al. 2001). It is also defined as the characteristic property of a solute (solid, liquid, or a gaseous substance) to dissolve in a solvent (solid, liquid, or a gaseous substance) to form a homogenous solution. Solubility of a solute occurs at a dynamic equilibrium and is expressed as concentration, molality, mole fraction, mole ratio and other units. LogP (partition coefficient), which defines the hydrophobicity/hydrophilicity of a compound is a measure of differential solubility of the compound in octanol (hydrophobic solvent) and water (hydrophilic solvent) (Savjani, Gajjar, and Savjani 2012). Based on the parts of solvent required for the solute to dissolve, the United States Pharmacopoeia (USP) and British Pharmacopoeia (BP) has classified the solubility classed provided in Table 1.1 (Savjani, Gajjar, and Savjani 2012). According to ICH M9 guideline, a drug molecule is considered highly soluble if the highest dose of the compound is completely soluble in 250 mL or less of aqueous media over a pH range of 1.2 to 6.8 at 37 ± 1 °C (ICH 2019).

Table 1.1: Solubility criteria as per USP and BP

S.no	Descriptive term	Part of solvent required per part of solute
1	Very soluble	<1
2	Freely soluble	From 1 - 10
3	Soluble	From 1 - 30
4	Sparingly soluble	From 30 - 100
5	Slightly soluble	From 100 - 1000
6	Very slightly soluble	From 1000 - 10000
7	Practically insoluble	>10000

It is already known that all the drugs irrespective of the mode of delivery, should possess at least limited aqueous solubility for desired pharmacologic activity as water is the major component of the body (Savjani, Gajjar, and Savjani 2012). In addition, solubility is considered as one of the critical parameters to achieve required concentration of the drug in systemic circulation to attain desired pharmacological response. Poor water solubility of drugs often leads to sub-optimal outcomes in the patients due to poor bioavailability and variable pharmacokinetics (Kalhapure et al. 2019). Poor aqueous solubility leads to poor dissolution and limits the bioavailability of drugs. It would be ideal to synthesize drug candidate with sufficient aqueous solubility for therapeutic activity (Ishikawa and Hashimoto 2011) however, it is estimated that nearly 40%-70% of the drugs marketed and 90% of drugs in pipeline are poorly soluble in water affecting their bioavailability (S. Gupta, Kesarla, and Omri 2013; Kalepu and Nekkanti 2015).

Permeability is defined as the flow of drug across a membrane. Mathematically, it is the diffusion coefficient of the drug across the membrane times the partition coefficient of the drug divided by the membrane thickness (Dahan, Miller, and Amidon 2009; Dahan and Miller 2012). Permeability is an important factor in drug delivery as poor membrane permeability leads to poor or non-existent efficacy or therapeutic response (Bennion et al. 2017). As solubility and permeability play a critical role in determining the bioavailability, drugs are classified into 4 main categories as per biopharmaceutics drug classification system (BCS classification) (ICH 2019).

BCS Classification

The BCS is a scientific framework for classifying a drug molecule based on its aqueous solubility and membrane permeability (C.-L. Cheng et al. 2004; Ishikawa and Hashimoto 2011). It is based on the physicochemical and physiological parameters. In the recent years, BCS system

is considered as one of the significant prognostic tools developed to facilitate the drug product development process. It has been adopted by various regulatory/health authority agencies such as United States Food and Drug Administration (USFDA), European Medicines Agency (EMA) and World Health Organization (WHO) for drug approvals (Dahan, Miller, and Amidon 2009). All the marketed drugs have been classified into 4 classes which include (Figure 1.1).

- Class I: High Solubility and High Permeability
- Class II: Low Solubility and High Permeability
- Class III: High Solubility and Low Permeability
- Class IV: Low Solubility and Low Permeability

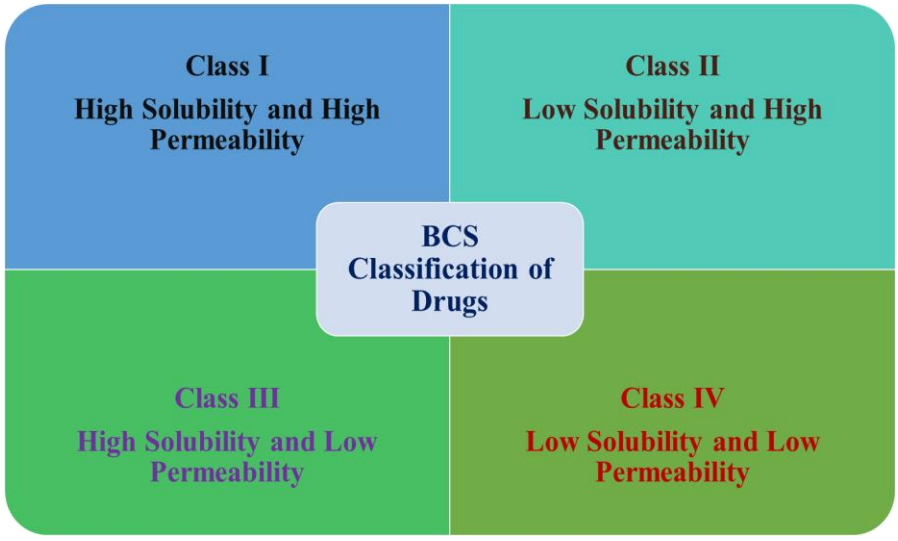

Figure 1.1: Biopharmaceutics classification system for drugs.

It is reported in the literature that >70% of the drugs are poorly soluble and belong to BCS class II and BCS class IV (X. Zhang et al. 2018). Therefore, solubility and permeability enhancement of poorly soluble/permeable drugs is required to improve the bioavailability of the drugs. Several techniques have been employed to improve the bioavailability which include

(Savjani, Gajjar, and Savjani 2012; X. Zhang et al. 2018; Tiwari et al. 2012; P. K. Bolla et al. 2018; Goli, Bolla, and Talla 2018).

1. Physical methods: Particle size reduction (milling, micronization and nanonization), crystal habit modification such as co-crystallization, and drug dispersions.

2. Chemical methods: Changes in pH of the solvent, use of buffers and permeation enhancers, salt formation, derivatization and complexation.

3. Formulation development: Nanoparticles (nanosuspensions, nanoemulsions, nanocrystals, polymeric nanoparticles and others), micelles, solid dispersions, lipid based drug delivery systems (self-emulsifying drug delivery systems, solid lipid nanoparticles (SLNs), liposomes, ufosomes, microemulsions), liquid solid techniques, and targeted therapy (surface modified drug delivery systems)

4. Miscellaneous methods: Super critical fluid process, use of adjuvants such as surfactants, solubilizers, cyclodextrins, co-solvents, hydrotrophy and novel excipients.

Of these, development of an adequate pharmaceutical formulations is considered as a good strategy to improve the solubility and permeability for existing drug molecules (Kalhapure et al. 2019).

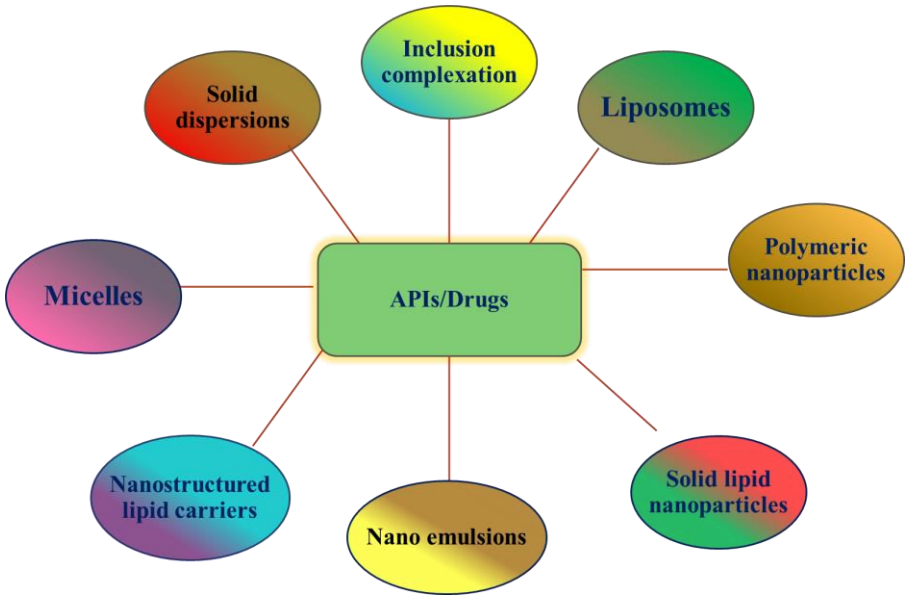

Figure 1.2: Formulation strategies to enhance solubility and permeability of drugs.

1.2. OBJECTIVE

The main objective of the dissertation is to develop novel formulations of Clotrimazole (an anti-fungal agent and a BCS class II drug), Lutein (a neuroprotective agent and BCS class II drug) and Furosemide Silver (a novel antibiotic and BCS class IV drug) to improve their solubility and permeability.

1.3. AIMS

1. To prepare and characterize clotrimazole loaded ufosomes for enhanced topical delivery.
2. To prepare and characterize folate decorated nanoparticles of lutein using PLGA-PEG-FOLATE polymer for enhanced uptake via folate receptor mediated endocytosis.
3. To prepare and characterize furosemide silver loaded solid lipid nanoparticles for enhanced antibacterial activity.

Chapter 2: Clotrimazole Loaded Ufosomes for Topical Delivery: Formulation Development and *In Vitro* Studies

Graphical abstract

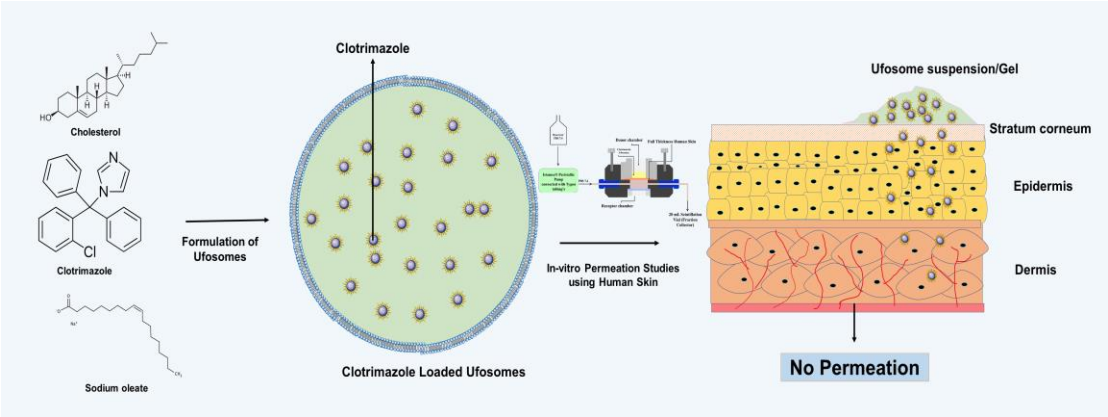

Illustration 2.1: Clotrimazole loaded ufosomes for topical delivery

Introduction

Global incidence of fungal infections has been on a significant rise since 1980's affecting approximately one billion people and are the primary cause of death in one million patients annually (Bongomin et al. 2017). Majority of fungal infections are opportunistic or secondary infections in immunocompromised patients with severe diseases such as acquired immune deficiency syndrome (AIDS), tuberculosis, cancer and chronic obstructive pulmonary disease. The surge in the incidence fungal infections in the recent times is due to the increased use of surgical and invasive procedures, immunosuppressants, and antibiotics (AbouSamra et al. 2019). Most commonly reported fungal infections are superficial in nature affecting skin, hair, nails, and mucosa however, systemic fungal infections are also reported (M. Gupta, Sharma, and Chauhan 2017; Bongomin et al. 2017). Superficial fungal infections caused by dermatophytes affect around 40 million people in developed and underdeveloped countries and is the fourth most common cause of infection (M. Gupta, Sharma, and Chauhan 2017; Shivakumar et al. 2012). Common

fungal pathogens responsible for fungal infections include *Candida, Aspergillus, Cryptococcus, Scedosporium, Zygomycetes* and other species (Bongomin et al. 2017; M. Gupta, Sharma, and Chauhan 2017). Various antifungal agents are used for the treatment of fungal infections which include azoles (triazoles and imidazoles), allylamines, polyene antibiotics, echinocandins, griseofulvin and others (AbouSamra et al. 2019; M. Gupta, Sharma, and Chauhan 2017).

Candidiasis, also referred to as yeast infection is the most common fungal superficial infection caused by the Candida species. *Candida albicans* is an ubiquitous fungal pathogen responsible for 50% of the Candida infections and is usually colonized in skin, vagina, mouth and intestinal tract (AbouSamra et al. 2019; M. A. Alam et al. 2017; Maheshwari et al. 2012). Other candida pathogens include *Candida. krusei*, *Candida. glabrata*, *Candida. lusitaniae*, *Candida. tropicalis*, and *Candida. Parapsilosis* (Nami et al. 2019). Topical formulations are intended to treat local infections on the topmost layer of the skin by effectively penetrating the drugs into the stratum corneum, thus destroying the fungi or the causative organism. Advantages associated with topical formulations include limited systemic bioavailability of the drug, which reduces the systemic adverse effects, potential self-medication, increased patient compliance and targeted or localized therapy. However, topical preparations have disadvantages such as poor dermal or ungual bioavailability, poor penetration into the stratum corneum, variable drug levels at the site of infection, greasiness or stickiness of ointments and creams, skin irritation, allergic reactions, and uncontrolled evaporation of drugs from the preparation (M. Gupta, Sharma, and Chauhan 2017; Bseiso et al. 2015; P. N. Gupta et al. 2005; Juluri et al. 2013; Juluri and Narasimha Murthy 2014). Therefore, there is a need for novel topical formulations to address the problems associated with the current existing formulations. Recently, formulation scientists have explored nanoparticle-based drug delivery systems to improve topical formulations. This is done by

delivering active drugs precisely to the infection site while enhancing skin penetration, reducing irritation and increasing the sustained effect (Pople and Singh 2011). Several novel drug delivery systems have been formulated to encapsulate antifungal agents and improve their efficacy. Some of them include microemulsions, nanoemulsions, niosomes, dendrimers, solid lipid nanoparticles, liposomes, ethosomes, lipid nanoparticles and polymeric nanoparticles (M. Gupta, Sharma, and Chauhan 2017).

Clotrimazole, a broad spectrum less toxic imidazole antifungal agent is widely used to treat Candidiasis. It acts by inhibiting cytochrome 14α-demethylase enzyme of the fungal cells responsible for cell wall synthesis (Santos et al. 2013). Chemically, clotrimazole is 1-((2-chlorophenyl) diphenylmethyl)-1H-imidazole, insoluble in water (0.49 mg/L) with Log P of 6.1 and pKa 6.7 (Waugh and Medical 2007; Ravani et al. 2013; M. Gupta, Sharma, and Chauhan 2017). It is the first oral azole approved for fungal infections; however, it is not used as an oral agent due to its limited oral absorption and systemic toxicity. Currently, clotrimazole is available as conventional topical formulations such as cream (Lotrimin AF and Gyne-Lotrimin), solution (Lotrimin AF) and lotion (Lotrimin AF) (M. Gupta, Sharma, and Chauhan 2017). Topical bioavailability of clotrimazole is very low ranging from 0.5%-10% due to its poor aqueous solubility (D. Waugh 2011). Therefore, clotrimazole must be loaded into a suitable drug delivery system to enhance its topical bioavailability at the infection site. It is reported in the literature that clotrimazole has been loaded into various novel drug delivery systems such as nanogels, microemulsions, solid lipid nanoparticles, nano-capsules, ethosomes, three-dimensionally structured hybrid vesicles, and liposomes (Santos et al. 2013; Esposito et al. 2013; Maheshwari et al. 2012; M. A. Alam et al. 2017; Manca et al. 2019). On the other hand, vesicular drug delivery systems have become more popular in recent times due to their advantages such as prolonged drug

release, improved drug penetration, targeted delivery to the site of infection, and improved physical stability. Very recently, Csongradi et al, reported the use of ufosomes as a potential topical drug delivery vehicle. They loaded roxithromycin, a poorly water-soluble antibiotic into ufosomes and evaluated its release and skin distribution. Results showed that significant amount of roxithromycin accumulation in the epidermis-dermis layer of the skin with no permeation across the skin layers (Csongradi et al. 2017). Ufosomes are lipid based vesicular drug delivery systems otherwise called unsaturated fatty acid liposomes. They are colloidal suspensions of fatty acids and ionized soaps which can form lipid bilayers and entrap active lipophilic drugs. Loading of clotrimazole into ufosomes can result in enhanced skin penetration due to the lipophilic nature of the vesicles. Ufosomes being fatty acid vesicles, could interact with the stratum corneum and enhance the topical bioavailability of clotrimazole (Csongradi et al. 2017; Patel, Patel, and Jani 2011). Moreover, preparation ufosomes is economical as the fatty acids are inexpensive compared to other lipids (Patel, Patel, and Jani 2011). Therefore, the present study aims to prepare and characterize clotrimazole loaded ufosomes using cholesterol and sodium oleate. Clotrimazole ufosomes were prepared by thin film hydration technique. Effect of drug to excipient ratio on size and entrapment efficiency was studied to optimize the formulation. Further, formulation was characterized, and skin diffusion studies were performed using human skin to determine the amount of clotrimazole accumulated in different layers of the skin.

Materials and Methods

Materials

Clotrimazole and cholesterol were purchased from Alfa Aesar (Ward Hill, MA, USA). Sodium oleate was purchased from TCI America (Portland, OR, USA). Methanol (ACS grade), methanol (HPLC grade), PBS (pH 7.4) and chloroform were procured from Fisher Chemicals

(Fair Lawn, NJ, USA). Hydroxy propyl methyl cellulose (HPMC) (MW: 86,000, viscosity 4,000 cP at 2% solution) was obtained from Acros Organics (Fair Lawn, NJ, USA). Cadaver skin for permeation and skin diffusion studies was obtained from Zen-Bio Inc., (Research Triangle Park, NC, USA). Marketed Clotrimazole 1% cream (Perrigo) was purchased from local pharmacy store in El Paso, TX, USA. Deionized water (resistivity of 18.2 MΩ) used for all experiments was obtained from in-house Milli-Q® IQ 7000 Ultrapure Water System (EMD Millipore, Bedford, MA, USA).

Methods

Preparation of ufosomes

Clotrimazole loaded ufosomes were prepared using thin film hydration method reported in the literature with slight modifications (Patel, Patel, and Jani 2011; Verma et al. 2014; Csongradi et al. 2017). Briefly, all the components of the vesicles (clotrimazole, sodium oleate and cholesterol) were dissolved in 10 mL of chloroform-methanol solution (1:2). Clear solution obtained was transferred to a beaker and kept on a magnetic stirrer for complete evaporation of the solvents until a thin film was formed. The thin film was then hydrated with 5 mL of PBS (pH 7.4) for 2 h. The formed vesicular dispersion was sonicated for 5 minutes to obtain ufosomes with uniform sizes. Optimization of the formulation was performed by screening six different ratios of clotrimazole, sodium oleate and cholesterol for vesicle size and entrapment efficiency. Ufosomal gels for permeation studies were prepared by adding 100 mg (2% w/v) and 50 mg (1% w/v) of HPMC to the optimized vesicular dispersion.

Determination of vesicle size, polydispersity index (PDI) and zeta potential (ZP)

Dynamic light scattering (DLS) technique applying photon correlation spectroscopy was used to measure vesicle size and PDI. Zeta potential was determined by measuring the

electrophoretic mobility. Ufosomal dispersion samples (100 µL) were diluted in 10 mL double distilled de-ionized water and measurements were obtained using Malvern Zetasizer (Nano ZS90, Malvern, Worcestershire, UK) at 25 °C. All the experiments were performed in triplicate.

Clotrimazole quantification by HPLC

The concentrations of clotrimazole in all the samples obtained during the analysis was determined using Waters Alliance e2695 HPLC with 2998 photodiode array detector and Empower 3.0 software. Clotrimazole separation was carried out on a reverse phase-C_{18} column (Phenomenex®; 250 mm × 4.6 mm; 5 µm particle size) at 25 °C under isocratic conditions. Mobile phase was methanol-water (90:10 v/v) at a flowrate of 1 mL/min. A sample of 20 µL was injected and the analyte was monitored at 229 nm for 10 minutes. Retention time of clotrimazole was 5.5 minutes. All standard samples were prepared with methanol and filtered through 0.45 µm filter before injection (Santos et al. 2013).

Determination of entrapment efficiency

Entrapment efficiency of the formulations was determined using ultra-centrifugation method (Salama and Aburahma 2016). In brief, the vesicular dispersions were transferred to tubes and centrifuged at 15,000 rpm for 4h at 4 °C (Beckman Ultracentrifuge). The supernatant was discarded to remove the unentrapped drug in the formulation. The lipid precipitate obtained was then mixed with methanol, bath sonicated for 30 minutes and kept overnight in shaking water bath (25 °C; 100 rpm) for complete extraction of entrapped clotrimazole. The resultant solution was centrifuged at 15,000 rpm for 30 minutes at 4 °C to separate methanol and lipid layer, if any. After centrifugation, supernatant was diluted appropriately and the concentration of entrapped clotrimazole was determined using HPLC. Entrapment efficiency was calculated using the following formula.

Entrapment efficiency (%EE) = (Amount of clotrimazole remained in vesicles)/(Initial amount of clotrimazole) × 100

Surface morphology

Quanta 600F scanning electron microscope with a high-resolution field emission source (ThermoFisher Scientific, Hillsboro, OR) was used to study surface morphology of ufosomes. Prior to imaging, samples were dispersed in methanol and the mixture was drop casted onto a piece of silicon wafer (5 mm × 5 mm) and fixed with double sided conductive tape. Further, samples were air dried and coated with gold using a gold sputter [Gatan 682 Precision Etching and Coating System (PECS) (Gatan, Inc., Pleasanton, CA)]. High resolution images of the ufosomes were visualized under high vacuum at an accelerated voltage of 20 keV.

X-ray diffraction (XRD) analysis

XRD analysis was carried out using Rigaku Miniflex X-Ray Diffractometer (Rigaku Corporation, Tokyo, Japan). A double-sided adhesive tape was applied over the sample holder and powdered (lyophilized) samples were poured onto the sample holder using a thin spatula. Intensity of diffracted beam was analyzed in 2θ range between 10° and 70°. All samples were analyzed using JADE software.

Differential Scanning Calorimetry (DSC)

DSC analysis was performed for lyophilized ufosomes, clotrimazole, sodium oleate and cholesterol using DSC822e (Mettler Toledo) instrument. Samples (5-10 mg) were weighed in 40 µL aluminum pans and hermetically sealed using a crimping device. An empty aluminum pan was used as a reference standard on the other side. Nitrogen was used as purge gas during the analysis at a flow rate of 20 mL/min. Samples were held at 0 °C isotherm for 5 minutes then heated

at 10 °C/minutes to 260 °C (from 0 °C - 260 °C, 260 °C - 0 °C, 0 °C - 260 °C and finally 260 °C – 0 °C). All the thermograms were recorded and analyzed using STARe software.

In vitro permeation studies

Preparation of skin

Skin penetration studies were performed using a human cadaver defatted skin from the abdominal region of a Caucasian male (ZenBio Inc., Lot#SKIN122117C). Skin acquired from the skin bank was stored in -20 °C freezer until needed. For permeation studies, the skin samples were thawed at 4 °C for 24 hours. On the day of permeation study, the skin samples were removed from the 4 °C and allowed to equilibrate at room temperature for 15 minutes. After equilibration, skin was shaved to remove any hair. Further, the skin was rehydrated in 150 mL of PBS (pH 7.4) for 30 minutes at room temperature (Barbero and Frasch 2016; Pere et al. 2018). Immediately after rehydration, the full thickness skin was appropriately cut to size of the PermeGear® in-line cells, 1.77 cm^2, and mounted between the donor and receptor compartments for skin diffusion studies (Hopf et al. 2014).

Automated flow through diffusion cells

In vitro permeation studies were performed using PermeGear® ILC-07 automated system (PermeGear, Riegelsville, PA) incorporated with seven in-line flow-through diffusion cells, made of Kel-F. Diffusion cells contain a donor and receptor chambers clamped using threaded rods with adjustable locking nuts. Inlet and outlet ports of the receptor chamber (254 µL receptor chamber volume) were connected to the Tygon tubings having 1/ 4-28 HPLC fittings and all cells were placed in cell warmer connected to a Julabo BC4 circulating water bath (Seelbach, Germany) to maintain the temperature at 37 °C. All the cells were connected to a multi-channel peristaltic pump® IPC (Ismatec, Zurich, Switzerland) which draws receptor solution from a reservoir

(Figure 2.1). The diameter of the diffusional area was 1 cm (total diffusional area: 0.785 cm^2). Full thickness skin (epidermis facing donor compartment) was mounted in the cells between the donor and receptor chambers and clamped using the adjustable locking nuts. Formulations were placed in the donor chamber and the receptor fluid (PBS pH 7.4) was pumped at a flow rate of 4 mL/h through each cell. Receptor fluid was collected in the receptor vials of 20 mL capacity at pre-determined time intervals up to 24 h (K. P. Bolla et al. 2020; De Leon et al. 2016; Córdoba-Díaz et al. 2000). The amount of clotrimazole permeated through the skin was determined by analyzing the samples using HPLC method described in the earlier sections.

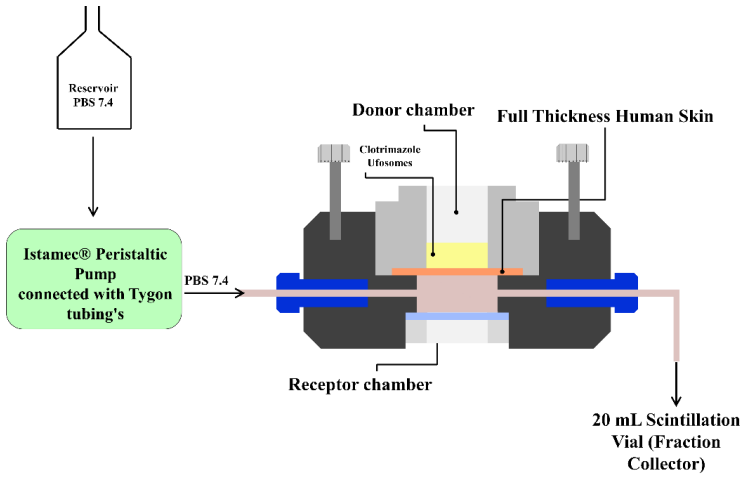

Figure 2.1: Automated flow through cells

Tape stripping

Tape stripping method reported in the literature was employed to determine the amount of clotrimazole accumulated in stratum corneum-epidermis and epidermis-dermis layers of the skin. After completion of skin permeation studies, the skin samples mounted were carefully removed from the cells and placed on a flat surface to view the diffusion area. The excess formulations on the skin surface was removed by gently dabbing the skin using soft tissue. Stratum corneum and some parts of epidermis layers was separated using 3M Scotch® Magic tape™. Pre-cut tapes were

pressed onto the skin with the thumb and removed immediately using forceps to remove stratum-corneum (first strip was discarded). An average of 10 strips were required to remove the stratum corneum completely. The remaining epidermis-dermis layers of the skin was cut into tiny pieces using clean surgical scissors. All the strips (except the first one) and skin pieces were transferred to a conical tube with 10 mL methanol and clotrimazole was extracted by sonicating in an ultrasonic water bath for 30 mins and left to stand overnight at 4 °C. After extraction, the resulting solution was centrifuged for 30 mins at 15,000 rpm and the drug content in the supernatant was analyzed using HPLC (Kahraman et al. 2018; Binder et al. 2018; Csongradi et al. 2017; Dwivedi et al. 2016).

Statistical analysis

Statistical analysis was performed using GraphPad Prism® software (version 5.0, San Diego, CA). Data are expressed as mean ± SD for DLS and entrapment efficiency results and mean ± SEM for skin diffusion results. One-way ANOVA followed by followed by Bonferroni's posttest was applied to determine statistical significance. A p-value of < 0.05 was considered as statistically significant.

Results and Discussion

Optimization of clotrimazole loaded ufosomes

Optimization studies were aimed to obtain smaller sized ufosomes with high entrapment efficiency. For this, different ratios of clotrimazole, cholesterol and sodium oleate were screened for vesicle size and entrapment efficiency. As most of the clotrimazole topical formulations available commercially are of 1%, the concentration of clotrimazole in all the formulations was constant at 1% w/v in all the formulations. The ratio of non-ionized fatty acids and ionized fatty acids determines the stability of ufosomes (Patel, Patel, and Jani 2011). Therefore, effect of six

different ratios of cholesterol and sodium oleate on vesicle size, PDI, ZP and entrapment efficiency were studied to obtain the optimized formulation. Cholesterol (neutral fatty acid) and sodium oleate (ionized fatty acid) were selected for formulation of ufosomes as they are widely used in lipid based topical formulations. Moreover, they are approved by USFDA as inactive ingredients (USFDA n.d.). Cholesterol, a naturally available unsaturated steroid is capable of forming phospholipid bilayers which entrap hydrophobic drugs. In addition, cholesterol enhanced the stability and permeability of the vesicles ("10 Final Report on the Safety Assessment of Cholesterol" 1986; Doppalapudi et al. 2017). It has been used in the preparation of various formulations which include liposomes, ufosomes, topical ointments and creams, transfersomes, niosomes, secosomes, and solid lipid nanoparticles (Kavian et al. 2019; Csongradi et al. 2017; Md et al. 2017; Roberts et al. 2017; Meng et al. 2019; Kravchenko et al. 2011). Sodium oleate is a salt of unsaturated fatty acid (oleic acid) and used as a permeation enhancer in topical formulations and is GRAS chemical (Csongradi et al. 2017; Witteveen 2018; Oliveira et al. 2015). As ufosomes are formed in narrow pH range of 7-9, phosphate buffered saline (PBS) 7.4 was used for hydration. Any differences in the pH of hydration medium will lead to the formation of oil droplets or precipitates (pH <7) or soluble micelles (pH >9) in the formulation (Salama and Aburahma 2016).

Determination of size, PDI and ZP

Table 2.1., summarizes the size, PDI and ZP of ufosomes prepared using different ratios of cholesterol, sodium oleate and clotrimazole. Results showed that increase in the concentration of sodium oleate and cholesterol led to the formation of ufosomes with smaller vesicle sizes. Ufosomes with particle sizes <300 nm was obtained with Ufo_6 (1:2:2 ratio) [clotrimazole (50 mg), sodium oleate (100 mg) and cholesterol (100 mg)]. However, all the formulations were polydisperse in nature with PDI ranging from 0.4 to 0.7. Size distribution analysis of all the

formulations is provided in Table 2.2. Ufo_6 formulation showed trimodal size distribution indicating the presence of vesicles with different sizes. Analysis of size distribution curves showed that the vesicle size was <200 nm for majority of the vesicles (Figure 2.2). Decrease in the vesicle size with increase in cholesterol could be attributed to higher packing densities and stability of vesicles with increased cholesterol concentration (Kravchenko et al. 2011). Similar findings were obtained when diclofenac was loaded into cholesterol vesicles (diclosomes) (Tavano, Mazzotta, and Muzzalupo 2018). As reported in the literature, ZP values for all the ufosomes was high ranging from -73.7 mV to -101 mV indicating high stability. Increase in the sodium oleate (ionized soap of fatty acid) concentration resulted in the shift of ZP to higher negative values.

Table 2.1: Summary of vesicle diameter, PDI and ZP results of ufosomes. Data are presented as mean ± SD (n=3)

Formulation	**Clotrimazole:Cholesterol:Sodium Oleate**	**Vesicle diameter (nm)**	**PDI**	**ZP (mV)**
Ufo_1	1:0.5:1	1177 ± 156	0.414 ± 0.164	-74 ± 3
Ufo_2	1:1:0.5	848 ± 239	0.638 ± 0.166	-74 ± 3
Ufo_3	1:1:1	432 ± 140	0.583 ± 0.069	-74 ± 5
Ufo_4	1:2:1	374 ± 67	0.589 ± 0.064	-75 ± 7
Ufo_5	1:1:2	752 ± 179	0.702 ± 0.067	-101 ± 5
Ufo_6	1:2:2	234 ± 59	0.581 ± 0.132	-98 ± 3

Table 2.2: Summary of size distribution analysis of ufosomes

Formulation	**Vesicle diameter (nm)**	**Size distribution (nm) (mean ± SD)**	**Intensity (%)**
Ufo_1	1282	1207 ± 342	93.7

		128 ± 27	5.2
		5560	1.1
Ufo_2	894	947 ± 191	82.7
		96 ± 17	17.3
Ufo_3	493	396 ± 80	72.5
		68 ± 12	27.5
Ufo_4	367	546 ± 140	65
		86 ± 21	35
Ufo_5	720	808 ± 167	59.6
		123 ± 28	40.4
Ufo_6	207	144 ± 50	71.6
		782 ± 194	19.4
		42 ± 9	9

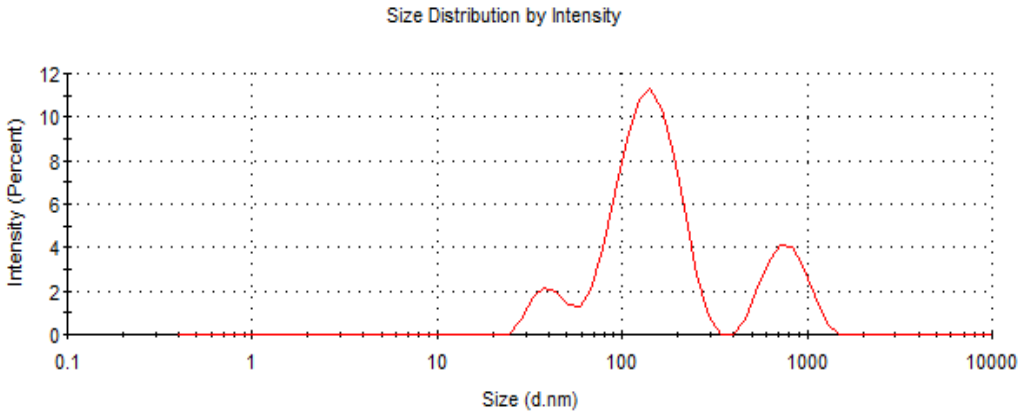

Figure 2.2: Size distribution curve of Ufo_6

Determination of Entrapment Efficiency

Overall, all formulations exhibited high clotrimazole entrapment with entrapment efficiency ranging from ~76% to ~87% indicating ufosomes as ideal carrier for entrapment of lipophilic drugs. Ufosomes contain fatty acids which are oriented in the form of a bilayer with

hydrophobic tails towards the interior resulting in greater entrapment of drugs (Patel, Patel, and Jani 2011). Ufo_6 formulation had high entrapment efficiency of ~99% for one sample among the triplicates analyzed (high standard deviation). Although, there was no significant difference between the formulations, a trend of greater entrapment was observed with increase in the drug lipid ratio. This could be attributed to higher rigidity of the ufosomal membrane leading to greater drug retention (Doppalapudi et al. 2017). Also, high entrapment efficiency at lower drug to lipid ratio could be attributed to the presence of the enough lipid for entrapment of clotrimazole (Das, Ng, and Tan 2012).

Based on the DLS and entrapment efficiency results, Ufo_6 formulation was chosen as the optimized formulation for further studies due to small vesicle size and high entrapment efficiency.

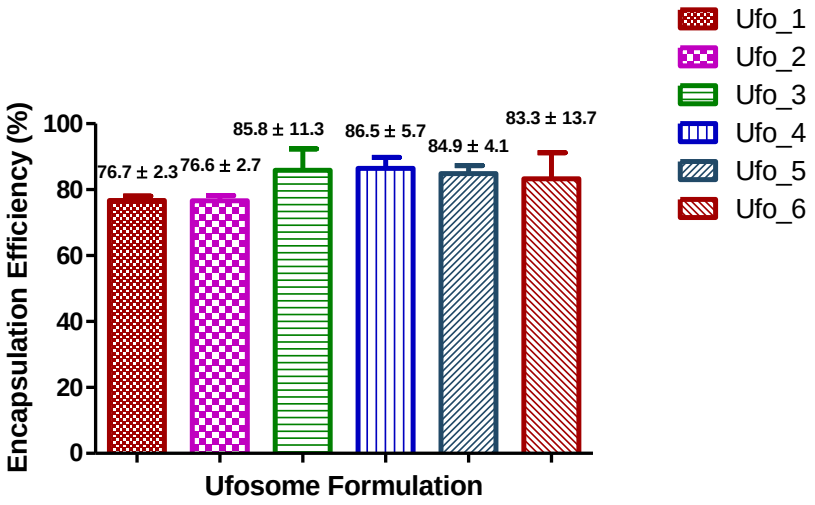

Figure 2.3: Summary of entrapment efficiency results of ufosomes. Data are presented as mean ± SD (n=3)

Surface morphology

Scanning electron microscopy (SEM) is one of the most widely used techniques to study the surface morphology of nano and microparticles. This technique uses electron beam as a probe

to acquire high resolution images of the particles whereas, DLS provide the hydrodynamic radius of the particles. SEM images of the ufosomes are provided in Figure 2.4. The images revealed that the ufosomes were roughly spherical with smooth surfaces. Vesicle size observed with SEM was larger compared to the sizes obtained from DLS. The difference in the sizes could be attributed to loss of water during the air-drying process resulting in collapse and fusion of vesicles.

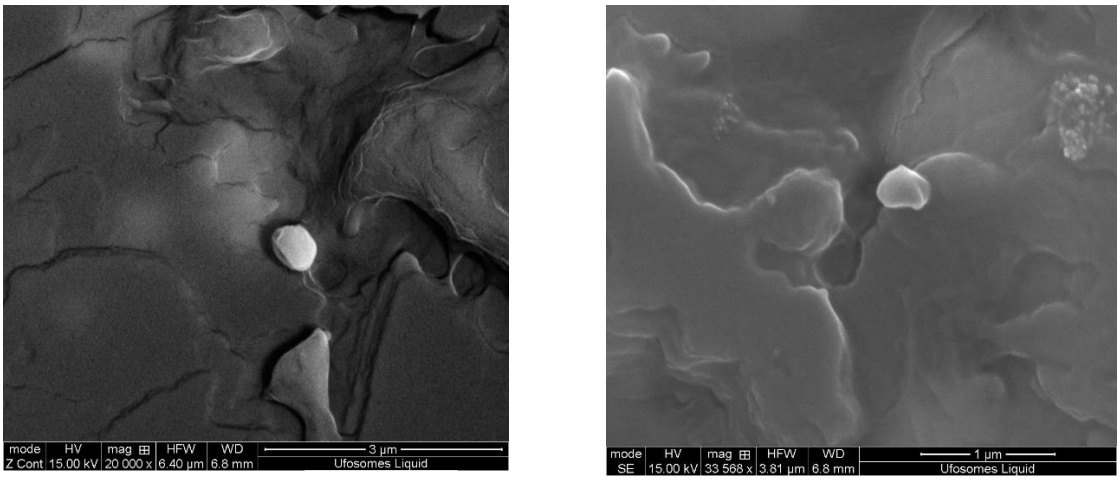

(a) (b)

Figure 2.4. SEM images of clotrimazole loaded ufosomes (Ufo_6).

XRD analysis

XRD studies were performed to study the polymorphic changes of compounds used in the formulation of ufosomes. Crystalline nature of the compounds affects important properties such as stability, solubility, and bioavailability. Amorphous forms of drug molecules are characterized with higher solubilities and increased bioavailability (P. K. Bolla et al. 2019; Renukuntla 2018a). XRD diffractograms for clotrimazole, cholesterol, sodium oleate and clotrimazole loaded ufosomes are provided in Figure 2.5. Results showed characteristic peaks at 10.8°, 13.2° (high intensity), 19.4°, 20.3°, 21.5°, 24.0°, 25.3°, and 26.2° confirming the crystalline nature of clotrimazole (Figure 2.5D). In addition, characteristic peaks were recorded for cholesterol (15.3°,

15.8°, and 30°) (Figure 2.5A) and sodium oleate (30.3°) (Figure 2.5C). However, XRD results of clotrimazole loaded ufosomes showed the absence of characteristic peaks of clotrimazole (Figure 2.5B). This confirms the entrapment of clotrimazole into ufosomes and transition of clotrimazole from crystalline to amorphous forms. Similar results were observed in other reports studying the entrapment of drug molecules into lipid-based drug delivery systems (Jaiswal et al. 2014; Bose and Michniak-Kohn 2013; AbouSamra et al. 2019; Das, Ng, and Tan 2012).

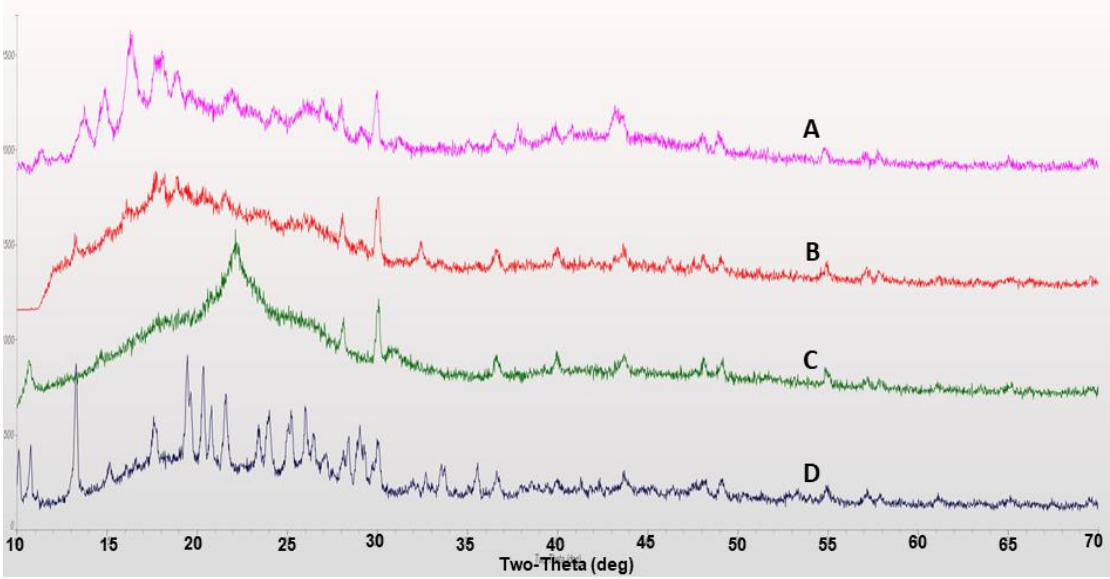

Figure 2.5: XRD diffractograms of (A) cholesterol, (B) clotrimazole loaded ufosomes, (C) sodium oleate and (D) clotrimazole.

DSC

DSC is a widely used technique to understand the melting and recrystallization behavior of drug molecules. It is a thermo-analytical technique, that determines the thermodynamic properties of materials by providing information about the polymorphic changes when subjected to a controlled heat flux (Ribeiro et al. 2016; Rodriguez et al. 2019). Thermal behavior of clotrimazole, cholesterol, sodium oleate and clotrimazole loaded ufosomes is provided in

Figure 2.6. DSC thermogram of clotrimazole showed a characteristic endothermic peak at 143.98 °C. In addition, cholesterol had a melting point of 147.63 °C. No specific thermal behavior was observed for sodium oleate and clotrimazole loaded ufosomes. Disappearance of characteristic endothermic peak of clotrimazole in lyophilized ufosomes confirm the entrapment and transformation from crystalline to amorphous form. DSC thermograms also confirm the internal arrangement drug in vesicles (Buchiraju et al. 2013). Clotrimazole is entrapped in cholesterol bilayer and carboxylic groups of sodium oleate are on the surface of vesicles. Overall, DSC results complemented the XRD results.

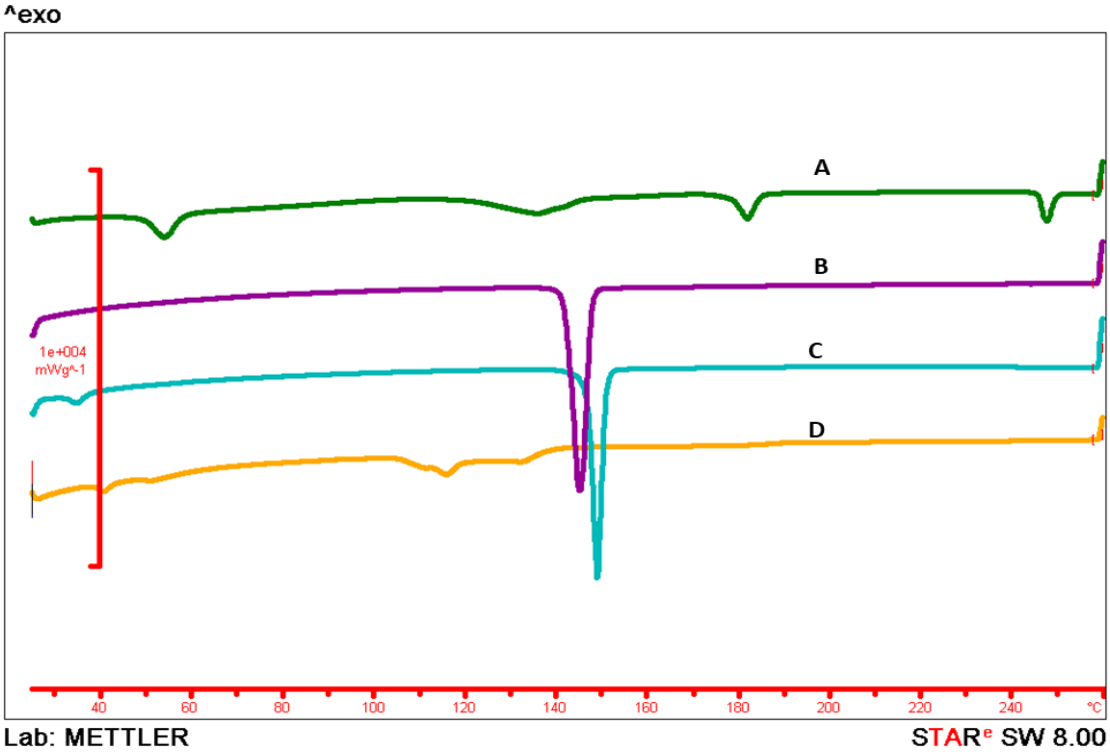

Figure 2.6: DSC Thermograms of (A) sodium oleate, (B) clotrimazole, (C) cholesterol and (D) clotrimazole loaded ufosomes. Sharp endothermic peaks in thermograms (B) and (C) indicates the melting points of clotrimazole and cholesterol at 147.63 °C and 143.98 °C, respectively. No peak related to drug was found in clotrimazole loaded ufosomes (D).

In vitro permeation studies

Skin diffusion studies

In formulation research and development, *in vitro* permeation studies are conducted to predict skin permeation of topical and transdermal formulations (Ruela et al. 2013; Azarmi, Roa, and Lobenberg 2007). Flow-through cells were used for continuous flow of receptor fluid to maintain sink conditions. Moreover, this type of system is more suitable to simulate *in vivo* conditions and preferred for several drug molecules (Cordoba-Diaz et al. 2000). For our experiments, 24-h permeation studies were conducted on human skin for ufosome suspension and ufosomes in HPMC gels (1% and 2%) with blanks as negative control. Permeation studies were also performed using a dialysis membrane to confirm the release of clotrimazole from the formulations. For comparison, permeation studies were also conducted for marketed Clotrimazole 1% cream (Perrigo) composed of benzyl alcohol, cetostearyl alcohol, cetyl esters wax, octyldodecanol, polysorbate 60, and sorbitan monostearate. Sampling intervals were 1, 2, 3, 4, 5, 6, 7, 8, 12, 16, 20, and 24 h. Results showed that clotrimazole was not permeated through the skin up to 24 h following the permeation studies from all the tested formulations. Similar results were observed in reports published in literature with clotrimazole microemulsions (Kaewbanjong et al. 2018), clotrimazole loaded three-dimensionally-structured hybrid vesicles (Manca et al. 2019) and roxithromycin ufosomes (Csongradi et al. 2017). As most of the fungal infections are localized on the surface of the skin, systemic bioavailability of clotrimazole is not required. Therefore, ufosomes could be a potential carrier for topical delivery of clotrimazole.

Skin retention study (Tape-stripping)

Tape-stripping experiments were performed to determine the penetration of clotrimazole into stratum-corneum, epidermis and dermis of the skin. Results showed that clotrimazole

accumulation in stratum corneum-epidermis and epidermis-dermis layers was significantly higher with ufosomes suspension compared to ufosomes gel and marketed cream ($p < 0.05$). Ufosome gels showed higher levels of clotrimazole in the skin, however, they were not significantly higher compared to the marketed cream ($p > 0.05$). These findings were consistent with other studies where entrapment of drugs into lipid vesicles enhanced the topical bioavailability of drugs. Enhancement of topical bioavailability could be attributed to simultaneous mechanisms such as: i) increased solubility due to transformation of clotrimazole from crystalline to amorphous form, ii) penetration enhancing property of cholesterol and sodium oleate, and iii) high interaction of lipids could modify the structure of stratum corneum and iv) enhanced thermodynamic activity (Csongradi et al. 2017; Dwivedi et al. 2016). The amount of clotrimazole accumulated in stratum corneum-epidermis and epidermis-dermis layers is provided in Figure 2.7 and Figure 2.8, respectively. Compared with marketed formulation, there was ~16-times, ~2.3-times, ~1.5-times enhanced penetration of clotrimazole into stratum corneum with ufosomes suspension, ufosome 1% gel and ufosomes 2% gel, respectively (Figure 2.7). Whereas, the amount of clotrimazole accumulated in the epidermis-dermis layer was ~6-fold, ~3.3-fold, and ~3.2-fold higher with ufosomes suspension, ufosome 1% gel and ufosomes 2% gel, compared to marketed formulation (Figure 2.8). Overall, topical diffusion studies revealed enhanced penetration and targeted delivery of clotrimazole only to the superior layers of the skin. This proves that ufosomes could be effective in enhancing the required drug concentrations at the target cutaneous tissues.

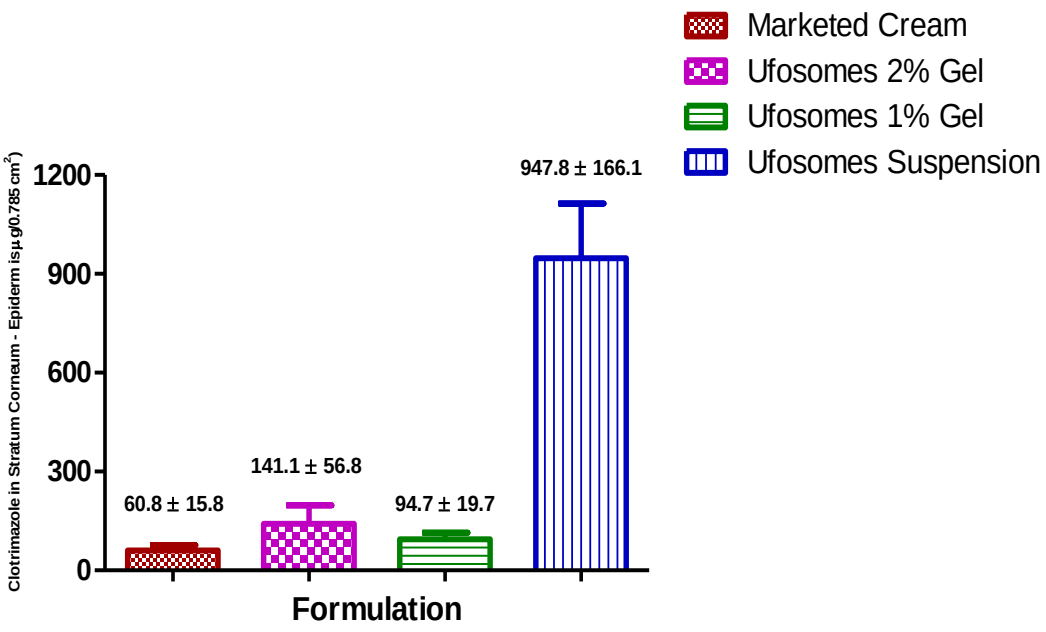

Figure 2.7: Amount of clotrimazole accumulated in stratum corneum-epidermis layers of skin. Data are represented as mean ± SEM (n=3)

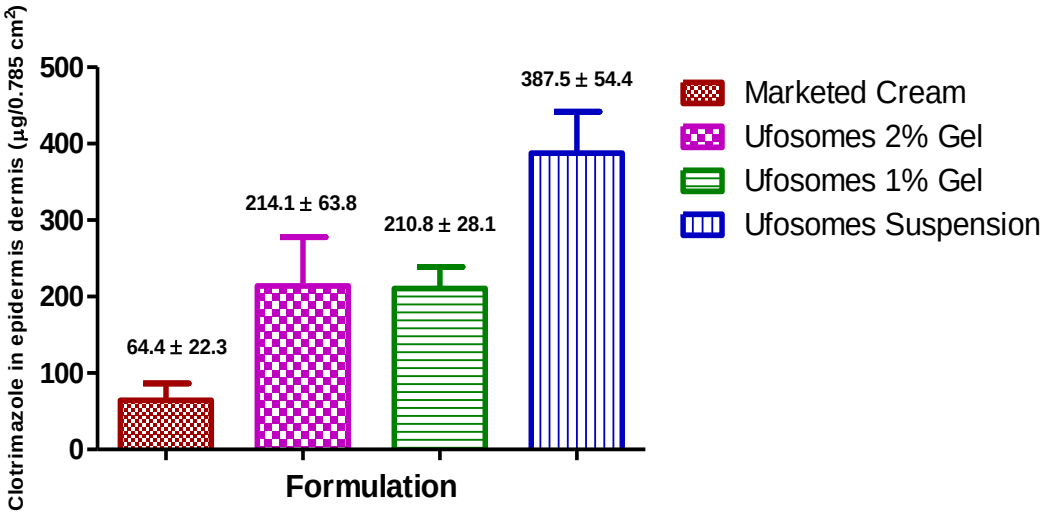

Figure 2.8: Amount of clotrimazole accumulated in epidermis-dermis layers of skin. Data are represented as mean ± SEM (n=3)

Conclusions

Entrapment of hydrophobic drugs into lipid-based vesicles can improve the topical bioavailability. In the present study, clotrimazole loaded ufosomes were successfully prepared using cholesterol and sodium oleate. Optimized formulation with vesicle size <250 nm and high entrapment efficiency was obtained with 1:2:2 ratio of clotrimazole (50 mg), cholesterol (100 mg) and sodium oleate (100 mg). DSC and XRD results confirmed the successful entrapment of clotrimazole into ufosomes. Spherical morphology of ufosomes was confirmed by SEM. *In vitro* permeation studies using human skin revealed that clotrimazole did not permeate through the skin. Topical diffusion studies (tape-stripping) confirmed that ufosomes suspension significantly increased the accumulation of highly lipophilic drug (clotrimazole) into the viable epidermis and dermis as compared to the ufosomes gels and commercially available cream. Thus, this study proves that ufosomes could be a potential carrier to enhance the topical bioavailability and targeted delivery of drugs. However, the results from this study are preliminary and should be further confirmed with in-depth formulation development, stability, and pre-clinical studies before clinical applications.

Future studies

In this dissertation project, I have successfully prepared and characterized novel ufosomes based formulation for enhancing the topical bioavailability of clotrimazole using several *in vitro* techniques. For extending this project, the future studies include: (1) Evaluation of *in vitro* antifungal activity of clotrimazole loaded ufosomes on different strains of *Candida albicans* and to evaluate the *in vivo* antifungal activity to compare with marketed formulation. (2) Further, *in vivo* pharmacokinetics and biodistribution of clotrimazole after topical application will be studied.

Chapter 3: Preparation and Characterization of Lutein Loaded Folate Conjugated Polymeric Nanoparticles

Graphical abstract

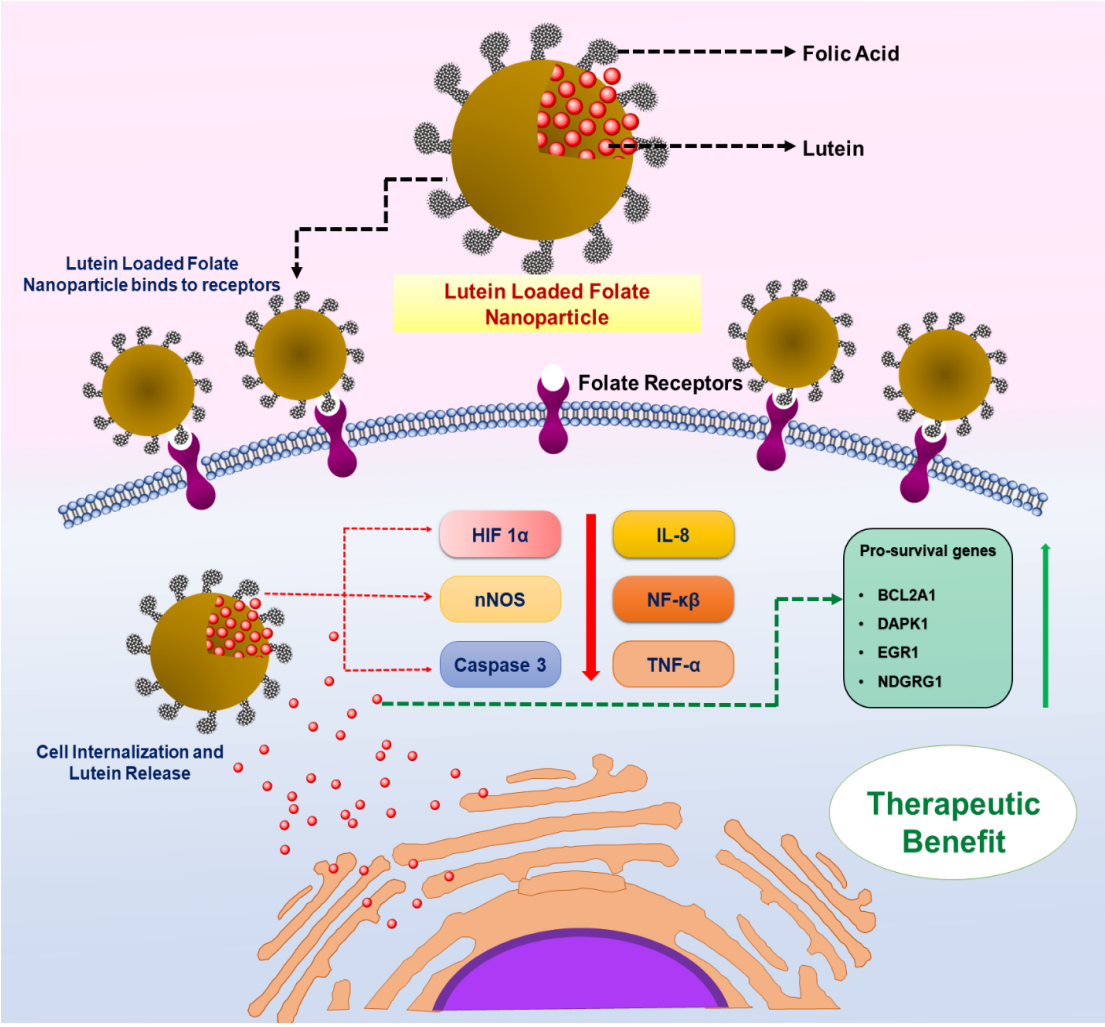

Illustration 3.1: Proposed mechanism of lutein loaded PLGA-PEG-FOLATE nanoparticles for treatment of neonatal HIE.

Introduction

Perinatal asphyxia (PA) caused due to a reduced oxygen supply to the brain at the time of birth is the main cause of mortality in one million neonates per year globally. Other causes for PA include various intricate perinatal events such as maternal/fetal hemorrhage, umbilical cord

compression, and uterine rupture leading to oxygen deprivation (Fattuoni et al. 2015). While the majority of neonates with PA recover from their episodes, in few cases, the condition complicates and causes hypoxic-ischemic brain injury, which subsequently leads to hypoxic-ischemic encephalopathy (HIE) (SE et al. 2011). Neonatal HIE affects approximately 0.1% to 0.3% of live births in developed nations and 2.6% in under-developed nations (Joseph et al. 2018). Globally, HIE is the main cause of mortality in about 23% of neonatal deaths. It is estimated that about, 15%-20% of the neonates with HIE die in the neonatal period and around 25% of the survivors develop severe neurological morbidities (SE et al. 2011; Joseph et al. 2018; Vannucci and Perlman 1997; Shankaran et al. 2005). Neurological/psychological morbidities associated with HIE include cerebral palsy, seizures, blindness, learning disabilities, cognitive delays, motor and intellectual disabilities (Vannucci and Perlman 1997; Fattuoni et al. 2015). Several biochemical mechanisms such as inflammation, excitotoxicity, and oxidative stress are involved in the pathophysiology of HIE, which ultimately leads to neuronal cell death (Foster et al. 2017; Busl and Greer 2010). In clinical settings, the most widely used treatment for HIE is therapeutic hypothermia, with a success rate of only 50%-60% (Joseph et al. 2018). Other classes of drugs used in the past include glucocorticoids, diuretics, and barbiturates for cerebral edema related to HIE (Vannucci and Perlman 1997). In recent times, there have been attempts to explore the use of various agents such as neuroprotective agents, anti-inflammatory agents, free-radical scavengers, and oxygen free radical generation inhibitors as an adjuvant therapy to hypothermia in clinical settings (Joseph et al. 2018; Vannucci and Perlman 1997). Efficacy of agents such as curcumin, melatonin, xenon, allopurinol, and erythropoietin, a brain-derived neurotrophic factor in preclinical models of HIE has been proven (Joseph et al. 2018; Y. Cheng et al. 1997; Martinello et al. 2017). However, none of these agents were effective in reducing the severity of HIE in clinical settings. Therefore, novel

strategies with new treatments are required to ameliorate the severity of HIE and reduce mortality and morbidity (Vannucci and Perlman 1997; Martinello et al. 2017).

One such promising therapeutic agent is Lutein. In 2017, Foster et al. evaluated the role of lutein as a neuroprotective agent in a rat model of neonatal hypoxic-ischemic brain injury. Results from this study had proven that there was significant reduction of histological brain injury scores, inflammatory mediators, and hypoxia-inducible proteins such as HIF-1α with lutein treatment. Also, lutein supplementation to rats resulted in the selective accumulation of lutein in neonatal rat brains through breast milk (Foster et al. 2017; Gong et al. 2017). Lutein is a dihydroxy xanthophyll carotenoid and is available abundantly from green leafy vegetables, fruits, flowers, and egg yolk etc. (Hu et al. 2012; Li et al. 2009). As animals/humans cannot synthesize lutein, it must be obtained from diet. The neuroprotective effects of Lutein are attributed to its anti-inflammatory and antioxidant properties (Li et al. 2009; Lim et al. 2016; do Prado Silva et al. 2017). Unfortunately, lutein has poor bioavailability due to high lipophilicity (Log P 7.9) and poor aqueous solubility (Ozawa et al. 2012; "Lutein" n.d.). Therefore, there is an unmet need for developing a new formulation of lutein with enhanced bioavailability.

The approach of utilizing polymeric nanoparticles to enhance bioavailability of drugs with poor biopharmaceutical properties has been proven effective (Joseph et al. 2018; El-Say and El-Sawy 2017). Furthermore, polymeric nanoparticles have advantages including biocompatibility, enhanced stability, sustained release, and improved efficacy (El-Say and El-Sawy 2017; Crucho and Barros 2017; Kumari, Yadav, and Yadav 2010; Khan, Saeed, and Khan 2017; Bahrami et al. 2017). Another advantage of polymeric nanoparticles is the possibility of covalent conjugation with ligands enabling targeted drug delivery to tissues of interest (Masood 2016). Polymeric nanoparticles are prepared using biodegradable polymers such as poly (lactide co-glycolide)

(PLGA), gelatin, chitosan, albumin, alginate, polycaprolactone, polyglycolides, poly (methyl methacrylate), and polyethylene glycol (PEG) (Banik, Fattahi, and Brown 2016; El-Say and El-Sawy 2017). Folate receptors are expressed in the brain and blood brain barrier and can be utilized for active targeting of drugs for neurological disorders such as HIE and brain cancer. As we know, neuronal cells after terminal maturation cannot be propagated *in vitro*, so lutein uptake studies were carried out in neuroblastoma cells as a model for brain cells. Neuroblastoma cell lines have been extensively used to study various neuronal properties including drug uptake studies. It has been reported that drugs such as doxorubicin, etoposide, docetaxel have been encapsulated in folate decorated NP formulations for brain tumors (Guo et al. 2017). Therefore, it is hypothesized that folate conjugated PEG-PLGA nanoparticles (PLGA-PEG-FOLATE) may increase the lutein uptake by brain cells through via receptor mediated endocytosis (Illustration 3.1) (Antony 1996; C. Alam et al. 2017; Zhao et al. 2011; Guo et al. 2017). Previously, lutein was encapsulated into various nano-formulations such as polymeric nanoparticles (PLGA, Polyvinyl pyrrolidone), liposomes, nano-emulsions, nanocrystals, lipid nano-capsules, and nano-dispersions. Nano-formulations of lutein were evaluated by *in vitro* studies and animal models for anti-oxidant, anti-inflammatory, anti-cancer, cognitive defects, and acute macular degeneration (Lim et al. 2016; Tan et al. 2016; Muhoza et al. 2018; Mitri et al. 2011; Steiner, McClements, and Davidov-Pardo 2018; do Prado Silva et al. 2017; Brum et al. 2017). The aim of the present study was to encapsulate lutein into polymeric nanoparticles (PLGA and PLGA-PEG-FOLATE) and evaluate its enhanced uptake in neuroblastoma cells.

Materials and Methods

Materials

Lutein (90%) was obtained from Acros Organics (New Jersey, USA). Dimethyl sulfoxide (DMSO), methanol (HPLC grade), tetrahydrofuran (HPLC grade), dichloromethane (DCM), n-hexane, sodium chloride, and potassium dihydrogen phosphate were procured from Fisher Scientific (Fair Lawn, NJ, USA). Sodium dodecyl sulphate, polyvinyl alcohol (PVA) (MW: 30,000 - 70,000), and disodium hydrogen phosphate were purchased from Sigma Aldrich (St. Louis, MO, USA). Milli-Q water (18.2 MΩ resistivity) was from Milli-Q® IQ 7000 Ultrapure Water System (EMD Millipore, Bedford, MA, USA). PLGA (50:50, MW: 10,000 – 15,000) and PLGA-PEG-FOLATE (50: 50; MW: 10,000 Da-2,000 Da) were procured from Akina PolySciTech, Inc, Indiana, USA. Fluorescein isothiocyanate (FITC) was purchased from Invitrogen, Labeling & Detection, Molecular Probes, ThermoFisher Scientific, USA. Cellulose ester dialysis tubing (Biotech grade; Mw: 300 kDa) was obtained from Spectrum Laboratories, Inc (CA, USA). Human neuroblastoma cell line, SK-N-BE(2) (ATCC CRL-2271), was purchased from American Type Culture Collection (ATCC, Manassas, VA, USA).

Methods

Preparation of polymeric Nanoparticles loaded with lutein

Lutein loaded polymeric nanoparticles were prepared using a slightly modified oil in water (O/W) emulsion-solvent evaporation method reported earlier (Figure 3.1) (Jwala et al. 2011; Sai HS. Boddu, R. Vaishya, J. Jwala, A. Vadlapudi 2012). In brief, 100 mg of polymer (PLGA or PLGA-PEG-FOLATE) was completely dissolved in 5 mL of DCM and lutein (20 mg) was separately dissolved in 2 mL DCM. The polymer and lutein solutions were mixed to form a homogenous organic phase. The organic phase was sonicated in a bath sonicator for 5 minutes

followed by its slow addition to aqueous solution of PVA (2% w/v) (20 mL) under constant stirring on a magnetic stirrer. Further, the resultant mixture was sonicated at 30% amplitude for 5 minutes using a Fisher Scientific™ Model 505 probe sonicator to obtain an emulsion. The sonication step was performed in cold conditions to prevent any overheating of the emulsion. After sonication, emulsion was kept overnight under gentle stirring at room temperature to completely evaporate DCM. The emulsion was washed three times with deionized water using Beckman ultracentrifuge at 22,000 × g for 1 h to remove any unentrapped lutein and PVA residue. Finally, the nanoparticles formed were lyophilized for 24 h using a benchtop freeze dryer (Harvest Right, North Salt Lake, UTAH, USA) (vacuum: <100 mTorr and condenser temperature: −50 °C).

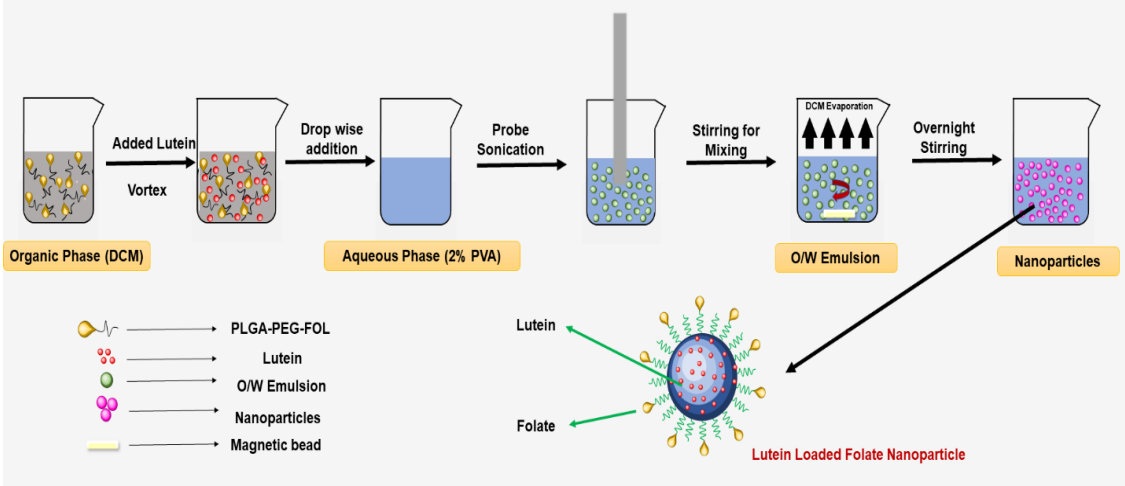

Figure 3.1: Oil in water emulsion-solvent evaporation method for preparation of lutein loaded PLGA-PEG-FOLATE nanoparticles

Determination of particle size, PDI and ZP

The particle diameter, PDI of lutein loaded PLGA and PLGA-PEG-FOLATE nanoparticles were measured using DLS technique. Zeta potential of nanoparticles was determined by measuring electrophoretic mobility of particles using Malvern Zetasizer. NP dispersions (200 µL) were

further dispersed in double distilled de-ionized water (10 mL) and size and ZP were analyzed with Malvern Zetasizer Nano ZS90 at 25 °C. All the measurements were performed on three different samples (n = 3).

Determination of lutein encapsulation efficiency (%EE) and drug loading (%DL)

The encapsulation and loading of lutein into nanoparticles were determined by quantifying the lutein content in freeze dried nanoparticles using high performance liquid chromatography (HPLC). Briefly, freeze dried nanoparticles (10 mg) were dissolved in 10 mL DMSO and the amount of lutein was determined using Waters Alliance e2695 HPLC equipped with 2998 photodiode array (PDA) detector and Empower 3.0 software. The separation was performed using Kromasil® C-18 column (5 µm; 250 mm × 4.6 mm) under isocratic conditions at a flow rate of 1 mL/minute at 25 °C. Mobile phase used was methanol: tetrahydrofuran at a ratio of 90: 10 and the analyte was monitored at 450 nm. Retention time of lutein was 3.85 minutes (Liu et al. 2014). Sample injection volume was 20 µL and the run time was 10 mins. The %EE and %DL of lutein in the nanoparticles was determined using the following formulae. All the measurements were performed on three different samples (n = 3).

%EE = (Amount of lutein remained in nanoparticles)/(Initial amount of lutein) × 100

Drug loading (%DL) = (Weight of lutein in nanoparticles)/(Weight of polymer used) × 100

DSC

Encapsulation of lutein into PLGA and PLGA-PEG-FOLATE was confirmed using DSC technique. Calorimetric analysis was performed for lutein, PVA, polymers (PLGA and PLGA-PEG-FOLATE), and lutein loaded nanoparticles using DSC822e (Mettler Toledo) instrument. Samples were weighed (3-11 mg) accurately in 40 µL capacity aluminum pans and were hermetically sealed using a crimping device. Reference standard was an empty aluminum pan on

the other side. Nitrogen was purged at a rate of 20 mL/minute during the analysis. Samples were held at 25 °C isotherm for 5 minutes and then heated at 10 °C/minute to 280 °C. All the thermograms recorded were analyzed using STARe software.

Fourier Transform Infrared Spectroscopy (FTIR)

The FTIR spectra of lutein, PVA, polymers (PLGA and PLGA-PEG-FOLATE), and lutein loaded polymeric nanoparticles were recorded on a JASCO-FT/IR 4600 instrument using Attenuated Total Reflection (ATR) technique. Sample compartment was flushed with argon prior to each run. The sample was ground to fine powder with a KBr pellet. The scanning range was from 500 – 4000 cm^{-1}. After the spectrum measurement, the spectral data were analyzed and plotted, CO_2 and H_2O peaks were subtracted from the original spectrum to obtain the final IR spectrum.

Surface Morphology

Quanta 600F scanning electron microscope with a high-resolution field emission source (ThermoFisher Scientific, Hillsboro, OR) was used to study the surface morphology of lutein loaded nanoparticles. Freeze dried nanoparticles suspended in milli-Q water were deposited on a copper grid and fixed with double-sided conductive tape. nanoparticles were coated with gold using a gold sputter [Precision Etching and Coating System (Gatan 682 PECS) (Gatan, Inc., Pleasanton, CA)] and allowed to evaporate. High resolution images of the nanoparticles were visualized under high vacuum at an accelerated voltage of 20 kV.

***In vitro* release studies**

Initially, various media were screened to identify the most suitable release medium for studies. Release media which were screened included phosphate buffered saline 7.4 with 0.2% w/v

sodium dodecyl sulphate, 20% (v/v) ethanol and phosphate buffered saline 7.4 with 0.2% w/v sodium dodecyl sulphate and 20% v/v ethanol. Excess lutein (~20 mg) was added to 2 mL of release medium in Eppendorf tubes (2 mL capacity) and were placed in a shaking water bath (100 rpm) at 37 °C. After 24 hours, samples were removed from the water bath and filtered through 0.45 µm cellulose acetate syringe filter. Aliquots of filtrate were diluted appropriately to determine the saturation solubility of lutein in release medium. After selecting the release medium, drug release behavior from lutein loaded PLGA and PLGA-PEG-FOLATE nanoparticles was determined using dialysis bag method (MWCO: 300 kDa) (Joseph et al. 2018). Phosphate buffered saline (pH 7.4) with 0.2% w/v sodium dodecyl sulphate was chosen as the suitable release medium for release studies to maintain sink conditions (Hu et al. 2012). In brief, 1 mL lutein loaded polymeric nanoparticles (~1 mg lutein) were transferred to individual dialysis tubing and release medium (1 mL) was added to the tubings. Leakage was prevented by sealing the tubing tightly at both ends. Sealed dialysis tubings loaded with nanoparticles were transferred to 250 mL beakers containing 100 mL of release medium in a shaking water bath (100 rpm) (maintained at 37 ± 0.5 °C). To prevent any evaporation of release medium, beakers were packed tightly with parafilm. At a pre-determined time-intervals (0.5, 1, 2, 3, 4, 5, 6, 7, 8, 24, and 48 h), samples (10 mL) were collected from each beaker and replaced with 10 mL of fresh release medium. Cumulative amount of drug released from the formulations was quantified using UV spectrophotometer (UV 1800, Shimadzu, Kyoto, Japan) by measuring the absorbance at λ_{max} of 436 nm at different timepoints. All experiments were performed on three different samples (n = 3).

Cell Culture studies

Neuroblastoma (SK-N-BE(2)) cells were used in this study to determine the cellular uptake of lutein loaded PLGA-PEG-FOLATE nanoparticles as compared to lutein and lutein loaded

PLGA nanoparticles. SK-N-BE(2) cells were purchased from ATCC (American Type Culture Collection, Virginia, USA) and were cultured according to manufacturer's protocol. In brief, DMEM: F-12 (1:1 ratio) culture media containing 10% (v/v) heat inactivated fetal bovine serum (FBS), 100 U/mL penicillin, and 100 µg/mL streptomycin, 1% (v/v) MEM Non-essential amino acids and 1% sodium bicarbonate was used for culturing SK-N-BE(2) cells. The cells were grown in T-75 Corning culture flask and incubated at 37 °C, 5% CO_2, and 95% relative humidity.

FITC Labelling

The cellular distribution of lutein loaded PLGA-PEG-FOLATE nanoparticles, lutein loaded PLGA nanoparticles and lutein was determined by labeling various treatment groups with FITC. FITC is widely used to label proteins (Chaganti, Venkatakrishnan, and Bose 2018), drugs (Michlewska et al. 2019) and polymers (Damgé, Maincent, and Ubrich 2007). FITC labeling was performed according to a previously published protocol (Mandal et al. 2017). Briefly, 10 µg equivalent of lutein loaded PLGA-PEG-FOLATE nanoparticles and PLGA nanoparticles were suspended in 50 mM phosphate buffered saline to make a 10 µg/mL of suspension of the nanoparticles. The final volume of the suspension was 8.0 mL. Separately, powdered FITC was dissolved in DMSO (1 mg/mL) since, FITC was not water soluble. The freshly prepared FITC solution (1.0 mL) was added to nanoparticles suspension (8.0 mL) and incubated at 4º C in dark for 12 hours. The incubation was followed by addition of 1 mL 50 mM ammonium chloride (NH_4Cl) to inactivate any unreacted FITC. Finally, the FITC labelled nanoparticles solution was subjected to dialysis using a 2,000 kDa dialysis filter to remove unreacted FITC, and other small molecules (NH_4Cl). Finally, the formulation was filtered through a 0.22 µm nylon syringe filter to ensure sterility of the FITC labelled nanoparticles. This fluorescent labelled nanoparticle solution was then aliquoted, protected from light and stored at -20°C until further use. A solution of FTIC

labelled lutein was also prepared in similar way as described above, except lutein was dissolved in DMSO (5 mg/mL) and then mixed with FITC solution.

In vitro uptake determination using flow cytometry [Fluorescence-activated cell sorting (FACS)]

The cellular uptake of FITC labelled nanoparticles in SK-N-BE(2) cells was determined by incubating the cells with the fluorescent treatment groups and then analyzing their time-dependent uptake using flow cytometry (FACS). SK-N-BE(2) cells were seeded in a 12-well plate at a density of 0.5×10^6 cells/well with 1 mL of DMEM: F-12 media and stored overnight in an incubator maintained at 37 ºC, 5% CO_2 and 95% RH. The overnight incubation was followed by treating the cells with 10 µL of various treatment groups which included (i) Control (DMSO), (ii) FITC-lutein PLGA nanoparticles and (iii) FITC-lutein PLGA-PEG-FOLATE nanoparticles. Then, the treated SK-N-BE(2) cells were incubated for various pre-determined time points (3, 6, 9, and 12 hours), which was followed by harvesting the cells, washing and acquiring the samples with FACS. At each time point, the media was removed from the wells and the cells were harvested using 200 µl of trypsin (TrypLE). This was followed by incubation (5 minutes) and addition of serum containing DMEM: F-12 media. The cells were then collected in FACS tubes and centrifuged at 20,000 rpm for 5 minutes to a obtain cell pellet. Further, the media was discarded, and the cells were washed twice with 1 mL of Dulbecco's Phosphate-Buffered Saline (DPBS) (Gibco's). The final sample was prepared using DPBS and acquired by flow cytometry to determine the mean FITC fluorescence intensity of the cells at an excitation wavelength of 490 nm. The mean FITC fluorescence intensity values obtained for all the samples were plotted using bar-graphs in GraphPad Prism (version 5.0) and the differences were observed.

In vitro uptake determination by confocal microscopy

Confocal laser scanning microscopy (CLSM) was used to determine the cellular distribution of FITC labelled nanoparticles and lutein in SK-N-BE(2) cells. FITC-lutein-PLGA-PEG-FOLATE nanoparticles, FITC-lutein PLGA nanoparticles and FITC-lutein were prepared using the same method described in earlier sections and were used as treatment groups. The unreacted FITC in all the samples was removed by adding 1 mL 50 mM NH_4Cl. FITC was adsorbed on the surface of the nanoparticles. SK-N-BE(2) cells were seeded in a 8- chamber confocal microscopy slide precoated with collagen (Nunc Lab-Tek 8 chambered, Thermo Fisher Scientific, Waltham, MA, USA) and 200 µL of complete DMEM: F-12 (1:1) media. These slides were stored overnight in an incubator maintained at 37 ºC, 5% CO2 and 95% R.H. This was followed by addition of 10 µL various treatment samples which included (i) control (DMSO), (ii) FITC-lutein, (iii) FITC-lutein PLGA nanoparticles, and (iv) FITC-lutein-PLGA-PEG-FOLATE nanoparticles into each chamber of the 8-chamber plate. Further, the treatment groups were incubated for 6 and 12 hours. At each time point, the culture media was removed, and the cells were washed twice with 300 µl of DPBS for 5 minutes. This was followed by fixing the cells with freshly prepared cold 4% buffered paraformaldehyde solution (200 µl) and incubation at 37 ºC for 20 minutes. After incubation, the fixation solution was removed, and the cells were washed again with 300 µl DPBS (3 times × 5 minutes each). Further, the nuclei of the cells were stained with 100 µl of DAPI (working solution of 10 µg/mL) for 15 minutes in dark. The cells were then mounted with mounting media and a sealed cover slip to prevent evaporation of the mounting media and dehydration of the cells. The SK-N-BE(2) cell slides were stored at 4ºC before the actual analysis. A Leica Confocal Laser Scanning Microscope (Leica TCS SP5, Wetzlar, Germany) was used to analyze the cells for green fluorescence-FITC and blue fluorescence-DAPI.

Determination of cellular uptake of lutein using HPLC

Cellular uptake studies were conducted in SK-N-BE(2) (ATCC CRL-2271), human neuroblastoma cell line. Cells were grown as described in previous sections and maintained in a humidified atmosphere with 95% air and 5% CO_2. Cells were seeded at a density of 10^6 cells/well in six-well plates for 24 h before treatment. After 24 h, the uptake study was initiated by adding lutein nano-formulation (1 mL) containing 20 µg of lutein to the wells and placed in an incubator maintained at 37 °C for 12 h. After incubation, the cells were washed two-times with phosphate buffered saline and supernatant was separated. Then, cells from the wells were lysed in 0.5 mL phosphate buffered saline with a microtube homogenizer. To extract lutein from the lysed cell suspension, 1.5 mL of DCM and methanol solution (1:2) was added to the suspension and mixed using vortex mixer for 5 minutes. Then, hexane (2 mL) was added to the mixture, and the resultant hexane-DCM layer (supernatant) was separated and dried to get lutein extract. The lower layer was similarly extracted twice. The extracted lutein was re-dissolved in 400 µl of methanol: dichloromethane (4:1) solution and analyzed using HPLC.

Physical stability Studies

A 60-day physical stability studies were conducted for all the nanoparticles at 4 °C and 25 °C. All nano-formulation dispersions were stored in glass scintillation vials for 60 days. At days 0, 30 and 60, all the samples were re-dispersed in milli-Q water (18.2 MΩ resistivity), and assessed for particle size, PDI, ZP using Malvern Zetasizer.

Statistical analysis

Statistical analysis was done using GraphPad Prism® software (Version 5.0, San Diego, CA). A non-parametric t-test followed by Bonferroni's multiple comparison post-test was used to

compare cellular uptake of nano-formulations. A 2-way analysis of variance (ANOVA) followed by Bonferroni's post-test was applied for stability studies.

Results and Discussion

Preparation and characterization of lutein loaded nanoparticles

PLGA and PLGA-PEG-FOLATE were chosen for the formulation of nanoparticles due to the biocompatibility, biodegradability, mechanical strength, targetability, and versatile biodegradation kinetics (Jain 2000; Mu and Feng 2003; Sahana et al. 2008). PLGA is metabolized to form safe degradation products such as lactate and glycolic acid, which are removed by Kreb's cycle. PVA was used for formulation of nanoparticles as it is the most widely used stabilizer for emulsions and helps in forming nanoparticles with smaller size and uniform size distribution (Turk et al. 2014). Moreover, both PLGA and PVA are US FDA approved inactive ingredients in various formulations (Mu and Feng 2003; Sahana et al. 2008). The size, PDI, and ZP of lutein loaded polymeric nanoparticles is provided in Table 3.1. Results show that all the lutein loaded nanoparticles had size < 200 nm with uniform size distribution (Figure 3.2). Size of lutein PLGA and PLGA-PEG-FOLATE nanoparticles were 189.6 ± 18.79 nm and 188.0 ± 4.06 respectively. PDI ranged from 0.083 ± 0.023 to 0.202 ± 0.009. ZP is a measurement of the surface charge on the nanoparticles and is a representative of stability of the nanoparticles (Suttiponparnit et al. 2010). Zeta potential results revealed that lutein loaded PLGA-PEG-FOLATE nanoparticles had higher ZP (-26.0 ± 1.27 mV) compared to lutein loaded PLGA nanoparticles (-10.7 ± 1.80 mV). Terminal carboxylic groups in the polymers is responsible for the negative ZP values (Sai HS. Boddu, R. Vaishya, J. Jwala, A. Vadlapudi 2012; Esmaeili et al. 2008), which could be a reason for higher shift of ZP of PLGA-PEG-FOLATE towards negativity.

Table 3.1: Size, PDI, ZP and %EE of lutein loaded PLGA and PLGA-PEG-FOLATE nanoparticles (n = 3). Data are expressed as mean ± SD

S.no	Particle type	Size (nm)	PDI	ZP (mV)	%EE
1	Lutein PLGA	189.6 ± 18.79	0.083 ± 0.023	-10.7 ± 1.80	60.95 ± 4.85
2	Lutein PLGA-PEG-FOLATE	188.0 ± 4.06	0.202 ± 0.009	-26.0 ± 1.27	72.87 ± 7.22

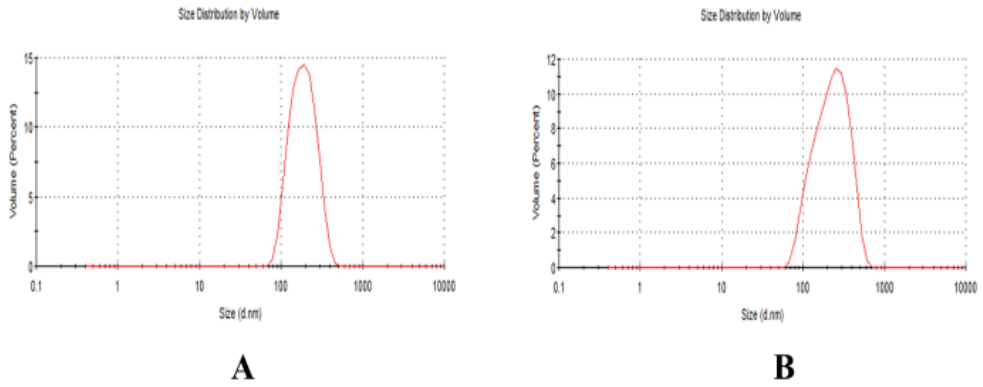

Figure 3.2: Size distribution curves of A) Lutein-PLGA and B) Lutein PLGA-PEG-FOLATE nanoparticles

%EE and %DL

The %EE of lutein was 60.95% ± 4.85% and 72.87% ± 7.22% for lutein PLGA and PLGA-PEG-FOLATE nanoparticles, respectively (Table 3.1). The lutein loading in PLGA and PLGA-PEG-FOLATE nanoparticles was ~12.2% and ~14.6%, respectively. Results showed that folate decorated nanoparticles had greater lutein encapsulation compared with PLGA nanoparticles. Greater encapsulation with PLGA-PEG-FOLATE polymer can be due to the presence of folate on the surface of nanoparticles, which could have increased the interaction between lutein and the

polymer. Similar results were obtained when docetaxel and SN-38 were encapsulated in folate decorated nanoparticles (Esmaeili et al. 2008; Ebrahimnejad et al. 2010).

Surface Morphology

SEM is one of the most widely used technique for understanding the surface morphology of nanoparticles. High resolution images of the nanoparticles were obtained using electron beam as a probe (Tsaousis et al. 2018). SEM images of lyophilized lutein loaded polymeric nanoparticles are shown in Figure 3.3. These images revealed that the nanoparticles were spherical in shape. The sizes obtained from the SEM images of all nanoparticles were below 200 nm and are well corroborated with the DLS results.

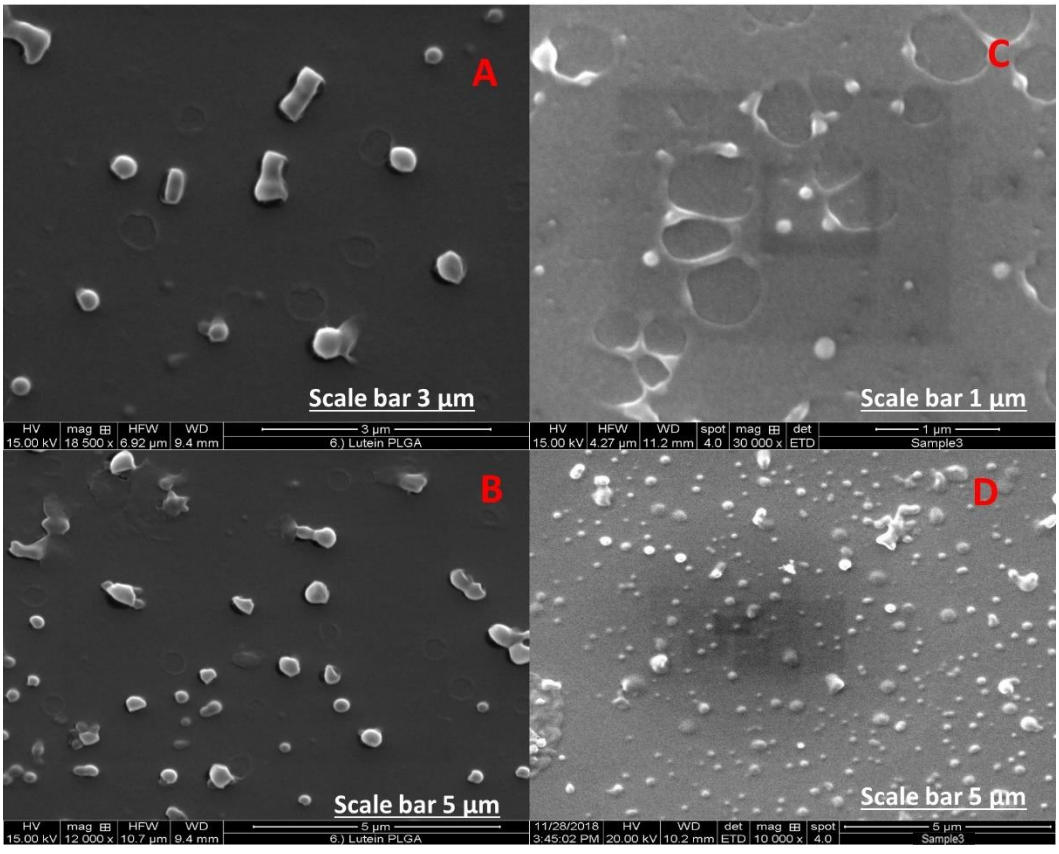

Figure 3.3: SEM images of Lutein-PLGA nanoparticles (A and B) and Lutein- PEG-PLGA - FOLATE nanoparticles (C and D). Scale bars are 1 μm for (C), 3 μm for (A) and 5 μm for (B and D).

DSC

DSC is one of the widely employed techniques to determine the polymorphic changes of the drugs and polymers in formulation research. Thermograms of lutein, polymers and lutein loaded nanoparticles are provided in Figure 3.4. Lutein had a sharp characteristic endothermic peak at 64.07 °C as per the thermogram. Also, PLGA had an endothermic at 45.28 °C. On the other hand, no specific peak/melting point was observed for PLGA-PEG-FOLATE and PVA confirming the amorphous nature of the polymers. The characteristic endothermic peak of lutein disappeared in thermograms of lutein loaded nanoparticles thereby confirming the complete encapsulation of lutein into the amorphous polymers. Transformation of lutein from crystalline form to amorphous form is important as amorphous forms are characterized with higher solubilities and increased bioavailability compared to crystalline forms (K. P. Bolla et al. 2019; Morissette et al. 2004; Kalhapure and Akamanchi 2013). Similar results (loss of characteristic peak) were obtained in other studies where crystalline drugs such as oxcarbazepine, prilocaine, and adefovir were encapsulated into PLGA micro and nanoparticles (Musumeci et al. 2018; Bragagni et al. 2018; Ayoub et al. 2018). Overall, DSC results confirmed the successful encapsulation of crystalline lutein into amorphous polymeric nanoparticles.

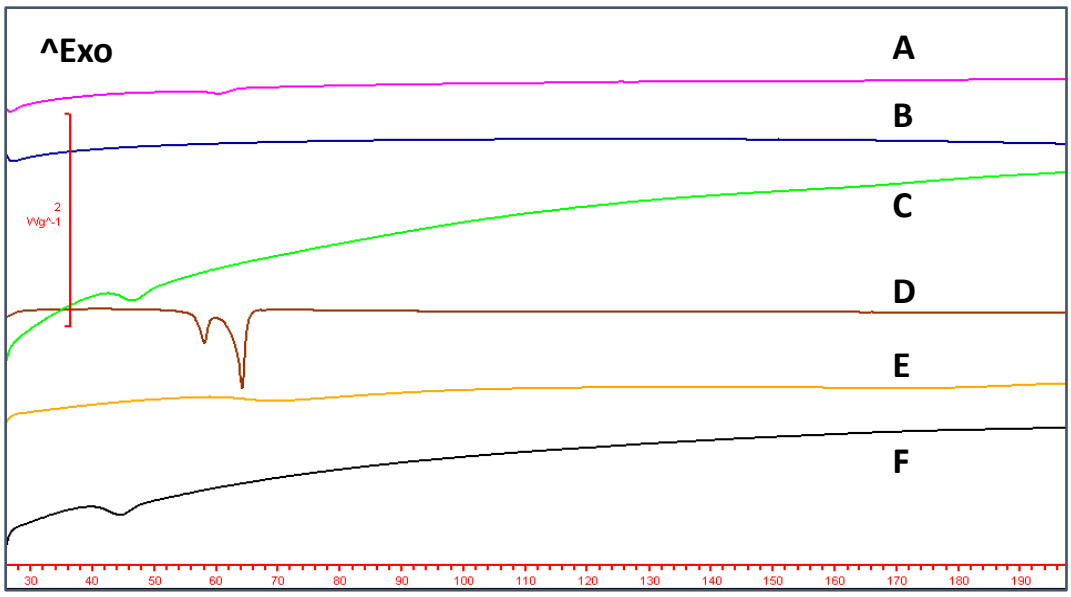

Figure 3.4: DSC thermograms of (A) lutein loaded PLGA-PEG-FOLATE nanoparticles, (B) PLGA-PEG-FOLATE, (C) lutein loaded PLGA nanoparticles, (D) Lutein, (E) PVA, and (F) PLGA.

FTIR analysis

The surface chemistry of lutein, PVA, PLGA, PLGA-PEG-FOLATE, lutein loaded PLGA and PLGA-PEG-FOLATE nanoparticles was evaluated using FTIR spectroscopy (Figure 3.5). The broad transmittance band of lutein between 3588.88 cm^{-1} and 3073.01 cm^{-1} corresponds to the O-H stretching vibrations, which was absent in lutein loaded PLGA and PLGA-PEG-FOLATE nanoparticles. In addition, characteristic C-H stretching bands at 2958 cm^{-1} and 2912 cm^{-1} were observed for lutein. A strong transmittance of lutein was observed at 1620.15 cm^{-1} which was absent in the spectra of the lutein-loaded PLGA-PEG-FOLATE and PLGA nanoparticles. There was no obvious difference in the spectra of the polymers (PLGA and PLGA-PEG-FOLATE) and lutein loaded polymeric nanoparticles. FTIR spectra obtained for PLGA-PEG-FOLATE in our study was similar to the spectra available in the literature (Fasehee et al. 2016; Sai HS. Boddu, R.

Vaishya, J. Jwala, A. Vadlapudi 2012). Results from FTIR confirm showed that the characteristic peaks of lutein were absent in the FTIR spectra of lutein loaded polymeric nanoparticles. This could be due to the strong interaction of lutein with the polymers which resulted in the absence of characteristic peaks. Similar results were observed for other nanoparticle systems (Ahlawat, Deemer, and Narayan 2019). Moreover, it is evident that the encapsulation of lutein into polymers did not result in any structural changes which might be attributed to either the small concentration of the drug or due to its bonding and non-bonding interactions with the surrounding matrix.

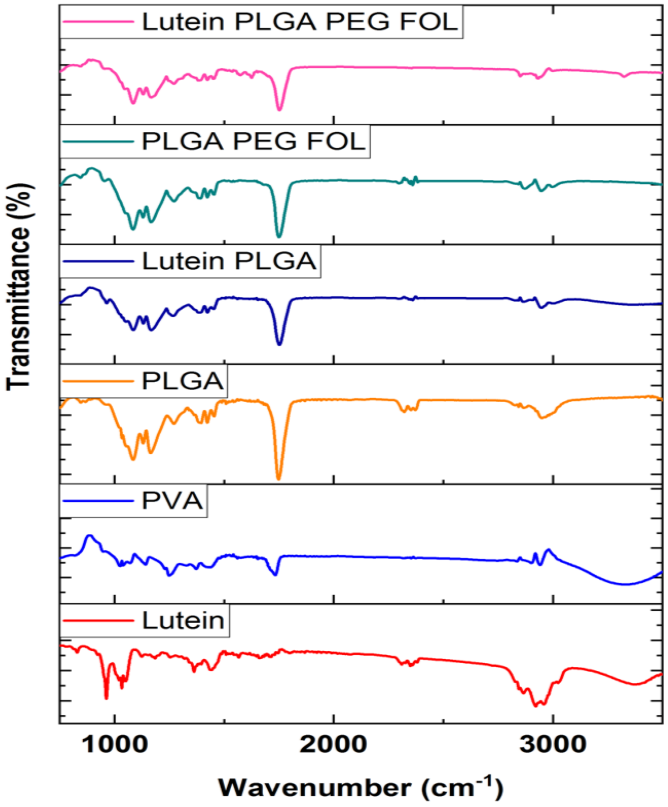

Figure 3.5: Fourier-transform infrared spectroscopy (FTIR) spectra of PLGA, PLGA-PEG-FOLATE, lutein loaded PLGA and PLGA-PEG-FOLATE nanoparticles, PVA and lutein.

In vitro release studies

After analyzing the solubility of lutein in various release media, phosphate buffered saline 7.4 with 0.2% sodium dodecyl sulphate was chosen as the release medium (Hu et al. 2012). *In vitro* release profile of lutein from PLGA and PLGA-PEG-FOLATE nanoparticles is provided in Figure 3.6. Release profiles showed that the nano-formulations showed initial burst-release (~50% and ~43% with PLGA and PLGA-PEG-FOLATE nanoparticles in 6 h), followed by sustained release pattern. Cumulative release of lutein was higher in PLGA nanoparticles with 100% release within 24 hours and ~80% in PLGA-PEG-FOLATE nanoparticles at 48 h. Similar release profiles were reported in literature when drugs such as SN-38 and docetaxel were encapsulated in folate decorated nanoparticles. The lower release of lutein from PLGA-PEG-FOLATE nanoparticles can be attributed to the high affinity of drug with the polymer or densely packed polymer system with low porosity, which hinders the immediate release of drug from the nanoparticles and also due to better arrangement of lutein in polymer matrix (Esmaeili et al. 2008; Ebrahimnejad et al. 2010; Sai HS. Boddu, R. Vaishya, J. Jwala, A. Vadlapudi 2012). Moreover, higher encapsulation of lutein in the PLGA-PEG-FOLATE polymer could have resulted in lesser space for polymer hydration and leading to slower release of lutein (Kamaly et al. 2016). Overall, release studies validate the sustained/controlled release of drugs from polymeric nanoparticles.

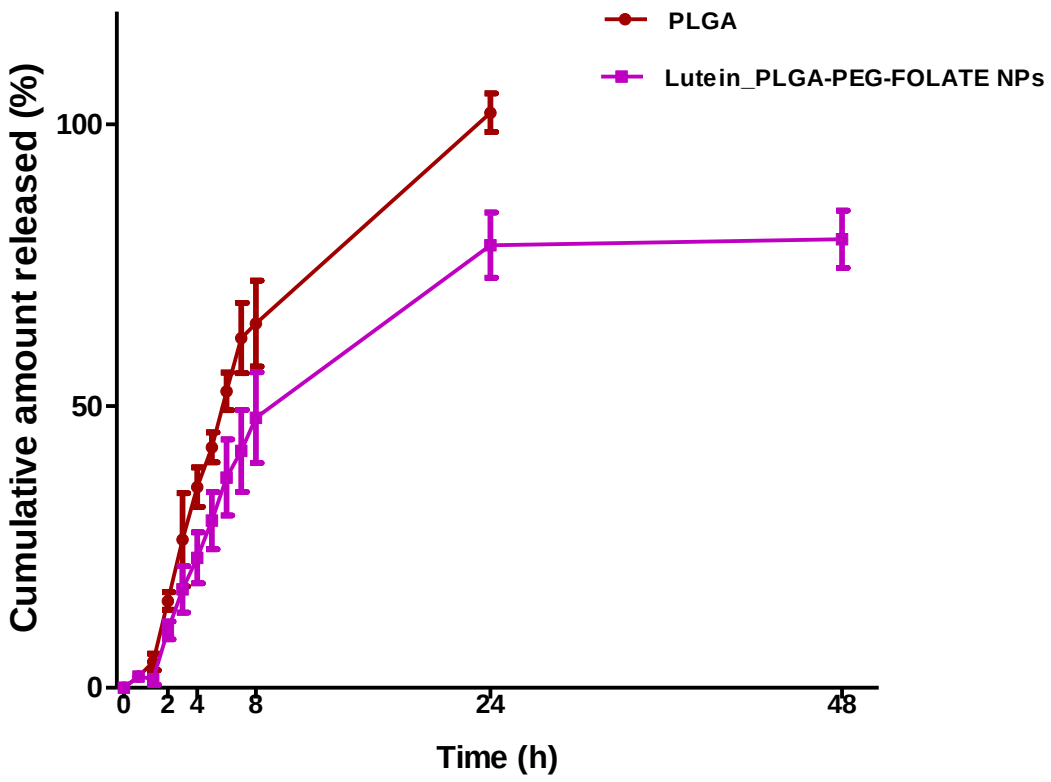

Figure 3.6: *In vitro* release of lutein loaded PLGA and PLGA-PEG-FOLATE nanoparticles. Data are expressed as mean ± SD (n=3).

In vitro cellular uptake studies

In vitro cellular uptake of lutein was determined in SK-N-BE(2) neuroblastoma cell line to understand the intracellular localization and uptake of the folate decorated nanoparticles loaded with lutein as compared to lutein PLGA nanoparticles and plain lutein. These studies also helped to compare the uptake of the lutein nanoparticles within the cytoplasm of SK-N-BE(2) cells. FACS and confocal microscopy were used as quantitative and a qualitative analysis method respectively, to determine the cellular uptake. Further, enhanced uptake of lutein with PLGA-PEG-FOLATE polymer was also determined by measuring the amount of lutein uptaken using HPLC.

FACS Analysis

FITC- labelled-lutein loaded nanoparticles were incubated with SK-N-BE(2) cells and were analyzed to determine *in vitro* uptake at predetermined time points by using flow cytometry. Figure 3.7 depicts the time dependent uptake of FITC-labelled nanoparticles in SK-N-BE(2) cells as measured by the mean FITC fluorescence intensity. Results show that there was a significant increase in the uptake of FITC-lutein-PLGA-PEG-FOLATE nanoparticles as compared to FITC-lutein PLGA nanoparticles at 6 hours and 9 hours. This enhanced uptake could be attributed to the receptor mediated endocytosis due to the presence of folate receptors on the surface of the SK-N-BE(2) cells, which aid in the higher uptake of the folate decorated lutein nanoparticles.

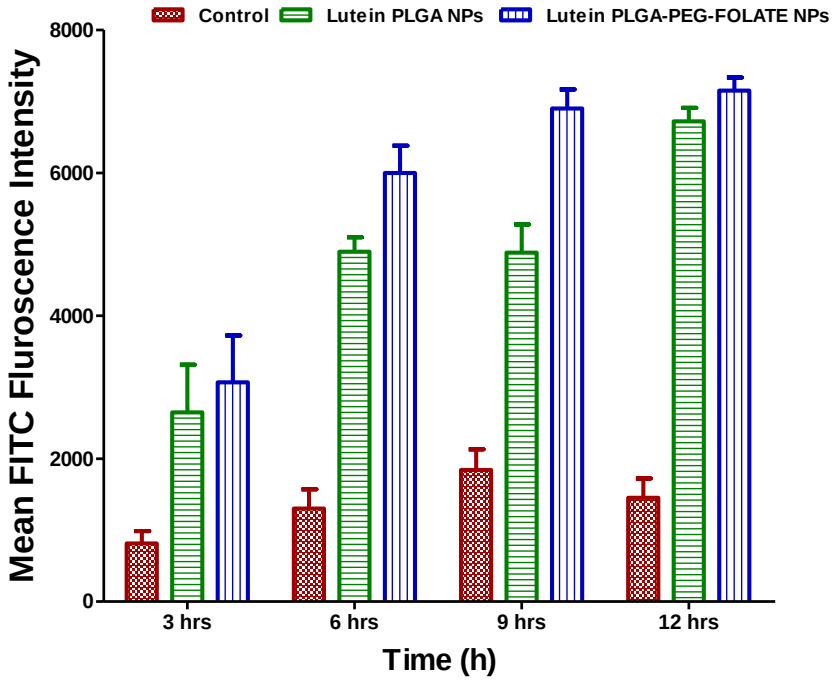

Figure 3.7: FACS analysis of lutein loaded polymeric nanoparticles (PLGA and PLGA-PEG-FOLATE) for 3-, 6-, 9-, and 12 hours. in SK-N-BE(2) cells. Data are represented as mean ± SEM.

Confocal microscopy

In vitro cellular uptake of FITC labelled lutein nanoparticles (PLGA and PLGA-PEG-FOLATE) and FITC labelled lutein was performed using confocal laser scanning microscopy for visual representation and qualitative analysis of lutein uptake by SK-N-BE(2) cells. The cells were incubated with the treatment groups for 6 and 12 hours. At the end of each time point the cells were washed, fixed, stained with DAPI and mounted on a slide for visualization by confocal laser scanning microscopy. Figure 3.8 and Figure 3.9 depicts the *in vitro* uptake of lutein nanoparticles (PLGA and PLGA-PEG-FOLATE) and FITC labelled lutein at 6 h and 12 h, respectively. It can be observed clearly that the fluorescence for FITC increases in all the treatment groups with time. It is also interesting to note that at all timepoints, the fluorescence in the cells treated with FITC-labelled lutein loaded polymeric nanoparticles (PLGA and PLGA-PEG-FOLATE) was higher than FITC- labelled lutein. These results are well corroborated with the results from the FACs analysis. This can imply that folate decorated lutein nanoparticles and lutein PLGA nanoparticles are well absorbed via the lipid bilayer of SK-N-BE(2) cells as compared to the free drug (lutein). Thus, the rate of internalization for lutein nanoparticles (PLGA and PLGA-PEG-FOLATE) into the cytoplasm and nuclei was higher than the drug alone. In addition, at 6-hour and 12- hour timepoints, a stronger fluorescence was observed with lutein loaded PLGA-PEG-FOLATE nanoparticles compared to lutein loaded PLGA nanoparticles. Thus, the results from confocal laser scanning microscopy analysis also confirm the greater uptake of lutein into the cells with lutein loaded PLGA-PEG-FOLATE nanoparticles through the folate receptor mediated endocytosis.

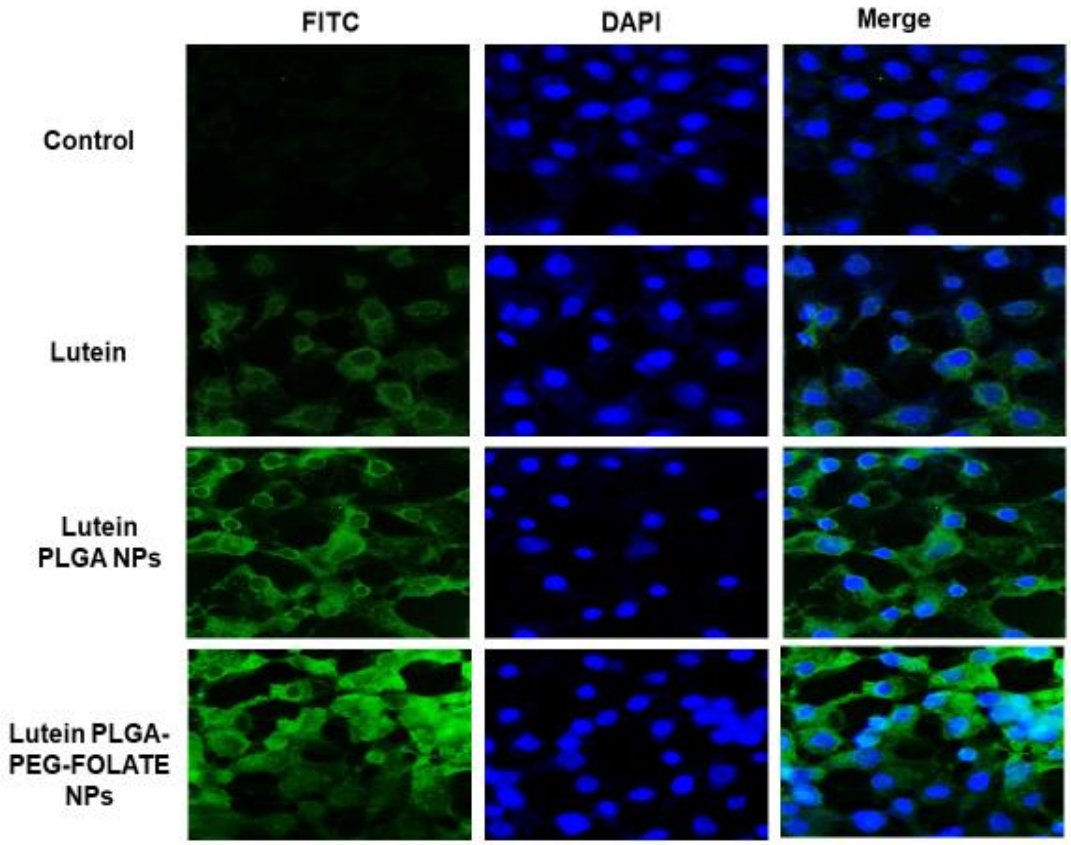

Figure 3.8: Confocal laser scanning microscopy images of FITC-labelled lutein and FITC-labelled lutein polymeric nanoparticles (PLGA and PLGA-PEG-FOLATE) at 6 hours in SK-N-BE(2) cells

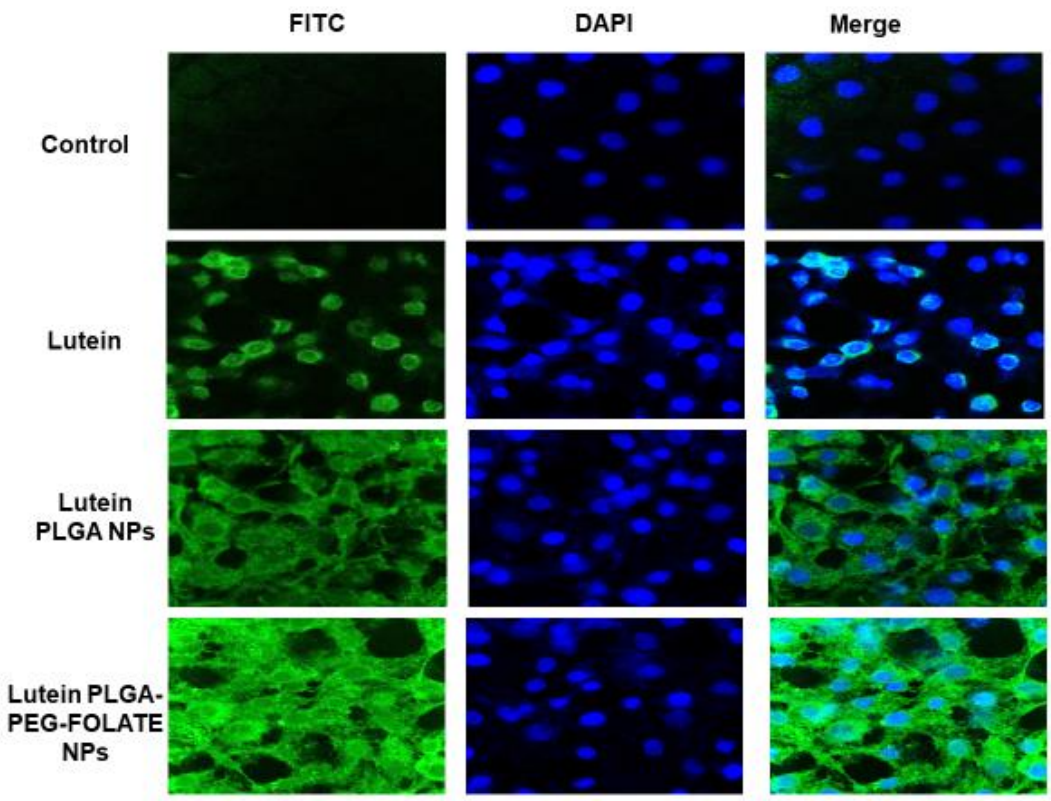

Figure 3.9: Confocal laser scanning microscopy images of FITC-labelled lutein and FITC-labelled lutein polymeric nanoparticles (PLGA and PLGA-PEG-FOLATE) at 12 hours in SK-N-BE(2) cells.

Cellular uptake studies using HPLC

In vitro cellular uptake studies were conducted to evaluate the enhanced uptake of lutein from folate decorated nanoparticles in neuroblastoma cells. Neuronal cells after terminal maturation cannot be propagated *in vitro*. Neuroblastoma cell lines have been extensively used to study various neuronal properties including drug uptake studies (Lashford, Hancock, and Kemshead 1991; Walton et al. 2004). Results revealed that there was a significant increase uptake of lutein with PLGA-PEG-FOLATE nanoparticles compared to PLGA nanoparticles and plain lutein ($p < 0.05$). There was ~1.6 fold and ~2-fold enhanced uptake of lutein from PLGA-PEG-

FOLATE nanoparticles compared with PLGA nanoparticles and plain lutein, respectively. The amount of lutein accumulated in the cells was 3.32 μg, 4.03 μg, and 6.5 μg for plain lutein, lutein loaded PLGA and PLGA-PEG-FOLATE nanoparticles, respectively (Figure 3.10). Thus, increased uptake of lutein was observed with folate decorated nanoparticles in neuroblastoma cells compared to plain lutein and lutein PLGA nanoparticles. Enhanced lutein uptake with PLGA-PEG-FOLATE polymer can be attributed to the hydrophilicity of folate at physiological conditions, which leads to receptor mediated uptake through folate receptors. Similar results of enhanced drug uptake were observed with folate decorated liposomes and PLGA nanoparticles loaded with doxorubicin and etoposide for brain tumors (Guo et al. 2017). We do know that lutein carried in lipoproteins (natural nanoparticles) cross blood - epithelial barriers (Thomas and Harrison 2016). Also, folate receptors are abundant in the blood brain barrier (BBB) (Wu and Pardridge 1999; Guo et al. 2017). It is also known that newborn babies tolerate lutein well and they naturally accumulate in the brain if supplemented (Vishwanathan et al. 2014). A synthetic biologic nanoparticle rich in lutein with capabilities to cross BBB and increase targeted delivery to brain during hypoxia-ischemia would be valuable. Another interesting prospect is in preterm newborn brain injury which is predominant and where lutein transport mechanisms are less effective (Costa et al. 2013; Giampietri et al. 2016).

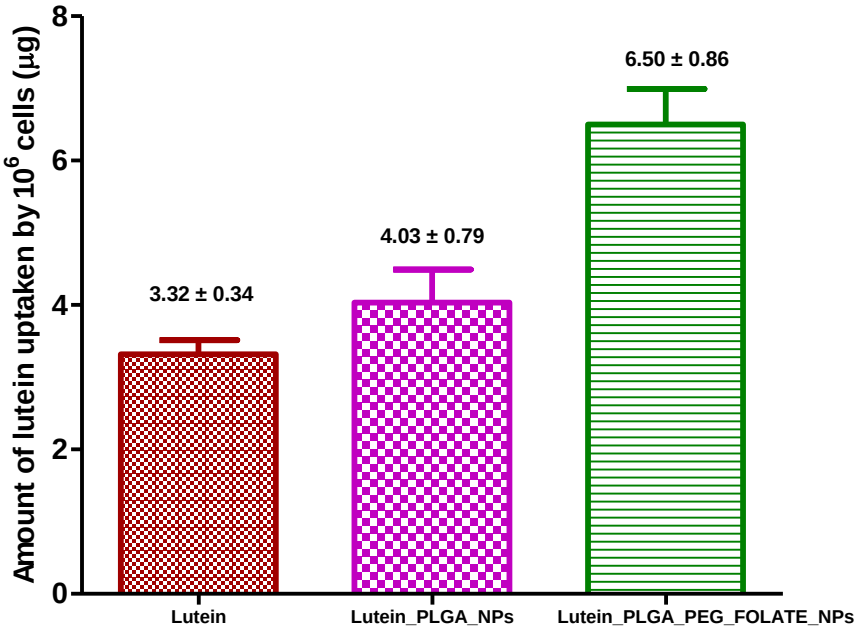

Figure 3.10: *In vitro* cellular uptake of lutein using plain lutein, lutein PLGA nanoparticles and lutein PLGA-PEG-FOLATE nanoparticles in SK-N-BE(2) cells.

Physical stability studies

Lutein loaded polymeric nanoparticles were evaluated for physical stability for 60 days stored at 4 °C and 25 °C. The effects of storage on the particle diameter, PDI and ZP of lutein loaded polymeric nanoparticles is provided in Table 3.2. Results revealed that there was no significant change in the particle diameter, PDI and ZP of lutein loaded nanoparticles from day 1 to days 30 and 60 with both the polymers at 4 °C and 25 °C ($p > 0.05$) (Figure 3.11). Similarly, there was a no signs of aggregation of nanoparticles. Physical stability results confirmed that lutein loaded PLGA-PEG-FOLATE nanoparticles were stable at 4 °C and 25 °C over the period of 60 days.

Table 3.2: Effect of storage on PDI and ZP of lutein polymeric nanoparticles at 4 °C and 25 °C.

	PDI				ZP (mV)			
Time (Days)	**Lutein PLGA**		**Lutein PLGA-PEG-FOLATE**		**Time (Days)**		**Lutein PLGA**	
	4 °C	25 °C	4 °C	25 °C	4 °C	25 °C	4 °C	25 °C
1	0.083 ± 0.023	0.104 ± 0.056	0.202 ± 0.009	0.202 ± 0.009	-10.7 ± 1.80	-10.7 ± 1.80	-26.0 ± 1.27	-26.0 ± 1.27
30	0.112 ± 0.043	0.063 ± 0.04	0.202 ± 0.013	0.148 ± 0.123	-9.16 ± 2.09	-13.8 ± 1.93	-24.5 ± 2.50	-31.7 ± 7.70
60	0.053 ± 0.021	0.113 ± 0.046	0.190 ± 0.027	0.394 ± 0.068	-12.7 ± 0.73	-12.5 ± 2.22	-21.3 ± 1.10	-22.7 ± 2.69

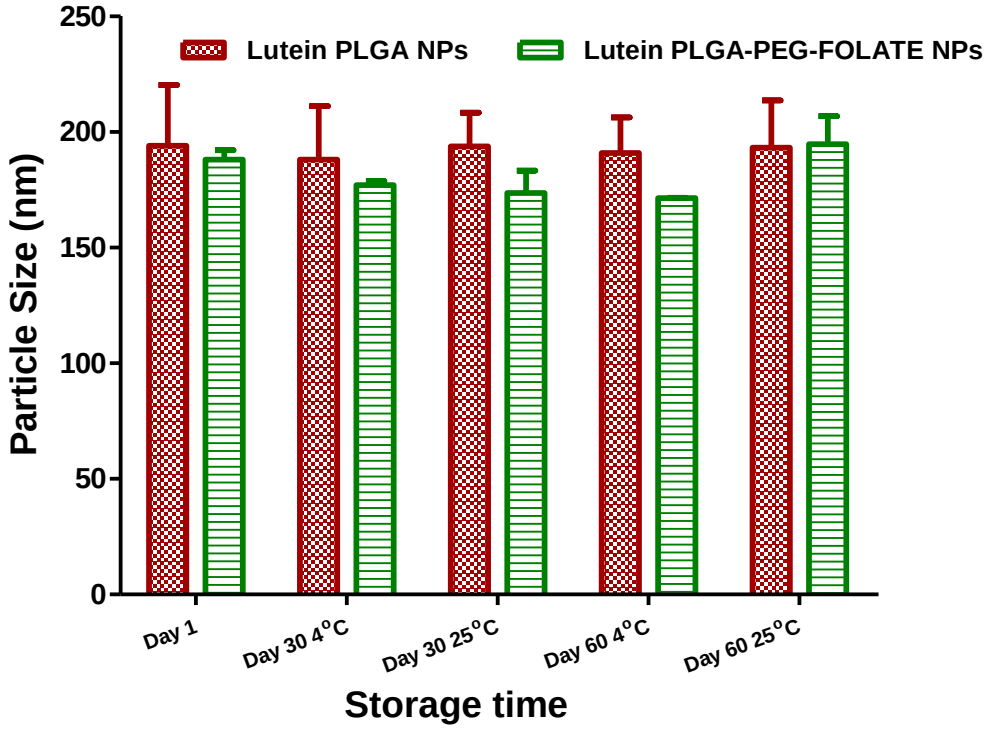

Figure 3.11: Effect of storage on particle diameter of lutein loaded polymeric nanoparticles at 4 °C and 25 °C

Conclusions

Encapsulation of hydrophobic drugs into polymeric nanoparticles can significantly enhance the bioavailability and release the drugs in sustained manner. In this study, lutein was successfully encapsulated into PLGA-PEG-FOLATE nanoparticles and significantly enhanced the lutein uptake in neuroblastoma cells. There was ~1.6 fold and ~2-fold enhanced uptake of lutein from PLGA-PEG-FOLATE nanoparticles compared with PLGA and lutein alone. Confocal microscopy and flow cytometry analysis also confirmed the enhanced uptake of lutein with lutein loaded PLGA-PEG-FOLATE nanoparticles. Size of lutein loaded PLGA-PEG-FOLATE nanoparticles was <200 nm with high %EE of >70%. SEM results confirmed the spherical surface morphology of the nanoparticles. Sustained release of lutein from nanoparticles was confirmed by *in vitro* release studies. Stability studies confirmed that there was no sign of NP aggregation within 60 days at 4 °C and 25 °C. Findings from this study confirmed the enhanced uptake of lutein from PLGA-PEG-FOLATE nanoparticles in neuroblastoma cells. However, these results are preliminary and enhanced uptake and neuroprotective properties of lutein from PLGA-PEG-FOLATE nanoparticles will be confirmed in rat model of HIE.

Future studies

In this dissertation project, I have successfully prepared and characterized lutein loaded folate decorated polymeric nanoparticles for enhancing the bioavailability of lutein in brain. Enhancement of lutein uptake in brain cells could result in effective treatment of HIE. Future studies include: (1) Investigation of neuroprotective effects of lutein loaded PLGA-PEG-FOL nanoparticles in neonatal HIE rat model (2) Evaluation of pharmacokinetics and tissue distribution of lutein loaded PLGA-PEG-FOL nanoparticles *in vivo*.

Chapter 4: Preparation of Solid Lipid Nanoparticles of Furosemide-Silver Complex and Evaluation of Antibacterial Activity

Graphical abstract

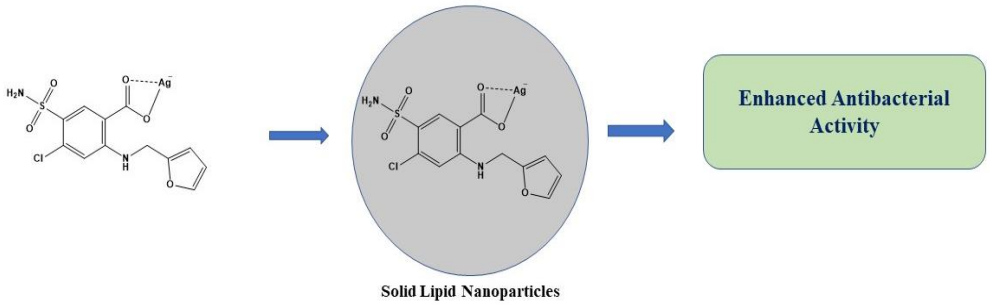

Illustration 4.1: Solid lipid nanoparticles of furosemide silver complex

Introduction

Antibiotics also referred to as “wonder drugs” have transformed the field of medicine by effectively treating microbial infections. They act mainly by inhibition of several important cellular processes such as cell wall and protein synthesis, and ultimately leading to bacterial cell death (Davies and Davies 2010; Richardson 2017). However, antibiotic resistance is one of the major challenges faced by the pharmaceutical and healthcare industries worldwide. Development of resistance can limit the efficacy of antibiotics (Ventola 2015b). Resistance to antibiotics can be developed by several biochemical, physiological and genetic mechanisms such as the development of efflux pumps, genetic mutations, inhibition of drug uptake, and alteration of drug target, etc. (Davies and Davies 2010). According to Center for Disease Control (CDC), the annual incidence of resistant infections is about 2 million and among these 23,000 patients die due to these infections. Economic burden due to antibiotic resistance on US healthcare system alone is 20 billion dollars in direct costs and 35 billion dollars in indirect costs, annually (Centers for

Disease Control and Prevention 2013). Overuse and misuse of antibiotics in clinics and poor new antibiotic pipeline in pharmaceutical industries have contributed to the current antibiotic crisis (Ventola 2015a; Centers for Disease Control and Prevention 2013). There has been a significant decline in the approval of new antibiotics by Food and Drug Administration (FDA) over the past three decades (Ventola 2015a; Spellberg et al. 2008). CDC has developed four core actions to combat antibiotic resistance which include i) prevention of infections and spread of resistance to micro-organisms, ii) tracking resistant bacteria, iii) improving the antibiotic use and iv) development of novel antibiotics and diagnostic tools (Ventola 2015b; Centers for Disease Control and Prevention 2013). Therefore, there is a need for the synthesis of new antibiotics with enhanced antibacterial activity and with novel mechanisms of action (Spellberg et al. 2008). Although, there have been attempts to develop novel antibiotics, regulatory barriers to their approval have limited their availability in the market (Ventola 2015b).

Historically, metal complexes of several drugs have been reported as antimicrobial agents and among these silver complexes have been most common ones. For example, silver sulfadiazine has been used in the clinics as a prophylactic and treatment for bacterial infections associated with skin burns (Rai, Yadav, and Gade 2009; Kalhapure et al. 2015; Marambio-Jones and Hoek 2010). Also, silver complexes of metronidazole (Kalinowska-Lis et al. 2015), nimesulide (de Paiva et al. 2012) and clotrimazole (Kalhapure et al. 2015) have been reported as antimicrobial agents. Silver complexes could be effective as broad-spectrum antibiotics due to their chemical nature. Moreover, due to multiple mechanisms of action of silver, development of bacterial resistance to silver complexes is difficult (Prabhu and Poulose 2012).

Lustri et. al., synthesized a novel antimicrobial, silver complex of furosemide (Ag-FSE), which was reported to have antibacterial properties against *Escherichia coli* (*E. coli*),

Staphylococcus aureus (*S. aureus*), and *Pseudomonas aeruginosa* (*P. aeruginosa*). However, its poor solubility in water and majority of organic solvents could limit its antibacterial activity (Lustri et al. 2017). Recently, there has been a report on formulation of nanosuspension of Ag-FSE, which resulted in significant enhancement of solubility and antibacterial activity (Renukuntla 2018b). Other approaches to enhance solubility of poorly water-soluble drugs include nanonization techniques such as the formulation of nano-emulsions, solid lipid nanoparticles (SLNs), liposomes and polymeric micelles (H. Chen et al. 2011; Khadka et al. 2014). Goal of this project was to encapsulate Ag-FSE into SLNs for achieving controlled and sustained drug release over a period of time.

SLNs are colloidal nanosized drug carrier systems (50 nm to 1000 nm in diameter) with matrix structure to encapsulate drugs. They are prepared from lipids which are solid at room and body temperature, and are stabilized using surfactants (Wissing, Kayser, and Muller 2004; Geszke-Moritz and Moritz 2016; Khadka et al. 2014). Compared to other formulations, SLNs offer advantages such as controlled and sustained drug release, enhanced drug solubility and stability, high drug payload, scale-up and, biocompatibility (Ghaffari et al. 2011; Hou et al. 2003; Potta et al. 2010). Researchers were successful in preparation of SLNs for improving solubility, drug loading and antimicrobial activity of drugs such as tretinoin (Ridolfi et al. 2012), ofloxacin (Xie et al. 2011), cortisone (Westesen, Bunjes, and Koch 1997), tilmicosin (Wang et al. 2012), nisin (Prombutara et al. 2012), vancomycin (Kalhapure et al. 2014), and amikacin (Ghaffari et al. 2011). Also, it was reported that encapsulation of clotrimazole silver complex into SLNs resulted in enhanced antibacterial activity against methicillin resistant *S. aureus* (MRSA) and *S. aureus* (Kalhapure et al. 2015). Therefore, the present study aims to encapsulate Ag-FSE into SLNs and evaluate its sustained and enhanced antibacterial activity.

Materials and Methods

Materials

Furosemide was purchased from Acros Organics (New Jersey, USA). Silver nitrate ($AgNO_3$), potassium hydroxide (KOH), dimethyl sulfoxide (DMSO), and Buffer salt packets were obtained from Fisher Scientific (Fair Lawn, NJ, USA). Kolliphor® RH 40 (RH 40), Kolliphor® HS 15 (SHS 15), and Tween® 80 (Tween 80) were procured from Sigma Aldrich (St. Louis, MO, USA). Powdered sucrose NF was obtained from PCCA (Houston, Texas, USA). Deionized water (resistivity of 18.2 MΩ) used for all experiments was obtained from in-house Milli-Q® IQ 7000 Ultrapure Water System (EMD Millipore, Bedford, MA, USA). Glycerol monostearate (GMS) and Poloxamer 188 were obtained from Alfa Aesar (Ward Hill, MA, USA). Bacterial strains were obtained from the American Type Culture Collection (ATCC). Muller-Hinton Broth (MHB) (CM0405) for bacterial cultures was obtained from Oxoid Microbiology Products, USA. Sterile microtiter plates were purchased from Fisher Scientific (Fair Lawn, NJ, USA).

Methods

Synthesis of Furosemide Silver Complex (Ag-FSE)

Furosemide silver complex was synthesized using a previously reported method (Illustration 4.2) (Renukuntla 2018b; Lustri et al. 2017). Briefly, aqueous solution (2 mL) of $AgNO_3$ (2.13 mM, 0.362 g) was added dropwise to methanolic solution of furosemide (0.704 g, 2.13 mM) (20 mL) and KOH (0.119 g, 2.13 mM) under stirring at 500 rpm on magnetic stirrer. The reaction mixture was subjected to continuous stirring (500 rpm) at room temperature for 2h. After 2h, the white precipitate was obtained by filtration, washed three times with cold water and dried in vacuum desiccator for 24 hours at room temperature.

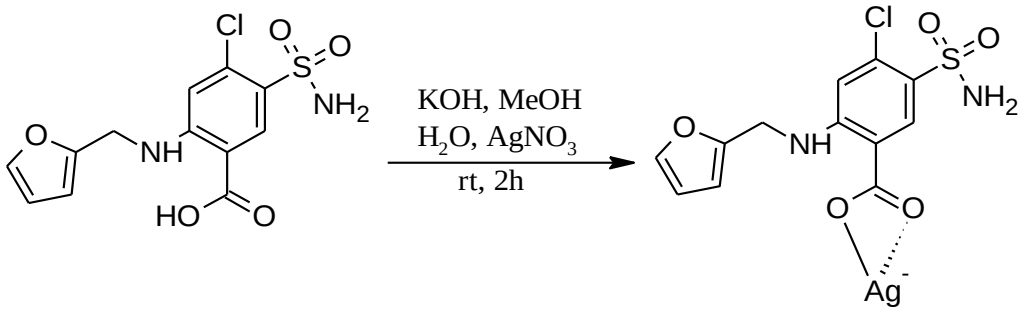

Illustration 4.2: Synthesis of Ag-FSE complex

Preparation of SLNs

SLNs were prepared using hot homogenization and ultrasonication technique described in the literature with slight modifications (Kalhapure et al. 2015). SLNs were prepared using GMS as the lipid matrix. GMS has been reported previously in the preparation of SLNs for controlled drug delivery (Mhango et al. 2017). Structurally, GMS is a fatty acid with a glycerol backbone and amphiphilic properties. Due to amphiphilic properties, GMS can self-assemble in both oil and water phases into various types of mesophases and stabilize emulsion systems. GMS is widely used as emulsifier in pharmaceutical and cosmetic industries (Talele, Sahu, and Mishra 2018). Moreover, GMS is biocompatible and biodegradable lipid with low melting point and high lipophilicity making it safe for biological applications (Mhango et al. 2017). Various surfactants (RH 40, SHS 15, Tween 80, and Poloxamer 188) at 1% concentration were screened during preliminary studies to obtain SLNs with minimum particle size and poly dispersity index (PDI). Based on these size results, surfactant was selected and other parameters such as surfactant concentration, homogenization and sonication time were evaluated to obtain optimized SLNs. All experiments were performed in three batches (n=3). In brief, GMS (200 mg) and Ag-FSE (20 mg) were heated at 80 ± 2 °C in a hot water bath. To the lipid and drug mixture Poloxamer 188 solution (1% w/v; 20 mL) heated separately at same temperature was added. This mixture was

homogenized at 5000 rpm using Fisherbrand™ 850 homogenizer for 5 minutes and immediately sonicated at 20% amplitude for 10 minutes with a probe sonicator (Fisher Scientific™ Model 505 Sonic Dismembrator). After sonication, emulsion was suddenly cooled to 20 °C in an ice bath. Blank SLNs were prepared by same method and same conditions without Ag-FSE. SLNs were freeze dried using powdered sucrose as a cryoprotectant. To freshly formulated Ag-FSE SLNs, sucrose dissolved in milli-Q water was added and the mixture was subjected to freeze drying using Freezone freeze dryer (Labconco, USA) for 24 hours.

Determination of size, poly dispersity index (PDI) and ZP

The size, PDI, and ZP of the SLNs were measured using DLS technique. SLNs (200 µL) were dispersed in 10 mL of deionized water and measurements were obtained using Malvern Zetasizer Nano ZS90 at 25 °C.

Encapsulation efficiency (EE%) and drug loading (DL%)

EE% of the SLNs was determined by ultrafiltration method (Kalhapure et al. 2015) using centrifugal filter tubes with a molecular weight cut-off of 10 kDa (MWCO 10 kDa). Ag-FSE SLN dispersion (500 µL) was transferred into centrifugal filter tubes and centrifuged at 10,000 rpm for 30 minutes at 20 °C. EE% was calculated by measuring the unencapsulated Ag-FSE in the filtrate and compared it with the total amount of drug added in the formulation. 300 µL of the filtrate was diluted to 3 mL with deionized water. Unencapsulated Ag-FSE was quantified by measuring absorbance at λ_{max} 277 nm using UV-visible spectrophotometer (Shimadzu, Kyoto, Japan) (Gulsun et al. 2018). The regression equation used for calculations was y = 0.0486x + 0.0135 with a linearity of 0.9995. All the determinations were performed in three batches (n=3). EE% and DL% were calculated using the following formulae (Kalhapure and Akamanchi 2013).

$$\text{Encapsulation efficiency (EE\%)} = (\text{Weight}_{\text{initialdrug}} - \text{Weight}_{\text{freedrug}})/(\text{Weight}_{\text{initialdrug}}) \times 100$$

Drug loading (%) = $(Weight_{initialdrug} - Weight_{freedrug})/(Weight_{lipid}) \times 100$

Where $Weight_{initialdrug}$ is the weight of the Ag-FSE used, $Weight_{freedrug}$ was the weight of unencapsulated Ag-FSE in the formulation and $Weight_{lipid}$ was the weight of the lipid used in the formulation.

SEM

Scanning electron microscope (Hitachi S- 4800 High Resolution Scanning Electron Microscope) was used to determine the surface morphology of Ag-FSE SLNs. Lyophilized SLNs were attached to a double-sided conductive tape on a stainless-steel stub and the SEM images were visualized at an accelerating voltage of 2kV.

XRD analysis

XRD analysis was performed using PANanlytical's X-ray diffractometer (PANanlytical's X'pert Pro Tokyo, Japan) equipped with X'Celerator high speed detector. XRD studies were performed for Poloxamer 188, GMS, Ag-FSE SLN and Ag-FSE. Powdered samples were placed on an aluminum sample holder and uniformly packed using a glass slide. Radiation source was CuKα operated at 45 kV and 40 mA. All measurements were recorded with a continuous scanning mode over a 2θ range of 5° to 70°.

DSC

DSC is the most frequently used technique to study recrystallization and melting properties of any material/formulation (Kalhapure and Akamanchi 2013). DSC was performed using DSC Q20 instrument with TA universal analysis software to obtain scans. Samples (5-10 mg) were weighed using microbalance and placed in aluminum pans and sealed. DSC analysis was

performed at a heating rate of 10 °C/minute over a range of 40 °C to 300 °C with a nitrogen flow of 20 mL/min.

In vitro release studies

Drug release behavior from Ag-FSE SLNs and free drug (Ag-FSE) in phosphate buffer saline (PBS) (pH 7.4) was evaluated using dialysis bag method (MW 8000 – 14,400 Da) (Mhango et al. 2017). In brief, 1 mL Ag-FSE SLNs, Blank SLNs and Ag-FSE in PBS were transferred into separate dialysis bags and 1 mL PBS was added to each tubing. Tubing's were tied at both ends to prevent any leakage. Dialysis tubing's loaded with Ag-FSE SLNs, Blank SLNs, and Ag-FSE were kept in conical tubes (50 mL capacity) containing 30 mL of PBS as release medium maintained at 37 ± 0.5 °C in a shaking water bath (100 rpm). 3 mL of the samples were collected from each conical tubes at pre-determined time-intervals. Samples were replaced with 3 mL of fresh PBS to maintain sink conditions. The pre-determined time intervals were 0.5, 1, 2, 3, 4, 5, 6, 7, 8, 24, 48, 72, and 96 h. The amount of drug released from the formulations at different timepoints was quantified using a UV-visible spectrophotometer (Shimadzu, Japan) at λmax of 277 nm using the regression equation provided in earlier sections. All the experiments were performed in triplicate.

Physical stability Studies

Physical stability studies were conducted for the freeze-dried Ag-FSE SLNs at room temperature (RT) and 4 °C for 60 days. All samples were stored in sealed glass scintillation vials at RT and 4 °C for 60 days. Freeze dried Ag-FSE SLNs were re-dispersed in milli-Q water, sonicated for 2 minutes and evaluated for size, PDI, ZP at days 1, 30 and 60.

In vitro anti-bacterial activity

Antibacterial activities of free Ag-FSE and Ag-FSE SLNs were evaluated using broth microdilution against *E. coli* (ATCC25922), *S. aureus* (ATCC25923) and *P. aeruginosa*

(ATCC27853) (Mhango et al. 2017). In brief, bacterial cultures were grown overnight in MHB at 37 °C in an incubator. After incubation, cell density of the bacterial cultures were adjusted to 0.5 Mcfarland. Each well of the 96-well microtiter plate was dispensed with 100 µL of the adjusted bacterial cell suspension. Immediately after dispensing, Ag-FSE SLNs, Ag-FSE in 10% w/v DMSO, Blank SLNs and MHB were serially diluted in each well so that the final volume of each well was maintained at 100 µL. The 96-well microtiter plates were incubated at 37 °C for 18 h and the minimum inhibitory concentration (MIC) was assessed as the concentration at which no bacterial growth was observed. Blank SLNs and MHB and 10% DMSO were used as controls. All the experiments were performed in triplicate (n=3).

Statistical analysis

Data are expressed as the mean ± standard deviation (SD). Statistical analysis was performed using GraphPad Prism® (Version 5.0, San Diego, CA). T-test followed by Bonferroni's multiple comparison test was used for optimizing the blank SLN formulations. A two-way ANOVA followed by Bonferroni posttest was applied for stability studies. A p value <0.05 was considered as statistically significant.

Results and Discussion

Optimization of blank SLNs

Screening of surfactants

The experiments were aimed to obtain blank SLNs with particle sizes < 200 nm. SHS 15, RH 40, Tween 80 and Poloxamer 188 at 1% concentration were screened initially with 5 minutes homogenization (5000 rpm) and 5 minutes sonication at 20% amplitude. Size, PDI and ZP for these formulations are provided in Table 4.1. Blank SLNs with sizes < 200 nm were obtained with

Tween 80 (113.4 ± 9.03 nm) and Poloxamer 188 (177.2 ± 3.99). However, SLNs prepared using Tween 80 were aggregated with particle size increasing up to 6.79 ± 3.88 µm. Therefore, Poloxamer 188 was chosen as the stabilizer for preparation of Ag-FSE loaded SLNs.

Table 4.1: Effect of surfactants (1% w/v) on size, PDI, and ZP of blank SLNs (5 minutes homogenization and 5 minutes sonication) Data are represented as mean ± SD (n=3)

S.no	Surfactant	Size (nm)	PDI	ZP (mV)
1	SHS 15	356.4 ± 53.88	0.586 ± 0.12	-12.7 ± 2.64
2	RH 40	352.9 ± 158.40	0.489 ± 0.23	-17.0 ± 4.00
3	Tween 80	113.4 ± 09.03	0.401 ± 0.09	-18.3 ± 5.71
4	Poloxamer 188	177.2 ± 03.99	0.145 ± 0.04	-16.9 ± 1.38

Effect of surfactant concentration on particle size, PDI and ZP

Based on initial experiments, Poloxamer 188 was chosen as the stabilizer for preparation of SLNs. Poloxamer 188 is a di-functional triblock copolymer surfactant with amphiphilic properties and soluble in water and organic solvents. It is composed of a hydrophobic block sandwiched between two hydrophilic polymer blocks. This unique structure of the surfactant helps in coating the hydrophobic nanoparticles effectively and stabilize the system by inducing stealth properties. Moreover, Poloxamer 188 has the ability to integrate into the membranes of the cells and affect various cellular functions (Pradhan, Singh, and Singh 2015; X. Chen et al. 2013; Pandya et al. 2018). Due to these properties, Poloxamer 188 has been used as a stabilizer for SLN formulations in various reports (W. Zhang et al. 2008; Müller, Mäder, and Gohla 2000; Allotey-Babington et al. 2018; Y. Zhang et al. 2010). Increase in the concentration of Poloxamer 188 did not have any significant effect on the particle size of blank SLNs (Figure 4.1). Therefore, 1%

Poloxamer 188 was considered as the optimum concentration for the formulation of Ag-FSE SLNs to limit any cytotoxicity associated with the use of surfactants (Kalhapure et al. 2014).

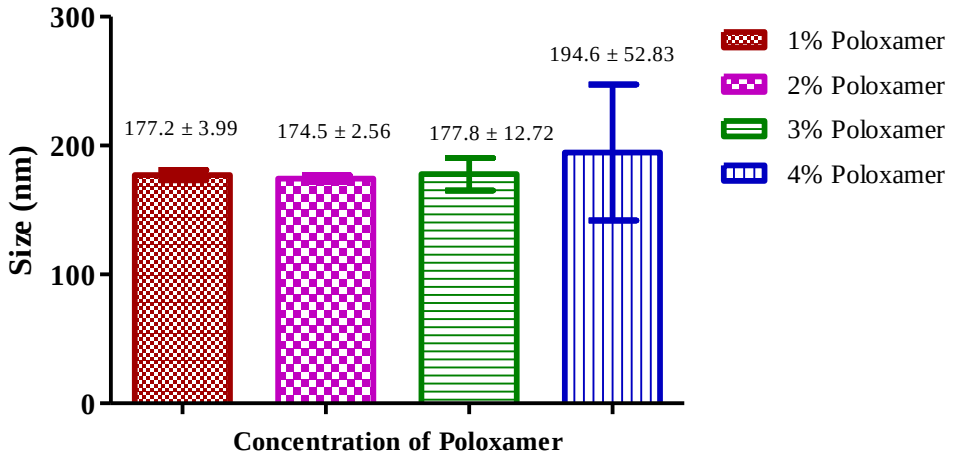

Figure 4.1: Effect of Poloxamer 188 concentration on particle size of blank SLNs. Data are represented as mean ± SD (n=3)

Effect of homogenization and sonication time on particle size, PDI and ZP

The effect of sonication and homogenization time on particle size, PDI, and ZP of blank SLNs is provided in Table 4.2. Based on the results, 5 minutes homogenization and 10 minutes sonication were considered as the optimum conditions for the formulation of Ag-FSE SLNs as those conditions gave SLNs with smaller particle size and PDI.

Table 4.2: Effect of sonication and homogenization time on the particle size, PDI and ZP of blank SLNs (1% Poloxamer 188). All the data are represented as mean ± SD (n=3).

S.no	Sonication time	Homogenization time	Size (nm)	PDI	ZP (mV)
1	5 min	5 min	177.2 ± 3.99	0.145 ± 0.04	-16.9 ± 1.38
2	10 min	5 min	162.5 ± 2.53	0.144 ± 0.03	-17.9 ± 1.56

3	20 min	5 min	166.8 ± 4.64	0.163 ± 0.013	-2.11 ± 3.10
4	10 min	10 min	179.2 ± 9.29	0.153 ± 0.03	-0.28 ± 0.65
5	10 min	20 min	184.9 ± 4.39	0.159 ± 0.03	-0.2 ± 0.88

Preparation of Ag-FSE SLNs

Based on the preliminary results, Poloxamer 188 1%, 5 minutes homogenization and 10 minutes sonication were considered as the optimum conditions for the formulation of Ag-FSE SLNs as those conditions gave SLNs with smaller particle size and PDI. The particle size, PDI and ZP of the optimized Ag-FSE SLNs were 129.8 ± 38.5 nm, 0.114 ± 0.033 and -23.9 ± 3.62 mV, respectively. Particle size for pure Ag-FSE dispersed in water was 1.42 ± 0.04 µm. Encapsulation of Ag-FSE into SLNs reduced the particle size significantly ($p < 0.05$). Mean particle size and ZP distribution curve are represented by Figure 4.2 and Figure 4.3, respectively. These curves represent the monodisperse nature of the formulation.

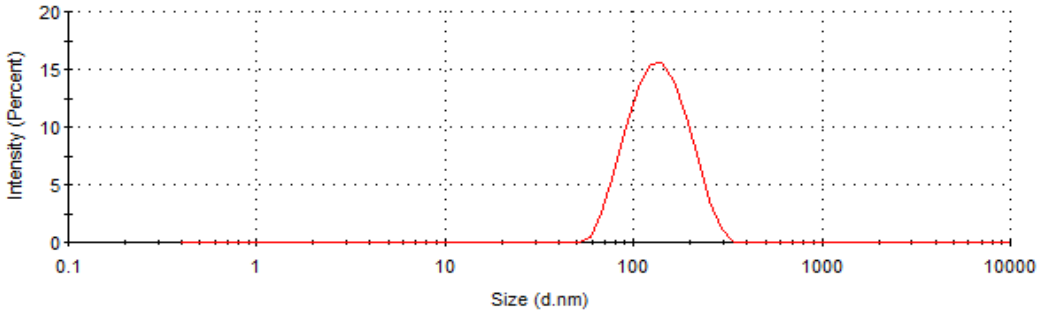

Figure 4.2: Size distribution curve of Ag-FSE SLNs

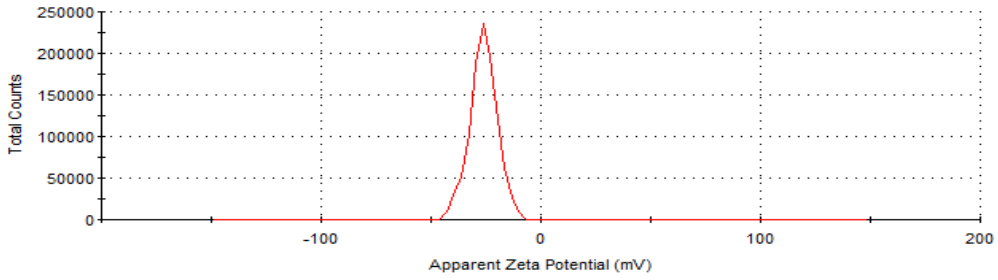

Figure 4.3: ZP distribution curve of Ag-FSE SLNs

Determination of EE% and DL%

Ag-FSE SLNs exhibited high EE% and DL%. EE% and DL% for Ag-FSE SLNs were 93.49 ± 0.391 and 9.35 ± 0.039, respectively. High encapsulation of Ag-FSE in the SLNs can be attributed to the drug-enriched core model of encapsulation. Drug distribution model in the SLNs can be explained with the differences in the melting points of drug used and lipids (Müller, Mäder, and Gohla 2000; X. Chen et al. 2013). Ag-FSE has higher melting point than GMS. When the formed SLNs were cooled, the solid Ag-FSE formed the core of the SLN and the liquid GMS and Poloxamer 188 were adsorbed on the surface of the core. Therefore, the Ag-FSE incorporation model was the core-shell model, drug enriched core. Similar type of encapsulation model has been reported for astragaloside loaded SLNs (X. Chen et al. 2013; Matougui et al. 2016). The unencapsulated Ag-FSE (~6.5%) could have formed nanocrystals during homogenization and ultrasonication process due to the stealth effect of Poloxamer 188.

SEM

SEM images of lyophilized Ag-FSE SLNs are shown in Figure 4.4. Morphology of the SLNs from the SEM images showed that the Ag-FSE SLNs were roughly spherical in shape with smooth surface (Figure 4.4). Aggregation was also noted in some images and could have occurred during lyophilization process.

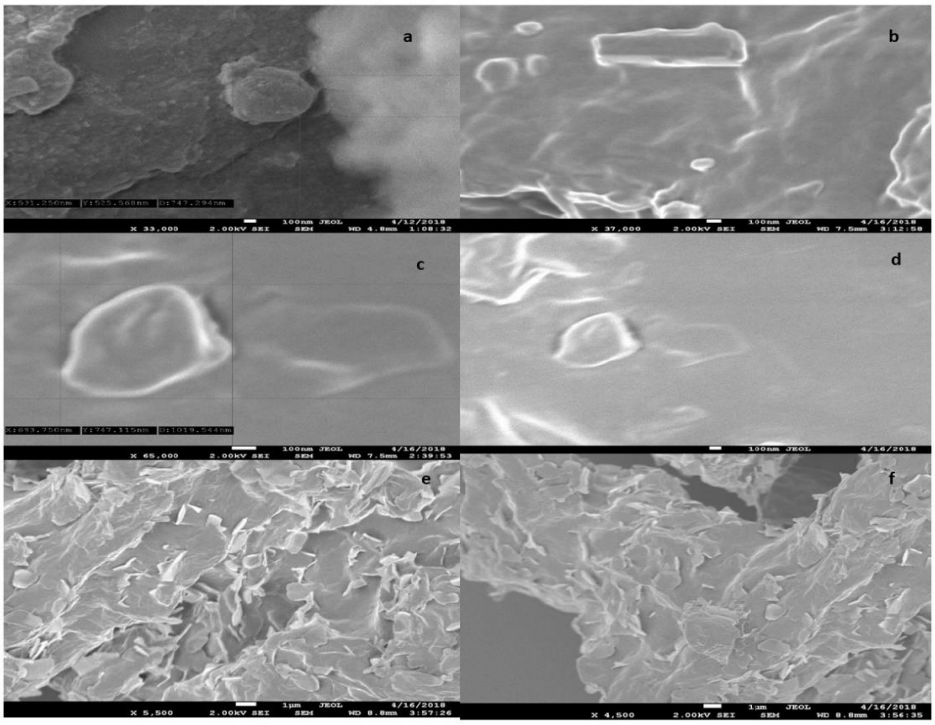

Figure 4.4: SEM images of Ag-FSE SLNs. Scale bars are (a-d) 100 nm (e-f) 1 µm

XRD analysis

Crystalline nature of drug molecules determines the important properties such as solubility, bioavailability, rate of dissolution, and stability (Kalhapure and Akamanchi 2013). XRD studies were used to confirm the crystalline nature of Ag-FSE, Ag-FSE SLNs and other excipients used in the formulation of SLNs. XRD results are provided in Figure 4.5 show that Ag-FSE exhibited crystalline nature with characteristic peaks at 6.18°, 10.28°, 18.48°, 25.92°, and 32.8°. However, the encapsulation of Ag-FSE into SLNs resulted in disappearance of these peaks confirming loss of crystallinity (Figure 4.5). Encapsulation of Ag-FSE into SLNs resulted in its transition from crystalline to amorphous form. Similar findings were observed with other SLN formulations (Kalhapure and Akamanchi 2013).

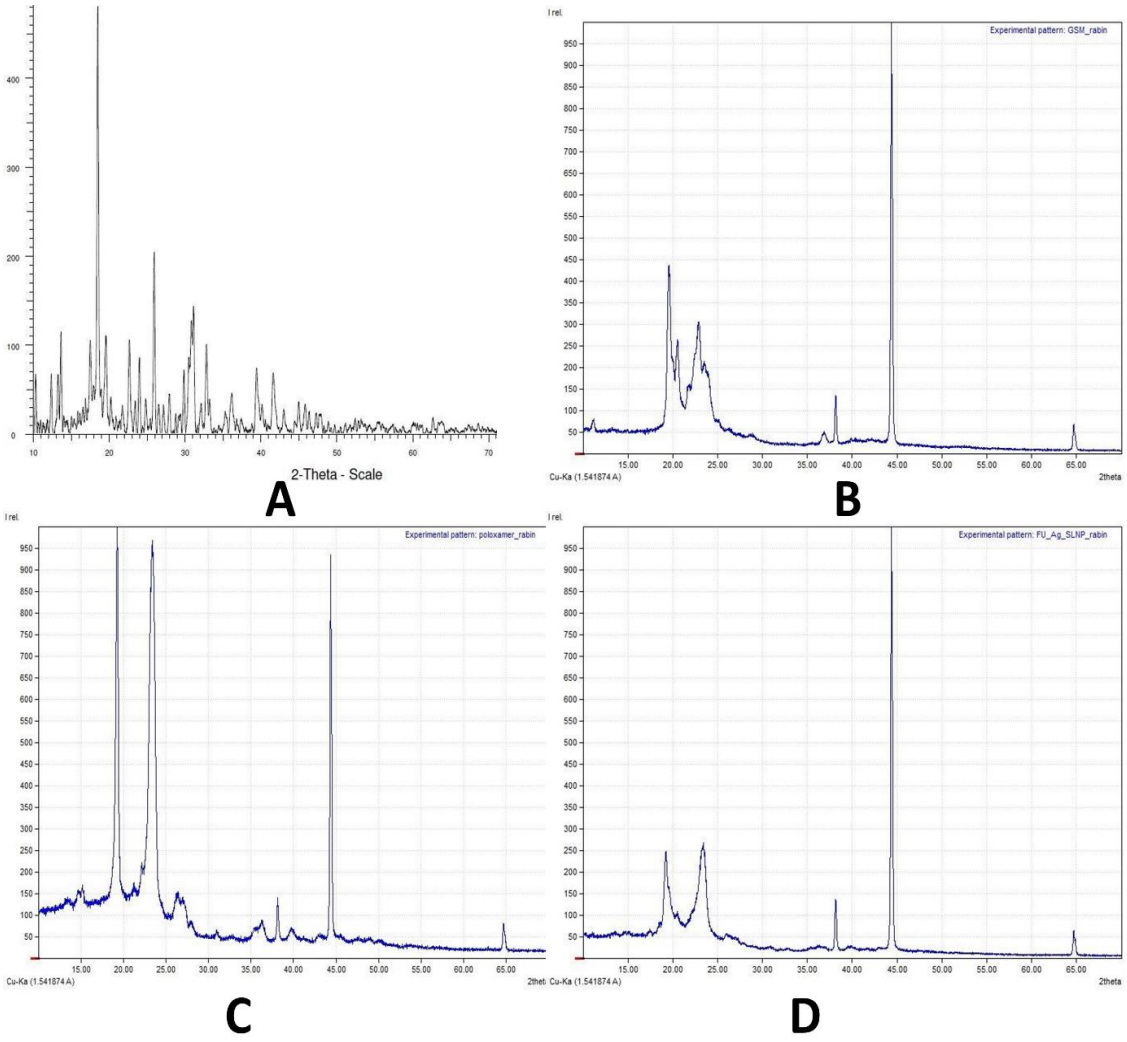

Figure 4.5: XRD of (A) Ag-FSE, (B) GMS, (C) Poloxamer 188, and (D) Ag-FSE SLN

DSC

Melting and crystalline behavior of all the materials used in the preparation of SLNs were evaluated by DSC. Ag-FSE showed a sharp exothermic peak at 211.69 °C (Figure 4.6A). GMS, and Poloxamer 188 showed sharp endothermic peaks at 74.47 °C, and 57.61 °C, respectively (Figure 4.6B and 4.6C). Absence of characteristic peak for Ag-FSE at 211.69 °C (Figure 4.6D) in the lyophilized Ag-FSE SLN confirms that the Ag-FSE was successfully encapsulated in the SLNs transforming into amorphous form from crystalline form. Compared to crystalline form, amorphous form of drug is characterized with higher solubilities and dissolution resulting in

increased bioavailability (Morissette et al. 2004). Also, a sharp endothermic peak of GMS at 74.47 °C disappeared in the Ag-FSE SLN and two new endothermic peaks were observed at lower temperatures of 54.86 °C and 68.60 °C (Figure 4.6D). Overall, DSC results complemented the XRD results.

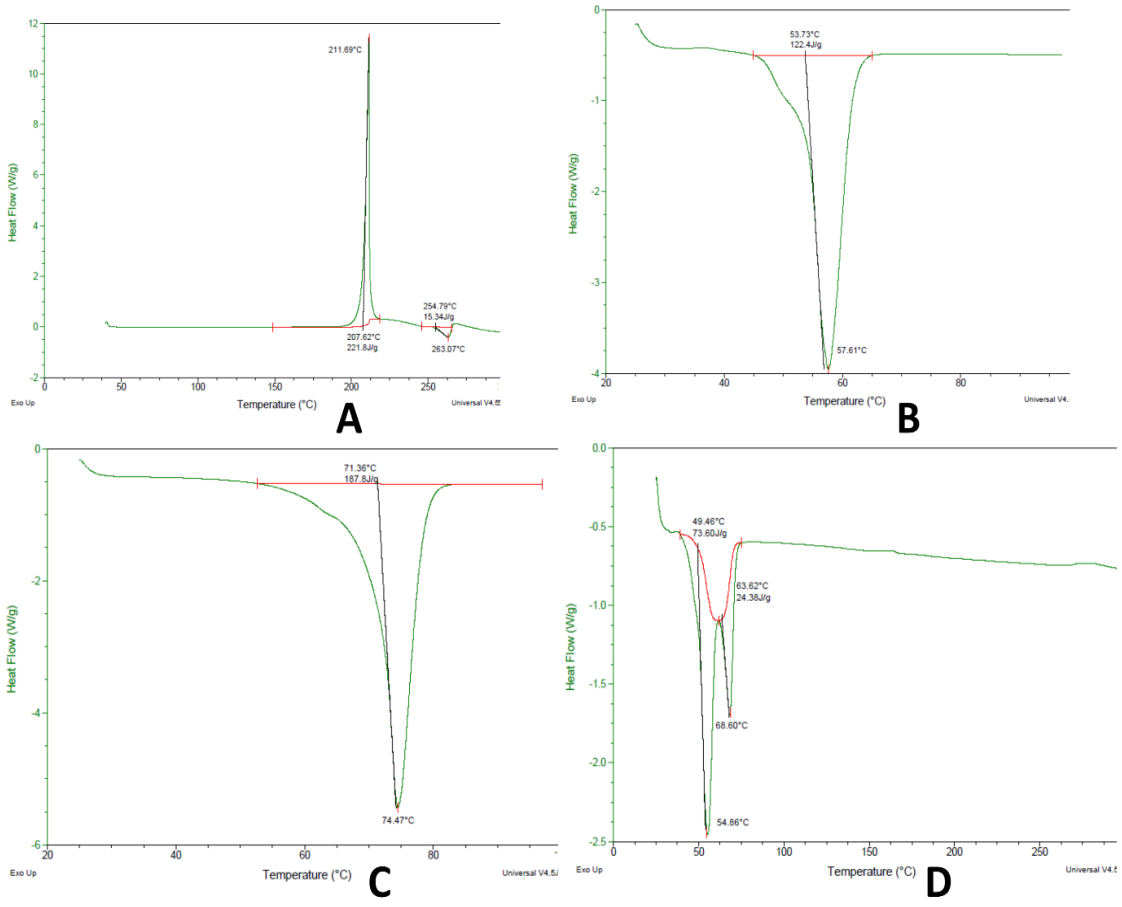

Figure 4.6: DSC of (A) Ag-FSE, (B) Poloxamer 188, (C) GMS, and (D) Ag-FSE SLN

In vitro release studies

In vitro release profile of Ag-FSE SLNs and Ag-FSE is presented in Figure 4.7. Release of Ag-FSE from the SLNs was observed to be in controlled manner with a ~94% of Ag-FSE released in 4 to 8 h and cumulative release of 91.46% at the end of 96 h. These results suggest that encapsulation of Ag-FSE into SLNs resulted in controlled release of the drug from lipid matrix.

Slow and controlled release of Ag-FSE from the SLNs could be due to the drug-enriched core model. Similar results of controlled release with SLNs was observed in other studies (Mhango et al. 2017; Kalhapure et al. 2017; X. Chen et al. 2013). Interestingly only ~22% release was released when Ag-FSE was dispersed in PBS. This could be due to precipitation of drug in PBS and subsequent diminished permeability through dialysis tubing. However, no precipitation for unentrapped Ag-FSE was observed in prepared SLNs. This could be due to formation of nanocrystals during homogenization and ultrasonication process by the stealth effect of Poloxamer 188. This was confirmed by subjecting Ag-FSE in Poloxamer 188 solution (1% w/v) to similar homogenization and sonication conditions as used during the preparation of SLNs. It was observed that there was formation of nanocrystals with average size of 356.5 ± 13.94 nm. However, sedimentation of these nanocrystals occurred within an hour. When Ag-FSE was dissolved in DMSO, 100% release was obtained within 2 h.

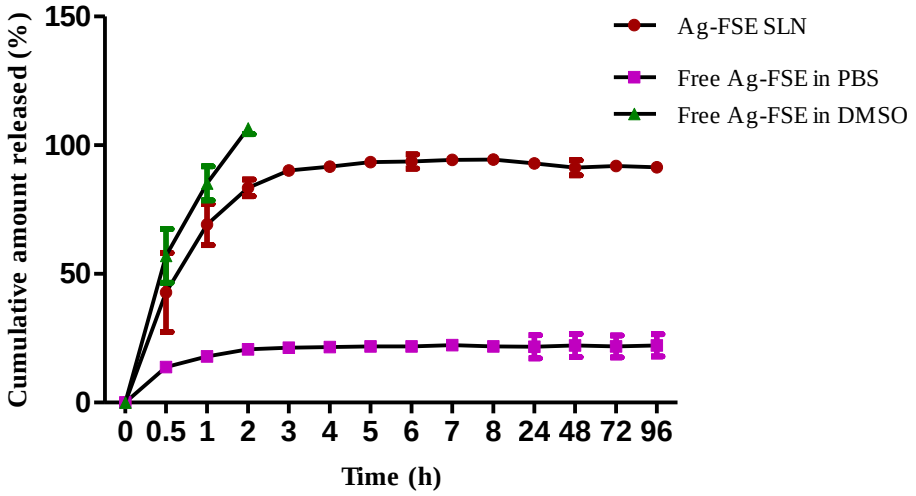

Figure 4.7: *In vitro* release profile of Ag-FSE SLNs, Ag-FSE in PBS, and Ag-FSE in DMSO. Data are expressed in mean ± SD (n = 3).

Physical stability studies

Freeze dried SLNs were evaluated for stability at 4 °C and 25 °C for 60 days. Initially, two concentrations of sucrose were evaluated to obtain particles with a minimum particle size. Results showed minimum particle size of 136.6 ± 15.93 nm was obtained with sucrose:GMS ratio of 1:1 (Table .3). Therefore, stability studies were conducted for freeze dried samples with sucrose to GMS concentration of 1:1 at days 1, 30 and 60.

Results showed that there was no significant difference in the particle size of SLNs at Day 1, 30 and Day 60 ($p > 0.05$) (Table 4.4). Also, there was no sign of aggregation of nanoparticles during the storage period at 4 °C and 25 °C. For samples stored at RT, the particle size at Day 1, Day 30 and Day 60 were 136.6 ± 15.93 nm, 143.8 ± 37.67 nm and 200.8 ± 27.38 nm, respectively. For samples stored at 4 °C, the particle size at Day 1, Day 30 and Day 60 were 136.6 ± 15.93 nm, 139.0 ± 23.19 nm and 146.8 ± 19.90 nm, respectively. ZP values at different timepoints also confirmed that the freeze-dried Ag-FSE SLNs were stable throughout the storage period.

Table 4.3: Effect of sucrose concentration on size, PDI and ZP of freeze-dried Ag-FSE SLNs.

All the data are represented as mean ± SD (n=3)

GMS to Sucrose Ratio	Size (nm)	PDI	ZP (mV)
1:0.5	201.9 ± 59.14	0.337 ± 0.06	-25.1 ± 0.72
1:1	136.6 ± 15.93	0.352 ± 0.09	-23.1 ± 2.10

Table 4.4: Effect of storage on particle size, PDI and ZP of freeze-dried Ag-FSE SLNs for 30 and 60 days at 4 °C and 25 °C. All the data are represented as mean ± SD (n=3)

Storage Condition	**Particle size (nm)**		**PDI**		**ZP**	
Time (Days)	**4 °C**	**RT**	**4 °C**	**RT**	**4 °C**	**RT**
1	136.6 ± 15.93	136.6 ± 15.93	0.352 ± 0.09	0.352 ± 0.09	-23.1 ± 2.10	-23.1 ± 2.10
30	139.0 ± 23.19	143.8 ± 37.67	0.411 ± 0.11	0.422 ± 0.13	-30.4 ± 0.58	-32.8 ± 1.59
60	146.8 ± 19.90	200.8 ± 27.38	0.374 ± 0.09	0.572 ± 0.10	-18.4 ± 4.12	-16.5 ± 3.41

***In vitro* antibacterial activity**

Antibacterial activity of SLNs was determined using broth dilution method. Results showed that encapsulation of Ag-FSE into SLNs significantly increased the antibacterial activity against *P. aeruginosa* and *S. aureus*. However, against *E. coli*, the antibacterial efficacy was similar for Ag-FSE and Ag-FSE SLNs. These results were consistent with other studies where encapsulation of antibiotics into SLNs enhanced the antibacterial activity. Enhancement in antibacterial activity can be attributed to multiple simultaneous mechanisms of actions of Ag-FSE loaded SLNs such as: i) transformation of Ag-FSE from crystalline to amorphous form; ii) enhanced drug diffusion onto bacterial cell wall as well as better interaction with the bacterial surface causing nanoparticle penetration into the cell due to lipidic shell of SLNs (Pignatello et al. 2018); iii) high binding avidity of silver for negatively charged side groups dispersed throughout the microbial cells (Kalhapure et al. 2015) and iv) capacity of silver to attack numerous sites in the

bacterial cell (Kalhapure et al. 2015; Suleman et al. 2015). No antibacterial activity was observed for blank SLNs and 10% DMSO. Compared to Ag-FSE, Ag-FSE SLNs had 4-fold and 2-fold enhancement in antibacterial activity against *S. aureus* (MIC: 15.625 µg/mL vs. 62.5 µg/mL) and *P. aeruginosa* (MIC: 15.625 µg/mL vs. 31.25 µg/mL), respectively (Table 4.5).

Results from this study are consistent with our previous study of Ag-FSE nanocrystals with few interesting findings (Table 4.6). Against *S. aureus* and *E. coli*, nanocrystals of Ag-FSE had better activity compared to Ag-FSE and Ag-FSE SLNs. Better activity with Ag-FSE nanocrystals against *S. aureus* could be due to: i) sodium dodecyl sulphate which was used as a stabilizer in nanocrystal formulation and ii) nanocrystals are unencapsulated nano form of a drug which would have made whole drug available immediately for exerting activity. Against *S. aureus*, Ag-FSE SLNs had better activity compared to Ag-FSE. This confirms that nanonization of Ag-FSE resulted in enhanced anti-bacterial activity compared to Ag-FSE.

Table 4.5: MIC values of antibacterial activities of Ag-FSE, 10% DMSO, Blank SLNs and Ag-FSE SLNs (n = 3).

Formulation	**MIC (µg/mL)**		
	***E. coli* (ATCC25922)**	***S. aureus* (ATCC25923)**	***P. aeruginosa* (ATCC27853)**
10% DMSO	NA	NA	NA
Blank SLNs	NA	NA	NA
Ag-FSE SLNs	125	15.625	15.625
Ag-FSE in 10% DMSO	125	62.5	31.25
NA = No activity			

Table 4.6: Comparison of antibacterial activities of Ag-FSE nanosuspension and Ag-FSE SLNs against *E. coli*, *S. aureus* and *P. aeruginosa*

Formulation	**Enhancement of antibacterial activity compared to Ag-FSE**		
	***E. coli* (ATCC25922)**	***S. aureus* (ATCC25923)**	***P. aeruginosa* (ATCC27853)**
Ag-FSE Nanosuspension	2-fold	8-fold	No difference
Ag-FSE SLN	No difference	4-fold	2-fold

Conclusions

Encapsulation of antibiotics into SLNs can significantly improve antibacterial bacterial activity and can sustain the drug release. In this study, Ag-FSE, a new antibacterial agent with poor solubility was successfully encapsulated into SLNs to enhance its antibacterial activity. Ag-FSE was encapsulated into SLNs with %EE of ~93%. *In vitro* release studies confirmed that encapsulation of Ag-FSE into SLNs resulted in sustained release of Ag-FSE over 96 h. Results also confirmed that there was a 2-fold and 4-fold enhancement of activity against *P. aeruginosa* and *S. aureus* respectively. Stability studies confirmed that there was no sign of aggregation of nanoparticles during the storage period at 4 °C and 25 °C. In conclusion, formulation of Ag-FSE SLNs significantly enhanced the antibacterial efficacy with sustained release profile. Ag-FSE SLNs can be considered as a promising topical antibacterial agent against bacterial infections. However, the findings in this study are preliminary and should be further confirmed with preclinical studies before clinical applications.

Future studies

In this dissertation project, I have successfully prepared and characterized solid lipid nanoparticles for enhancing the antibacterial activity of furosemide silver complex using several *in vitro* techniques. Future studies for extension of this project includes: (1) Determination of *in vivo* antibacterial efficacy of Ag-FSE SLNs in MRSA infected mice model and (2) To evaluate the *in vivo* pharmacokinetics and tissue distribution of Ag-FSE loaded SLNs.

Chapter 5: Impact on Public Health

The primary aim of developing new formulations/drug delivery systems is to improve the therapeutic performance, achieve sustained efficacy and better patient compliance. In this dissertation, I have developed three novel formulations for drugs (clotrimazole, lutein and furosemide silver complex) with low aqueous solubility, affecting the efficacy/bioavailability.

Globally, fungal infections affect around one billion people and are the primary cause of death in one million patients annually. These infections are usually associated as secondary infections in immunocompromised patients such as AIDs and tuberculosis. Clotrimazole, an antifungal agent is widely used to treat these infections. It is the first oral azole approved for fungal infections; however, it is not used orally sue to systemic toxicity. It is currently available as topical formulations such as cream, solution and lotion, however, the bioavailability is very low (5-10%) due to poor solubility. In the first study, I loaded clotrimazole into novel lipid-based drug delivery system (ufosomes) prepared using cholesterol and sodium oleate. There was a significant increase in the topical bioavailability of clotrimazole. Moreover, cholesterol and sodium oleate are inexpensive and easy to procure. Overall, clotrimazole loaded ufosomes could be advantageous in treating fungal infections effectively, help in increasing patient compliance due to reduced frequency in application.

In the second study I have formulated lutein loaded folate decorated nano-formulation to enhance the uptake of a neuroprotective agent, lutein. Neonatal HIE affects approximately 0.1% to 0.3% of live births in developed nations and 2.6% in under-developed nations and is responsible for 23% of neonatal deaths. Survivors of neonatal HIE develop severe neurological abnormalities such as cerebral palsy, seizures, and blindness. Currently therapeutic hypothermia is the only gold standard treatment; however, it is successful only in 50-60% of the cases. Lutein, a neuroprotective agent has shown to be effective in reducing inflammatory mediators, brain injury and HIF-α. However, poor solubility limits its bioavailability in neonates and mother's milk. Supplementation of lutein with the prepared nano-formulation to the mother and neonate is expected to increase

lutein levels in the brain and reduce the hypoxic ischemic shock. This novel formulation could be valuable in reducing the deaths associated with HIE.

There is a significant rise in the incidence of antibiotic resistant infections. According to the CDC, mortality associated with these infections is around 23,000 patients annually and causes an annual economic burden of 20 billion dollars in direct costs and 35 billion dollars in indirect costs in the US alone. The CDC has recommended the development of new antibiotics to combat these infections. Silver complexes have been used as a prophylactic and treatment for bacterial infections associated with skin burns. Furosemide-silver is a novel synthetic agent effective against wide range of bacterial infections however, poor solubility limits its activity. I have developed a novel solid lipid nanoparticle formulation for furosemide silver complex and enhanced its activity and provided a sustained release profile. This formulation could potentially be used as a novel topical antibacterial agent for treating infections associated with burns and reduce the systemic effects of silver toxicity.

Thus, the new formulations developed have advantages such as dose flexibility, easier administration, and better acceptance by all patient population.

References

"10 Final Report on the Safety Assessment of Cholesterol." 1986. *Journal of the American College of Toxicology* 5 (5): 491–516. https://doi.org/10.3109/10915818609141922.

AbouSamra, Mona M, Mona Basha, Ghada E A Awad, and Soheir S Mansy. 2019. "A Promising Nystatin Nanocapsular Hydrogel as an Antifungal Polymeric Carrier for the Treatment of Topical Candidiasis." *Journal of Drug Delivery Science and Technology* 49: 365–74. https://doi.org/https://doi.org/10.1016/j.jddst.2018.12.014.

Ahlawat, Jyoti, M Eva Deemer, and Mahesh Narayan. 2019. "Chitosan Nanoparticles Rescue Rotenone-Mediated Cell Death." *Materials* . https://doi.org/10.3390/ma12071176.

Alam, Camille, Md Tozammel Hoque, Richard H Finnell, I David Goldman, and Reina Bendayan. 2017. "Regulation of Reduced Folate Carrier (RFC) by Vitamin D Receptor at the Blood-Brain Barrier." *Molecular Pharmaceutics* 14 (11): 3848–58. https://doi.org/10.1021/acs.molpharmaceut.7b00572.

Alam, Mohd Aftab, Fahad I Al-Janoobi, Khaled A Alzahrani, Mohammad H Al-Agamy, Ahmed A Abdelgalil, and Abdullah M Al-Mohizea. 2017. "In-Vitro Efficacies of Topical Microemulsions of Clotrimazole and Ketoconazole; and in-Vivo Performance of Clotrimazole Microemulsion." *Journal of Drug Delivery Science and Technology* 39: 408–16. https://doi.org/https://doi.org/10.1016/j.jddst.2017.04.025.

Allotey-Babington, Grace Lovia, Henry Nettey, Sucheta D'Sa, Kimberly Braz Gomes, and Martin J D'Souza. 2018. "Cancer Chemotherapy: Effect of Poloxamer Modified Nanoparticles on Cellular Function." *Journal of Drug Delivery Science and Technology* 47: 181–92. https://doi.org/https://doi.org/10.1016/j.jddst.2018.06.012.

Antony, A C. 1996. "Folate Receptors." *Annual Review of Nutrition* 16: 501–21.

https://doi.org/10.1146/annurev.nu.16.070196.002441.

Ayoub, Margrit M, Neveen G Elantouny, Hanan M El-Nahas, and Fakhr El-Din S Ghazy. 2018. "Injectable PLGA Adefovir Microspheres; the Way for Long Term Therapy of Chronic Hepatitis-B." *European Journal of Pharmaceutical Sciences : Official Journal of the European Federation for Pharmaceutical Sciences* 118 (June): 24–31. https://doi.org/10.1016/j.ejps.2018.03.016.

Azarmi, Shirzad, Wilson Roa, and Raimar Lobenberg. 2007. "Current Perspectives in Dissolution Testing of Conventional and Novel Dosage Forms." *International Journal of Pharmaceutics* 328 (1): 12–21. https://doi.org/10.1016/j.ijpharm.2006.10.001.

Bahrami, Behdokht, Mohammad Hojjat-Farsangi, Hamed Mohammadi, Enayat Anvari, Ghasem Ghalamfarsa, Mehdi Yousefi, and Farhad Jadidi-Niaragh. 2017. "Nanoparticles and Targeted Drug Delivery in Cancer Therapy." *Immunology Letters* 190 (October): 64–83. https://doi.org/10.1016/j.imlet.2017.07.015.

Banik, Brittany L, Pouria Fattahi, and Justin L Brown. 2016. "Polymeric Nanoparticles: The Future of Nanomedicine." *Wiley Interdisciplinary Reviews. Nanomedicine and Nanobiotechnology* 8 (2): 271–99. https://doi.org/10.1002/wnan.1364.

Barbero, Ana M, and H Frederick Frasch. 2016. "Effect of Frozen Human Epidermis Storage Duration and Cryoprotectant on Barrier Function Using Two Model Compounds." *Skin Pharmacology and Physiology* 29 (1): 31–40. https://doi.org/10.1159/000441038.

Bennion, Brian J, Nicholas A Be, M Windy McNerney, Victoria Lao, Emma M Carlson, Carlos A Valdez, Michael A Malfatti, et al. 2017. "Predicting a Drug's Membrane Permeability: A Computational Model Validated With in Vitro Permeability Assay Data." *The Journal of Physical Chemistry B* 121 (20): 5228–37. https://doi.org/10.1021/acs.jpcb.7b02914.

Binder, Lisa, Johannes Jatschka, Eva Maria Kulovits, Simone Seeböck, Hanspeter Kählig, and Claudia Valenta. 2018. “Simultaneous Penetration Monitoring of Oil Component and Active Drug from Fluorinated Nanoemulsions.” *International Journal of Pharmaceutics* 552 (1): 312–18. https://doi.org/https://doi.org/10.1016/j.ijpharm.2018.10.012.

Bolla, K Pradeep, A Bradley Clark, Abhishek Juluri, S Hanumanth Cheruvu, and Jwala Renukuntla. 2020. “Evaluation of Formulation Parameters on Permeation of Ibuprofen from Topical Formulations Using Strat-M® Membrane.” *Pharmaceutics* . https://doi.org/10.3390/pharmaceutics12020151.

Bolla, K Pradeep, A Carlos Meraz, A Victor Rodriguez, Isaac Deaguero, Mahima Singh, K Venkata Yellepeddi, and Jwala Renukuntla. 2019. “Clotrimazole Loaded Ufosomes for Topical Delivery: Formulation Development and In-Vitro Studies.” *Molecules* . https://doi.org/10.3390/molecules24173139.

Bolla, Pradeep Kumar, Rahul S. Kalhapure, Victor A. Rodriguez, David V. Ramos, Amit Dahl, and Jwala Renukuntla. 2019. “Preparation of Solid Lipid Nanoparticles of Furosemide-Silver Complex and Evaluation of Antibacterial Activity.” *Journal of Drug Delivery Science and Technology*. https://doi.org/10.1016/j.jddst.2018.10.035.

Bolla, Pradeep Kumar, Victor A Rodriguez, Rahul S Kalhapure, and Jwala Renukuntla. 2018. “A Review on PH and Temperature Responsive Gels and Other Less Explored Drug Delivery Systems.” *Journal of Drug Delivery Science and Technology* 46 (May): 416–35. https://doi.org/10.1016/j.jddst.2018.05.037.

Bongomin, Felix, Sara Gago, O Rita Oladele, and W David Denning. 2017. “Global and Multi-National Prevalence of Fungal Diseases—Estimate Precision.” *Journal of Fungi* . https://doi.org/10.3390/jof3040057.

Bose, Sonali, and Bozena Michniak-Kohn. 2013. “Preparation and Characterization of Lipid Based Nanosystems for Topical Delivery of Quercetin.” *European Journal of Pharmaceutical Sciences* 48 (3): 442–52. https://doi.org/https://doi.org/10.1016/j.ejps.2012.12.005.

Bragagni, Marco, Maria Esther Gil-Alegre, Paola Mura, Marzia Cirri, Carla Ghelardini, and Lorenzo Di Cesare Mannelli. 2018. “Improving the Therapeutic Efficacy of Prilocaine by PLGA Microparticles: Preparation, Characterization and in Vivo Evaluation.” *International Journal of Pharmaceutics* 547 (1–2): 24–30. https://doi.org/10.1016/j.ijpharm.2018.05.054.

Brum, Aelson Aloir Santana, Priscilla Pereira dos Santos, Médelin Marques da Silva, Karina Paese, Silvia Stanisçuaski Guterres, Tania Maria Haas Costa, Adriana Raffin Pohlmann, André Jablonski, Simone Hickmann Flôres, and Alessandro de Oliveira Rios. 2017. “Lutein-Loaded Lipid-Core Nanocapsules: Physicochemical Characterization and Stability Evaluation.” *Colloids and Surfaces A: Physicochemical and Engineering Aspects* 522: 477–84. https://doi.org/https://doi.org/10.1016/j.colsurfa.2017.03.041.

Bseiso, Eman Ahmed, Maha Nasr, Omaima Sammour, and Nabaweya A Abd El Gawad. 2015. “Recent Advances in Topical Formulation Carriers of Antifungal Agents.” *Indian Journal of Dermatology, Venereology and Leprology* 81 (5): 457–63. https://doi.org/10.4103/0378-6323.162328.

Buchiraju, Ravi, Dr. Nama Sreekanth, Sakala Bhargavi, C H RAO, Arun Kommu, Jaya Kishore, Babu Chebrolu, Narasimhamurthy Yedulapurapu, and Don Bosco. 2013. “Vesicular Drug Delivery System -An Over View,” July.

Busl, Katharina M, and David M Greer. 2010. “Hypoxic-Ischemic Brain Injury: Pathophysiology, Neuropathology and Mechanisms.” *NeuroRehabilitation* 26 (1): 5–13.

https://doi.org/10.3233/NRE-2010-0531.

Centers for Disease Control and Prevention, C D C. 2013. “Antibiotic Resistance Threats in the United States, 2013.” *Atlanta: CDC*. http://www.cdc.gov/drugresistance/threat-report-2013/%5Cnhttp://www.cdc.gov/drugresistance/threat-report-2013/pdf/ar-threats-2013-508.pdf.

Chaganti, Lalith K, Navneet Venkatakrishnan, and Kakoli Bose. 2018. “An Efficient Method for FITC Labelling of Proteins Using Tandem Affinity Purification.” *Bioscience Reports* 38 (6): BSR20181764. https://doi.org/10.1042/BSR20181764.

Chen, Huabing, Chalermchai Khemtong, Xiangliang Yang, Xueling Chang, and Jinming Gao. 2011. “Nanonization Strategies for Poorly Water-Soluble Drugs.” *Drug Discovery Today* 16 (7–8): 354–60. https://doi.org/10.1016/j.drudis.2010.02.009.

Chen, Xi, Li-Hua Peng, Ying-Hui Shan, Ni Li, Wei Wei, Lian Yu, Qi-Mei Li, Wen-Quan Liang, and Jian-Qing Gao. 2013. “Astragaloside IV-Loaded Nanoparticle-Enriched Hydrogel Induces Wound Healing and Anti-Scar Activity through Topical Delivery.” *International Journal of Pharmaceutics* 447 (1): 171–81. https://doi.org/https://doi.org/10.1016/j.ijpharm.2013.02.054.

Cheng, Ching-Ling, Lawrence X Yu, Hwei-Ling Lee, Chyun-Yu Yang, Chang-Sha Lue, and Chen-Hsi Chou. 2004. “Biowaiver Extension Potential to BCS Class III High Solubility-Low Permeability Drugs: Bridging Evidence for Metformin Immediate-Release Tablet.” *European Journal of Pharmaceutical Sciences : Official Journal of the European Federation for Pharmaceutical Sciences* 22 (4): 297–304. https://doi.org/10.1016/j.ejps.2004.03.016.

Cheng, Y, J M Gidday, Q Yan, A R Shah, and D M Holtzman. 1997. “Marked Age-Dependent

Neuroprotection by Brain-Derived Neurotrophic Factor against Neonatal Hypoxic-Ischemic Brain Injury." *Annals of Neurology* 41 (4): 521–29. https://doi.org/10.1002/ana.410410416.

Cordoba-Diaz, M, M Nova, B Elorza, D Cordoba-Diaz, J R Chantres, and M Cordoba-Borrego. 2000. "Validation Protocol of an Automated In-Line Flow-through Diffusion Equipment for in Vitro Permeation Studies." *Journal of Controlled Release : Official Journal of the Controlled Release Society* 69 (3): 357–67.

Córdoba-Díaz, M, M Nova, B Elorza, D Córdoba-Díaz, J R Chantres, and M Córdoba-Borrego. 2000. "Validation Protocol of an Automated In-Line Flow-through Diffusion Equipment for in Vitro Permeation Studies." *Journal of Controlled Release : Official Journal of the Controlled Release Society* 69 (3): 357—367. https://doi.org/10.1016/s0168-3659(00)00306-0.

Costa, Simonetta, Carmen Giannantonio, Costantino Romagnoli, Giovanni Vento, Jacopo Gervasoni, Silvia Persichilli, Cecilia Zuppi, and Francesco Cota. 2013. "Effects of Lutein Supplementation on Biological Antioxidant Status in Preterm Infants: A Randomized Clinical Trial." *The Journal of Maternal-Fetal & Neonatal Medicine : The Official Journal of the European Association of Perinatal Medicine, the Federation of Asia and Oceania Perinatal Societies, the International Society of Perinatal Obstetricians* 26 (13): 1311–15. https://doi.org/10.3109/14767058.2013.783801.

Crucho, Carina I C, and Maria Teresa Barros. 2017. "Polymeric Nanoparticles: A Study on the Preparation Variables and Characterization Methods." *Materials Science and Engineering: C* 80: 771–84. https://doi.org/https://doi.org/10.1016/j.msec.2017.06.004.

Csongradi, Candice, Jeanetta du Plessis, Marique Elizabeth Aucamp, and Minja Gerber. 2017. "Topical Delivery of Roxithromycin Solid-State Forms Entrapped in Vesicles." *European*

Journal of Pharmaceutics and Biopharmaceutics : Official Journal of Arbeitsgemeinschaft Fur Pharmazeutische Verfahrenstechnik e.V 114 (May): 96–107. https://doi.org/10.1016/j.ejpb.2017.01.006.

D. Waugh, Christine. 2011. "Clotrimazole." In *XPharm: The Comprehensive Pharmacology Reference*, 1–4. https://doi.org/10.1016/B978-008055232-3.61499-0.

Dahan, Arik, and Jonathan M Miller. 2012. "The Solubility-Permeability Interplay and Its Implications in Formulation Design and Development for Poorly Soluble Drugs." *The AAPS Journal* 14 (2): 244–51. https://doi.org/10.1208/s12248-012-9337-6.

Dahan, Arik, Jonathan M Miller, and Gordon L Amidon. 2009. "Prediction of Solubility and Permeability Class Membership: Provisional BCS Classification of the World's Top Oral Drugs." *The AAPS Journal* 11 (4): 740–46. https://doi.org/10.1208/s12248-009-9144-x.

Damgé, Christiane, Philippe Maincent, and Nathalie Ubrich. 2007. "Oral Delivery of Insulin Associated to Polymeric Nanoparticles in Diabetic Rats." *Journal of Controlled Release* 117 (2): 163–70. https://doi.org/https://doi.org/10.1016/j.jconrel.2006.10.023.

Das, Surajit, Wai Kiong Ng, and Reginald B H Tan. 2012. "Are Nanostructured Lipid Carriers (NLCs) Better than Solid Lipid Nanoparticles (SLNs): Development, Characterizations and Comparative Evaluations of Clotrimazole-Loaded SLNs and NLCs?" *European Journal of Pharmaceutical Sciences* 47 (1): 139–51. https://doi.org/https://doi.org/10.1016/j.ejps.2012.05.010.

Davies, Julian, and Dorothy Davies. 2010. "Origins and Evolution of Antibiotic Resistance." *Microbiology and Molecular Biology Reviews : MMBR*. https://doi.org/10.1128/MMBR.00016-10.

Doppalapudi, Sindhu, Anjali Jain, Dhiraj Kumar Chopra, and Wahid Khan. 2017. "Psoralen

Loaded Liposomal Nanocarriers for Improved Skin Penetration and Efficacy of Topical PUVA in Psoriasis." *European Journal of Pharmaceutical Sciences* 96: 515–29. https://doi.org/https://doi.org/10.1016/j.ejps.2016.10.025.

Dwivedi, Anupma, Anisha Mazumder, Lizelle T Fox, Alicia Brümmer, Minja Gerber, Jan L du Preez, Richard K Haynes, and Jeanetta du Plessis. 2016. "In Vitro Skin Permeation of Artemisone and Its Nano-Vesicular Formulations." *International Journal of Pharmaceutics* 503 (1): 1–7. https://doi.org/https://doi.org/10.1016/j.ijpharm.2016.02.041.

Ebrahimnejad, Pedram, Rassoul Dinarvand, Abolghasem Sajadi, Mahmoud Reza Jaafari, Ali Reza Nomani, Ebrahim Azizi, Mazda Rad-Malekshahi, and Fatemeh Atyabi. 2010. "Preparation and in Vitro Evaluation of Actively Targetable Nanoparticles for SN-38 Delivery against HT-29 Cell Lines." *Nanomedicine : Nanotechnology, Biology, and Medicine* 6 (3): 478–85. https://doi.org/10.1016/j.nano.2009.10.003.

El-Say, Khalid M, and Hossam S El-Sawy. 2017. "Polymeric Nanoparticles: Promising Platform for Drug Delivery." *International Journal of Pharmaceutics* 528 (1–2): 675–91. https://doi.org/10.1016/j.ijpharm.2017.06.052.

Esmaeili, Farnaz, Mohammad Hossein Ghahremani, Seyed Nasser Ostad, Fatemeh Atyabi, Mohammad Seyedabadi, Mazda Rad Malekshahi, Mohsen Amini, and Rassoul Dinarvand. 2008. "Folate-Receptor-Targeted Delivery of Docetaxel Nanoparticles Prepared by PLGA-PEG-Folate Conjugate." *Journal of Drug Targeting* 16 (5): 415–23. https://doi.org/10.1080/10611860802088630.

Esposito, Elisabetta, Laura Ravani, Catia Contado, Andrea Costenaro, Markus Drechsler, Damiano Rossi, Enea Menegatti, Alessandro Grandini, and Rita Cortesi. 2013. "Clotrimazole Nanoparticle Gel for Mucosal Administration." *Materials Science and*

Engineering: C 33 (1): 411–18. https://doi.org/https://doi.org/10.1016/j.msec.2012.09.007.

Fasehee, Hamidreza, Rassoul Dinarvand, Ardeshir Ghavamzadeh, Mehdi Esfandyari-Manesh, Hanieh Moradian, Shahab Faghihi, and Seyed Hamidollah Ghaffari. 2016. "Delivery of Disulfiram into Breast Cancer Cells Using Folate-Receptor-Targeted PLGA-PEG Nanoparticles: In Vitro and in Vivo Investigations." *Journal of Nanobiotechnology* 14 (1): 32. https://doi.org/10.1186/s12951-016-0183-z.

Fattuoni, Claudia, Francesco Palmas, Antonio Noto, Vassilios Fanos, and Luigi Barberini. 2015. "Perinatal Asphyxia: A Review from a Metabolomics Perspective." *Molecules (Basel, Switzerland)* 20 (4): 7000–7016. https://doi.org/10.3390/molecules20047000.

Foster, Chase H, Devaraj Sambalingam, Xiaoming Gong, and Lewis P Rubin. 2017. "Neuroprotective Effects of Lutein in Neonatal Hypoxic-Ischemic Brain Injury." *The FASEB Journal* 31 (1_supplement): 635.9-635.9. https://doi.org/10.1096/fasebj.31.1_supplement.635.9.

Geszke-Moritz, Małgorzata, and Michał Moritz. 2016. "Solid Lipid Nanoparticles as Attractive Drug Vehicles: Composition, Properties and Therapeutic Strategies." *Materials Science and Engineering: C* 68: 982–94. https://doi.org/https://doi.org/10.1016/j.msec.2016.05.119.

Ghaffari, Solmaz, Jaleh Varshosaz, Afrooz Saadat, and Fatemeh Atyabi. 2011. "Stability and Antimicrobial Effect of Amikacin-Loaded Solid Lipid Nanoparticles." *International Journal of Nanomedicine* 6 (December): 35–43. https://doi.org/10.2147/IJN.S13671.

Giampietri, Matteo, Francesca Lorenzoni, Francesca Moscuzza, Antonio Boldrini, and Paolo Ghirri. 2016. "Lutein and Neurodevelopment in Preterm Infants." *Frontiers in Neuroscience* 10 (September): 411. https://doi.org/10.3389/fnins.2016.00411.

Goli, Naresh, Pradeep Kumar Bolla, and Venu Talla. 2018. "Antibody-Drug Conjugates (ADCs):

Potent Biopharmaceuticals to Target Solid and Hematological Cancers- an Overview." *Journal of Drug Delivery Science and Technology*, August. https://doi.org/10.1016/j.jddst.2018.08.022.

Gong, Xiaoming, Devaraj Sambalingam, Min Li, Mario G Ferruzzi, and Lewis P Rubin. 2017. "Lutein Selectively Accumulates in the Neonatal Rat Brain via Breast Milk." *The FASEB Journal* 31 (1_supplement): 170.5-170.5. https://doi.org/10.1096/fasebj.31.1_supplement.170.5.

Gulsun, Tugba, Sahand E Borna, Imran Vural, and Selma Sahin. 2018. "Preparation and Characterization of Furosemide Nanosuspensions." *Journal of Drug Delivery Science and Technology* 45: 93–100. https://doi.org/https://doi.org/10.1016/j.jddst.2018.03.005.

Guo, Jianfeng, Michele Schlich, John F Cryan, and Caitriona M O'Driscoll. 2017. "Targeted Drug Delivery via Folate Receptors for the Treatment of Brain Cancer: Can the Promise Deliver?" *Journal of Pharmaceutical Sciences* 106 (12): 3413–20. https://doi.org/10.1016/j.xphs.2017.08.009.

Gupta, Madhu, Vikas Sharma, and Nagendra S Chauhan. 2017. "Chapter 11 - Promising Novel Nanopharmaceuticals for Improving Topical Antifungal Drug Delivery." In , edited by Alexandru Mihai B T - Nano- and Microscale Drug Delivery Systems Grumezescu, 197–228. Elsevier. https://doi.org/https://doi.org/10.1016/B978-0-323-52727-9.00011-X.

Gupta, Prem N, Vivek Mishra, Amit Rawat, Praveen Dubey, Sunil Mahor, Sanyog Jain, D P Chatterji, and Suresh P Vyas. 2005. "Non-Invasive Vaccine Delivery in Transfersomes , Niosomes and Liposomes : A Comparative Study" 293: 73–82. https://doi.org/10.1016/j.ijpharm.2004.12.022.

Gupta, Shweta, Rajesh Kesarla, and Abdelwahab Omri. 2013. "Formulation Strategies to

Improve the Bioavailability of Poorly Absorbed Drugs with Special Emphasis on Self-Emulsifying Systems." Edited by J Reynisson, A S Zidan, and S Simovic. *ISRN Pharmaceutics* 2013: 848043. https://doi.org/10.1155/2013/848043.

Hopf, N B, A Berthet, D Vernez, E Langard, P Spring, and R Gaudin. 2014. "Skin Permeation and Metabolism of Di(2-Ethylhexyl) Phthalate (DEHP)." *Toxicology Letters* 224 (1): 47–53. https://doi.org/https://doi.org/10.1016/j.toxlet.2013.10.004.

Hou, DongZhi, ChangSheng Xie, KaiJin Huang, and ChangHong Zhu. 2003. "The Production and Characteristics of Solid Lipid Nanoparticles (SLNs)." *Biomaterials* 24 (10): 1781–85.

Hu, Daode, Changchun Lin, Liang Liu, Sining Li, and Yaping Zhao. 2012. "Preparation, Characterization, and in Vitro Release Investigation of Lutein/Zein Nanoparticles via Solution Enhanced Dispersion by Supercritical Fluids." *Journal of Food Engineering* 109 (3): 545–52. https://doi.org/https://doi.org/10.1016/j.jfoodeng.2011.10.025.

ICH. 2019. "BIOPHARMACEUTICS CLASSIFICATION SYSTEM BASED BIOWAIVERS - M9." https://database.ich.org/sites/default/files/M9_Guideline_Step4_2019_1116.pdf.

Ishikawa, Minoru, and Yuichi Hashimoto. 2011. "Improvement in Aqueous Solubility in Small Molecule Drug Discovery Programs by Disruption of Molecular Planarity and Symmetry." *Journal of Medicinal Chemistry* 54 (6): 1539–54. https://doi.org/10.1021/jm101356p.

Jain, Rajeev A. 2000. "The Manufacturing Techniques of Various Drug Loaded Biodegradable Poly(Lactide-Co-Glycolide) (PLGA) Devices." *Biomaterials* 21 (23): 2475–90. https://doi.org/https://doi.org/10.1016/S0142-9612(00)00115-0.

Jaiswal, Manish K, Arpan Pradhan, Rinti Banerjee, and Dhirendra Bahadur. 2014. "Dual PH and Temperature Stimuli-Responsive Magnetic Nanohydrogels for Thermo-Chemotherapy." *Journal of Nanoscience and Nanotechnology* 14 (6): 4082–89.

Joseph, Andrea, Thomas Wood, Chih-Chung Chen, Kylie Corry, Jessica M. Snyder, Sandra E. Juul, Pratik Parikh, and Elizabeth Nance. 2018. "Curcumin-Loaded Polymeric Nanoparticles for Neuroprotection in Neonatal Rats with Hypoxic-Ischemic Encephalopathy." *Nano Research*, no. June. https://doi.org/10.1007/s12274-018-2104-y.

Juluri, Abhishek, Naresh Modepalli, Seongbong Jo, Michael A Repka, H Nanjappa Shivakumar, and S Narasimha Murthy. 2013. "Minimally Invasive Transdermal Delivery of Iron-Dextran." *Journal of Pharmaceutical Sciences* 102 (3): 987–93. https://doi.org/10.1002/jps.23429.

Juluri, Abhishek, and S Narasimha Murthy. 2014. "Transdermal Iontophoretic Delivery of a Liquid Lipophilic Drug by Complexation with an Anionic Cyclodextrin." *Journal of Controlled Release : Official Journal of the Controlled Release Society* 189 (September): 11–18. https://doi.org/10.1016/j.jconrel.2014.06.014.

Jwala, Jwala, Sai H S Boddu, Sujay Shah, Suman Sirimulla, Dhananjay Pal, and Ashim K Mitra. 2011. "Ocular Sustained Release Nanoparticles Containing Stereoisomeric Dipeptide Prodrugs of Acyclovir." *Journal of Ocular Pharmacology and Therapeutics* 27 (2): 163–72. https://doi.org/10.1089/jop.2010.0188.

Kaewbanjong, J, T Amnuaikit, E B Souto, and P Boonme. 2018. "Antidermatophytic Activity and Skin Retention of Clotrimazole Microemulsion and Microemulsion-Based Gel in Comparison to Conventional Cream." *Skin Pharmacology and Physiology* 31 (6): 292–97. https://doi.org/10.1159/000491756.

Kahraman, Emine, Neşet Neşetoğlu, Sevgi Güngör, Duri Şehvar Ünal, and Yıldız Özsoy. 2018. "The Combination of Nanomicelles with Terpenes for Enhancement of Skin Drug Delivery." *International Journal of Pharmaceutics* 551 (1): 133–40.

https://doi.org/https://doi.org/10.1016/j.ijpharm.2018.08.053.

Kalepu, Sandeep, and Vijaykumar Nekkanti. 2015. “Insoluble Drug Delivery Strategies: Review of Recent Advances and Business Prospects.” *Acta Pharmaceutica Sinica B* 5 (5): 442–53. https://doi.org/https://doi.org/10.1016/j.apsb.2015.07.003.

Kalhapure, Rahul S, and Krishnacharya G Akamanchi. 2013. “A Novel Biocompatible Bicephalous Dianionic Surfactant from Oleic Acid for Solid Lipid Nanoparticles.” *Colloids and Surfaces. B, Biointerfaces* 105 (May): 215–22. https://doi.org/10.1016/j.colsurfb.2013.01.011.

Kalhapure, Rahul S, Pradeep Kumar Bolla, Sai H S Boddu, and Jwala Renukuntla. 2019. “Evaluation of Oleic Acid and Polyethylene Glycol Monomethyl Ether Conjugate (PEGylated Oleic Acid) as a Solubility Enhancer of Furosemide.” *Processes* 7 (8). https://doi.org/10.3390/pr7080520.

Kalhapure, Rahul S, Chunderika Mocktar, Dhiraj R Sikwal, Sandeep J Sonawane, Muthu K Kathiravan, Adam Skelton, and Thirumala Govender. 2014. “Ion Pairing with Linoleic Acid Simultaneously Enhances Encapsulation Efficiency and Antibacterial Activity of Vancomycin in Solid Lipid Nanoparticles.” *Colloids and Surfaces. B, Biointerfaces* 117 (May): 303–11. https://doi.org/10.1016/j.colsurfb.2014.02.045.

Kalhapure, Rahul S, Dhiraj R Sikwal, Sanjeev Rambharose, Chunderika Mocktar, Sanil Singh, Linda Bester, Jung Kwon Oh, Jwala Renukuntla, and Thirumala Govender. 2017. “Enhancing Targeted Antibiotic Therapy via PH Responsive Solid Lipid Nanoparticles from an Acid Cleavable Lipid.” *Nanomedicine: Nanotechnology, Biology and Medicine* 13 (6): 2067–77. https://doi.org/10.1016/j.nano.2017.04.010.

Kalhapure, Rahul S, Sandeep J Sonawane, Dhiraj R Sikwal, Mahantesh Jadhav, Sanjeev

Rambharose, Chunderika Mocktar, and Thirumala Govender. 2015. “Solid Lipid Nanoparticles of Clotrimazole Silver Complex: An Efficient Nano Antibacterial against Staphylococcus Aureus and MRSA.” *Colloids and Surfaces. B, Biointerfaces* 136 (December): 651–58. https://doi.org/10.1016/j.colsurfb.2015.10.003.

Kalinowska-Lis, Urszula, Aleksandra Felczak, Lilianna Checinska, Katarzyna Zawadzka, Emilia Patyna, Katarzyna Lisowska, and Justyn Ochocki. 2015. “Synthesis, Characterization and Antimicrobial Activity of Water-Soluble Silver(i) Complexes of Metronidazole Drug and Selected Counter-Ions.” *Dalton Transactions (Cambridge, England : 2003)* 44 (17): 8178–89. https://doi.org/10.1039/c5dt00403a.

Kamaly, Nazila, Basit Yameen, Jun Wu, and Omid C Farokhzad. 2016. “Degradable Controlled-Release Polymers and Polymeric Nanoparticles: Mechanisms of Controlling Drug Release.” *Chemical Reviews* 116 (4): 2602–63. https://doi.org/10.1021/acs.chemrev.5b00346.

Kavian, Zahra, Seyedeh Hoda Alavizadeh, Shiva Golmohamadzadeh, Ali Badiee, Ali Khamesipour, and Mahmoud Reza Jaafari. 2019. “Development of Topical Liposomes Containing Miltefosine for the Treatment of Leishmania Major Infection in Susceptible BALB/c Mice.” *Acta Tropica* 196: 142–49. https://doi.org/https://doi.org/10.1016/j.actatropica.2019.05.018.

Khadka, Prakash, Jieun Ro, Hyeongmin Kim, Iksoo Kim, Jeong Tae Kim, Hyunil Kim, Jae Min Cho, Gyiae Yun, and Jaehwi Lee. 2014. “Pharmaceutical Particle Technologies: An Approach to Improve Drug Solubility, Dissolution and Bioavailability.” *Asian Journal of Pharmaceutical Sciences* 9 (6): 304–16. https://doi.org/https://doi.org/10.1016/j.ajps.2014.05.005.

Khan, Ibrahim, Khalid Saeed, and Idrees Khan. 2017. “Nanoparticles: Properties, Applications

and Toxicities." *Arabian Journal of Chemistry*. https://doi.org/https://doi.org/10.1016/j.arabjc.2017.05.011.

Kravchenko, Iryna, Yuriy Boyko, N Novikova, A Egorova, and S Andronati. 2011. "Influence of Cholesterol and Its Esters on Skin Penetration in Vivo and in Vitro in Rats and Mice." *Ukr. Bioorg. Acta* 1 (January): 17–21.

Kumari, Avnesh, Sudesh Kumar Yadav, and Subhash C Yadav. 2010. "Biodegradable Polymeric Nanoparticles Based Drug Delivery Systems." *Colloids and Surfaces B: Biointerfaces* 75 (1): 1–18. https://doi.org/https://doi.org/10.1016/j.colsurfb.2009.09.001.

Lashford, L S, J P Hancock, and J T Kemshead. 1991. "Meta-Iodobenzylguanidine (MIBG) Uptake and Storage in the Human Neuroblastoma Cell Line SK-N-BE(2C)." *International Journal of Cancer* 47 (1): 105–9.

Leon, A S De, M Molina, S Wedepohl, A Munoz-Bonilla, J Rodriguez-Hernandez, and M Calderon. 2016. "Immobilization of Stimuli-Responsive Nanogels onto Honeycomb Porous Surfaces and Controlled Release of Proteins." *Langmuir : The ACS Journal of Surfaces and Colloids* 32 (7): 1854–62. https://doi.org/10.1021/acs.langmuir.5b04166.

Li, Suk-Yee, Zhong-Jie Fu, Huan Ma, Wai-Chi Jang, Kwok-Fai So, David Wong, and Amy C Y Lo. 2009. "Effect of Lutein on Retinal Neurons and Oxidative Stress in a Model of Acute Retinal Ischemia/Reperfusion." *Investigative Ophthalmology & Visual Science* 50 (2): 836–43. https://doi.org/10.1167/iovs.08-2310.

Lim, Chaemin, Da-won Kim, Taehoon Sim, Ngoc Ha Hoang, Jun Won Lee, Eun Seong Lee, Yu Seok Youn, and Kyung Teak Oh. 2016. "Preparation and Characterization of a Lutein Loading Nanoemulsion System for Ophthalmic Eye Drops." *Journal of Drug Delivery Science and Technology* 36: 168–74.

https://doi.org/https://doi.org/10.1016/j.jddst.2016.10.009.

Lipinski, C A, F Lombardo, B W Dominy, and P J Feeney. 2001. "Experimental and Computational Approaches to Estimate Solubility and Permeability in Drug Discovery and Development Settings." *Advanced Drug Delivery Reviews* 46 (1–3): 3–26.

Lipinski, Christopher A, Franco Lombardo, Beryl W Dominy, and Paul J Feeney. 1997. "Experimental and Computational Approaches to Estimate Solubility and Permeability in Drug Discovery and Development Settings." *Advanced Drug Delivery Reviews* 23 (1): 3–25. https://doi.org/https://doi.org/10.1016/S0169-409X(96)00423-1.

Liu, Chi Hsien, Hao Che Chiu, Wei Chi Wu, Soubhagya Laxmi Sahoo, and Ching Yun Hsu. 2014. "Novel Lutein Loaded Lipid Nanoparticles on Porcine Corneal Distribution." *Journal of Ophthalmology* 2014 (July). https://doi.org/10.1155/2014/304694.

Lustri, Bruna Cardinali, Antonio Carlos Massabni, Maria Aline C. Silva, Flávia Aparecida Resende Nogueira, Renata Aquino, André C. Amaral, Antonio Carlos Massabni, and Hernane da Silva Barud. 2017. "Spectroscopic Characterization and Biological Studies in Vitro of a New Silver Complex with Furosemide: Prospective of Application as an Antimicrobial Agent." *Journal of Molecular Structure* 1134: 386–94. https://doi.org/10.1016/j.molstruc.2016.12.056.

"Lutein." n.d. Accessed December 15, 2018. https://www.drugbank.ca/drugs/DB00137.

Maheshwari, Rahul G S, Rakesh K Tekade, Piyoosh A Sharma, Gajanan Darwhekar, Abhishek Tyagi, Rakesh P Patel, and Dinesh K Jain. 2012. "Ethosomes and Ultradeformable Liposomes for Transdermal Delivery of Clotrimazole: A Comparative Assessment." *Saudi Pharmaceutical Journal* 20 (2): 161–70. https://doi.org/https://doi.org/10.1016/j.jsps.2011.10.001.

Manca, Maria Letizia, Iris Usach, José Esteban Peris, Antonella Ibba, Germano Orrù, Donatella Valenti, Elvira Escribano-Ferrer, et al. 2019. “Optimization of Innovative Three-Dimensionally-Structured Hybrid Vesicles to Improve the Cutaneous Delivery of Clotrimazole for the Treatment of Topical Candidiasis.” *Pharmaceutics* 11 (6). https://doi.org/10.3390/pharmaceutics11060263.

Mandal, Abhirup, Kishore Cholkar, Varun Khurana, Ankit Shah, Vibhuti Agrahari, Rohit Bisht, Dhananjay Pal, and Ashim K Mitra. 2017. “Topical Formulation of Self-Assembled Antiviral Prodrug Nanomicelles for Targeted Retinal Delivery.” *Molecular Pharmaceutics* 14 (6): 2056–69. https://doi.org/10.1021/acs.molpharmaceut.7b00128.

Marambio-Jones, Catalina, and Eric M. V. Hoek. 2010. “A Review of the Antibacterial Effects of Silver Nanomaterials and Potential Implications for Human Health and the Environment.” *Journal of Nanoparticle Research* 12 (5): 1531–51. https://doi.org/10.1007/s11051-010-9900-y.

Martinello, Kathryn, Anthony R Hart, Sufin Yap, Subhabrata Mitra, and Nicola J Robertson. 2017. “Management and Investigation of Neonatal Encephalopathy: 2017 Update.” *Archives of Disease in Childhood - Fetal and Neonatal Edition* 102 (4): F346--F358. https://doi.org/10.1136/archdischild-2015-309639.

Masood, Farha. 2016. “Polymeric Nanoparticles for Targeted Drug Delivery System for Cancer Therapy.” *Materials Science and Engineering: C* 60: 569–78. https://doi.org/https://doi.org/10.1016/j.msec.2015.11.067.

Matougui, Nada, Lukas Boge, Anne-Claire Groo, Anita Umerska, Lovisa Ringstad, Helena Bysell, and Patrick Saulnier. 2016. “Lipid-Based Nanoformulations for Peptide Delivery.” *International Journal of Pharmaceutics* 502 (1): 80–97.

https://doi.org/https://doi.org/10.1016/j.ijpharm.2016.02.019.

Md, Shadab, Shadabul Haque, Thiagarajan Madheswaran, Farrukh Zeeshan, Venkata Srikanth Meka, Ammu K Radhakrishnan, and Prashant Kesharwani. 2017. "Lipid Based Nanocarriers System for Topical Delivery of Photosensitizers." *Drug Discovery Today* 22 (8): 1274–83. https://doi.org/https://doi.org/10.1016/j.drudis.2017.04.010.

Meng, Shikang, Lin Sun, Lun Wang, Zibei Lin, Zeyu Liu, Long Xi, Zhenping Wang, and Ying Zheng. 2019. "Loading of Water-Insoluble Celastrol into Niosome Hydrogels for Improved Topical Permeation and Anti-Psoriasis Activity." *Colloids and Surfaces B: Biointerfaces* 182: 110352. https://doi.org/https://doi.org/10.1016/j.colsurfb.2019.110352.

Mhango, Ellen K G, Rahul S Kalhapure, Mahantesh Jadhav, Sandeep J Sonawane, Chunderika Mocktar, Suresh Vepuri, Mahmoud Soliman, and Thirumala Govender. 2017. "Preparation and Optimization of Meropenem-Loaded Solid Lipid Nanoparticles: In Vitro Evaluation and Molecular Modeling." *AAPS PharmSciTech* 18 (6): 2011–25. https://doi.org/10.1208/s12249-016-0675-z.

Michlewska, Sylwia, Malgorzata Kubczak, Marta Maroto-Diaz, Natalia Sanz Del Olmo, Paula Ortega, Dzmitry Shcharbin, Rafael Gomez Ramirez, Francisco Javier de la Mata, Maksim Ionov, and Maria Bryszewska. 2019. "Synthesis and Characterization of FITC Labelled Ruthenium Dendrimer as a Prospective Anticancer Drug." *Biomolecules* 9 (9). https://doi.org/10.3390/biom9090411.

Mitri, Khalil, Ranjita Shegokar, Sven Gohla, Cecilia Anselmi, and Rainer H Muller. 2011. "Lutein Nanocrystals as Antioxidant Formulation for Oral and Dermal Delivery." *International Journal of Pharmaceutics* 420 (1): 141–46. https://doi.org/10.1016/j.ijpharm.2011.08.026.

Morissette, Sherry L, Örn Almarsson, Matthew L Peterson, Julius F Remenar, Michael J Read, Anthony V Lemmo, Steve Ellis, Michael J Cima, and Colin R Gardner. 2004. "High-Throughput Crystallization: Polymorphs, Salts, Co-Crystals and Solvates of Pharmaceutical Solids." *Advanced Drug Delivery Reviews* 56 (3): 275–300. https://doi.org/https://doi.org/10.1016/j.addr.2003.10.020.

Mu, L, and S S Feng. 2003. "A Novel Controlled Release Formulation for the Anticancer Drug Paclitaxel (Taxol): PLGA Nanoparticles Containing Vitamin E TPGS." *Journal of Controlled Release : Official Journal of the Controlled Release Society* 86 (1): 33–48.

Muhoza, Bertrand, Yating Zhang, Shuqin Xia, Jibao Cai, Xiaoming Zhang, and Jiakun Su. 2018. "Improved Stability and Controlled Release of Lutein-Loaded Micelles Based on Glycosylated Casein via Maillard Reaction." *Journal of Functional Foods* 45: 1–9. https://doi.org/https://doi.org/10.1016/j.jff.2018.03.035.

Müller, Rainer H, Karsten Mäder, and Sven Gohla. 2000. "Solid Lipid Nanoparticles (SLN) for Controlled Drug Delivery – a Review of the State of the Art." *European Journal of Pharmaceutics and Biopharmaceutics* 50 (1): 161–77. https://doi.org/https://doi.org/10.1016/S0939-6411(00)00087-4.

Musumeci, Teresa, Maria Francesca Serapide, Rosalia Pellitteri, Alessandro Dalpiaz, Luca Ferraro, Roberta Dal Magro, Angela Bonaccorso, et al. 2018. "Oxcarbazepine Free or Loaded PLGA Nanoparticles as Effective Intranasal Approach to Control Epileptic Seizures in Rodents." *European Journal of Pharmaceutics and Biopharmaceutics : Official Journal of Arbeitsgemeinschaft Fur Pharmazeutische Verfahrenstechnik e.V* 133 (December): 309–20. https://doi.org/10.1016/j.ejpb.2018.11.002.

Nami, Sanam, Ali Aghebati-Maleki, Hamid Morovati, and Leili Aghebati-Maleki. 2019.

"Current Antifungal Drugs and Immunotherapeutic Approaches as Promising Strategies to Treatment of Fungal Diseases." *Biomedicine & Pharmacotherapy* 110: 857–68. https://doi.org/https://doi.org/10.1016/j.biopha.2018.12.009.

No Title. 2014. Washington (DC). https://doi.org/10.17226/18616.

Oliveira, Marcela Brito, Giovana Calixto, Márcia Graminha, Hugo Cerecetto, Mercedes González, and Marlus Chorilli. 2015. "Performance of Fluconazole-Loaded Microemulsions for the Topical Treatment of Cutaneous Leishmaniasis" 2015.

Ozawa, Yoko, Mariko Sasaki, Noriko Takahashi, Mamoru Kamoshita, Seiji Miyake, and Kazuo Tsubota. 2012. "Neuroprotective Effects of Lutein in the Retina." *Current Pharmaceutical Design* 18 (1): 51–56.

Paiva, Raphael E F de, Camilla Abbehausen, Alexandre F Gomes, Fábio C Gozzo, Wilton R Lustri, André L B Formiga, and Pedro P Corbi. 2012. "Synthesis, Spectroscopic Characterization, DFT Studies and Antibacterial Assays of a Novel Silver(I) Complex with the Anti-Inflammatory Nimesulide." *Polyhedron* 36 (1): 112–19. https://doi.org/https://doi.org/10.1016/j.poly.2012.02.002.

Pandya, Nilima T, Parva Jani, Jigar Vanza, and Hemal Tandel. 2018. "Solid Lipid Nanoparticles as an Efficient Drug Delivery System of Olmesartan Medoxomil for the Treatment of Hypertension." *Colloids and Surfaces B: Biointerfaces* 165: 37–44. https://doi.org/https://doi.org/10.1016/j.colsurfb.2018.02.011.

Patel, D M, C N Patel, and Rushiraj Jani. 2011. "Ufasomes: A Vesicular Drug Delivery." *Systematic Reviews in Pharmacy* 2 (July). https://doi.org/10.4103/0975-8453.86290.

Pere, Cristiane Patricia Pissinato, Sophia N Economidou, Gurprit Lall, Clémentine Ziraud, Joshua S Boateng, Bruce D Alexander, Dimitrios A Lamprou, and Dennis Douroumis.

2018. “3D Printed Microneedles for Insulin Skin Delivery.” *International Journal of Pharmaceutics* 544 (2): 425–32. https://doi.org/https://doi.org/10.1016/j.ijpharm.2018.03.031.

Pignatello, Rosario, Antonio Leonardi, Virginia Fuochi, Giulio Petronio Petronio, Antonio Greco, and Pio Furneri. 2018. “A Method for Efficient Loading of Ciprofloxacin Hydrochloride in Cationic Solid Lipid Nanoparticles: Formulation and Microbiological Evaluation.” *Nanomaterials* . https://doi.org/10.3390/nano8050304.

Pople, Pallavi V, and Kamalinder K Singh. 2011. “Development and Evaluation of Colloidal Modified Nanolipid Carrier: Application to Topical Delivery of Tacrolimus.” *European Journal of Pharmaceutics and Biopharmaceutics : Official Journal of Arbeitsgemeinschaft Fur Pharmazeutische Verfahrenstechnik e.V* 79 (1): 82–94. https://doi.org/10.1016/j.ejpb.2011.02.016.

Potta, Sriharsha Gupta, Sriharsha Minemi, Ravi Kumar Nukala, Chairmane Peinado, Dimitrios A Lamprou, Andrew Urquhart, and D Douroumis. 2010. “Development of Solid Lipid Nanoparticles for Enhanced Solubility of Poorly Soluble Drugs.” *Journal of Biomedical Nanotechnology* 6 (6): 634–40.

Prabhu, Sukumaran, and Eldho K Poulose. 2012. “Silver Nanoparticles: Mechanism of Antimicrobial Action, Synthesis, Medical Applications, and Toxicity Effects.” *International Nano Letters* 2 (1): 32. https://doi.org/10.1186/2228-5326-2-32.

Pradhan, Madhulika, Deependra Singh, and Manju Rawat Singh. 2015. “Development Characterization and Skin Permeating Potential of Lipid Based Novel Delivery System for Topical Treatment of Psoriasis.” *Chemistry and Physics of Lipids* 186: 9–16. https://doi.org/https://doi.org/10.1016/j.chemphyslip.2014.11.004.

Prado Silva, Jessica Thais do, Julia Maria Tonin Geiss, Sara Marchesan Oliveira, Evelyne da Silva Brum, Sara Cristina Sagae, Daniela Becker, Fernanda Vitoria Leimann, Rafael Porto Ineu, Gustavo Petri Guerra, and Odinei Hess Goncalves. 2017. "Nanoencapsulation of Lutein and Its Effect on Mice's Declarative Memory." *Materials Science & Engineering. C, Materials for Biological Applications* 76 (July): 1005–11. https://doi.org/10.1016/j.msec.2017.03.212.

Prombutara, Pinitphon, Yokruethai Kulwatthanasal, Nuttapun Supaka, Issara Sramala, and Supat Chareonpornwattana. 2012. "Production of Nisin-Loaded Solid Lipid Nanoparticles for Sustained Antimicrobial Activity." *Food Control* 24 (1): 184–90. https://doi.org/https://doi.org/10.1016/j.foodcont.2011.09.025.

Rai, Mahendra, Alka Yadav, and Aniket Gade. 2009. "Silver Nanoparticles as a New Generation of Antimicrobials." *Biotechnology Advances* 27 (1): 76–83. https://doi.org/https://doi.org/10.1016/j.biotechadv.2008.09.002.

Ravani, Laura, Elisabetta Esposito, Christian Bories, Vanessa Lievin-Le Moal, Philippe M Loiseau, Madeleine Djabourov, Rita Cortesi, and Kawthar Bouchemal. 2013. "Clotrimazole-Loaded Nanostructured Lipid Carrier Hydrogels: Thermal Analysis and in Vitro Studies." *International Journal of Pharmaceutics* 454 (2): 695–702. https://doi.org/https://doi.org/10.1016/j.ijpharm.2013.06.015.

Renukuntla, Jwala. 2018a. "FSE–Ag Complex NS: Preparation and Evaluation of Antibacterial Activity." *IET Nanobiotechnology* 1: 1–5. https://doi.org/10.1049/iet-nbt.2017.0284.

———. 2018b. "FSE–Ag Complex NS: Preparation and Evaluation of Antibacterial Activity." *IET Nanobiotechnology*, April. http://digital-library.theiet.org/content/journals/10.1049/iet-nbt.2017.0284.

Ribeiro, Lígia N M, Michelle Franz-Montan, Márcia C Breitkreitz, Ana C S Alcântara, Simone R Castro, Viviane A Guilherme, Raquel M Barbosa, and Eneida de Paula. 2016. "Nanostructured Lipid Carriers as Robust Systems for Topical Lidocaine-Prilocaine Release in Dentistry." *European Journal of Pharmaceutical Sciences* 93: 192–202. https://doi.org/https://doi.org/10.1016/j.ejps.2016.08.030.

Richardson, Lauren A. 2017. "Understanding and Overcoming Antibiotic Resistance." *PLOS Biology* 15 (8): e2003775. https://doi.org/10.1371/journal.pbio.2003775.

Ridolfi, Daniela M, Priscyla D Marcato, Giselle Z Justo, Livia Cordi, Daisy Machado, and Nelson Duran. 2012. "Chitosan-Solid Lipid Nanoparticles as Carriers for Topical Delivery of Tretinoin." *Colloids and Surfaces. B, Biointerfaces* 93 (May): 36–40. https://doi.org/10.1016/j.colsurfb.2011.11.051.

Roberts, M S, Y Mohammed, M N Pastore, S Namjoshi, S Yousef, A Alinaghi, I N Haridass, et al. 2017. "Topical and Cutaneous Delivery Using Nanosystems." *Journal of Controlled Release* 247: 86–105. https://doi.org/https://doi.org/10.1016/j.jconrel.2016.12.022.

Rodriguez, Victor A., Pradeep Kumar Bolla, Rahul S. Kalhapure, Sai Hanuman Sagar Boddu, Rabin Neupane, Julian Franco, and Jwala Renukuntla. 2019. "Preparation and Characterization of Furosemide-Silver Complex Loaded Chitosan Nanoparticles." *Processes* 7 (4): 206. https://doi.org/10.3390/pr7040206.

Ruela, AndrÃ\copyright LuÃ\-s Morais, Eduardo Costa Figueiredo, Aline Gravinez Perissinato, Ana Carolina Zogbi Lima, Magali Benjamim AraÃ\textordmasculinejo, and Gislaine Ribeiro Pereira. 2013. "In Vitro Evaluation of Transdermal Nicotine Delivery Systems Commercially Available in Brazil." *Brazilian Journal of Pharmaceutical Sciences* 49: 579–88. http://www.scielo.br/scielo.php?script=sci_arttext&pid=S1984-

82502013000300020&nrm=iso.

Ruiz, María Esperanza, and Sebastián Scioli Montoto. 2018. “Routes of Drug Administration.” In *ADME Processes in Pharmaceutical Sciences: Dosage, Design, and Pharmacotherapy Success*, edited by Alan Talevi and Pablo A M Quiroga, 97–133. Cham: Springer International Publishing. https://doi.org/10.1007/978-3-319-99593-9_6.

Sahana, D K, G Mittal, V Bhardwaj, and M N V Ravi Kumar. 2008. “PLGA Nanoparticles for Oral Delivery of Hydrophobic Drugs: Influence of Organic Solvent on Nanoparticle Formation and Release Behavior in Vitro and in Vivo Using Estradiol as a Model Drug.” *Journal of Pharmaceutical Sciences* 97 (4): 1530–42. https://doi.org/10.1002/jps.21158.

Sai HS. Boddu, R. Vaishya, J. Jwala, A. Vadlapudi, D. Pal and A.K. Mitra. 2012. “Preparation and Characterization of Folate Conjugated Nanoparticles of Doxorubicin Using PLGA-PEG-FOL Polymer.” *Medicinal Chemistry* 2 (4): 068–075. https://doi.org/10.4172/2161-0444.1000117.

Salama, Alaa Hamed, and Mona Hassan Aburahma. 2016. “Ufasomes Nano-Vesicles-Based Lyophilized Platforms for Intranasal Delivery of Cinnarizine: Preparation, Optimization, Ex-Vivo Histopathological Safety Assessment and Mucosal Confocal Imaging.” *Pharmaceutical Development and Technology* 21 (6): 706–15. https://doi.org/10.3109/10837450.2015.1048553.

Santos, Sara S, Alessandra Lorenzoni, Luana M Ferreira, Juliane Mattiazzi, Andréa I H Adams, Laura B Denardi, Sydney H Alves, Scheila R Schaffazick, and Letícia Cruz. 2013. “Clotrimazole-Loaded Eudragit® RS100 Nanocapsules: Preparation, Characterization and in Vitro Evaluation of Antifungal Activity against Candida Species.” *Materials Science and Engineering: C* 33 (3): 1389–94. https://doi.org/https://doi.org/10.1016/j.msec.2012.12.040.

Savjani, Ketan T, Anuradha K Gajjar, and Jignasa K Savjani. 2012. “Drug Solubility: Importance and Enhancement Techniques.” Edited by G Aktay, Y.-Z. Du, and J Torrado. *ISRN Pharmaceutics* 2012: 195727. https://doi.org/10.5402/2012/195727.

SE, Jacobs, Morley CJ, Inder TE, and et al. 2011. “Whole-Body Hypothermia for Term and near-Term Newborns with Hypoxic-Ischemic Encephalopathy: A Randomized Controlled Trial.” *Archives of Pediatrics & Adolescent Medicine* 165 (8): 692–700. https://doi.org/10.1001/archpediatrics.2011.43.

Shankaran, Seetha, Abbot R Laptook, Richard A Ehrenkranz, Jon E Tyson, Scott A McDonald, Edward F Donovan, Avroy A Fanaroff, et al. 2005. “Whole-Body Hypothermia for Neonates with Hypoxic–Ischemic Encephalopathy.” *New England Journal of Medicine* 353 (15): 1574–84. https://doi.org/10.1056/NEJMcps050929.

Shivakumar, H N, Abhishek Juluri, B G Desai, and S Narasimha Murthy. 2012. “Ungual and Transungual Drug Delivery.” *Drug Development and Industrial Pharmacy* 38 (8): 901–11. https://doi.org/10.3109/03639045.2011.637931.

Spellberg, Brad, Robert Guidos, David Gilbert, John Bradley, Helen W Boucher, W Michael Scheld, John G Bartlett, and John Jr Edwards. 2008. “The Epidemic of Antibiotic-Resistant Infections: A Call to Action for the Medical Community from the Infectious Diseases Society of America.” *Clinical Infectious Diseases : An Official Publication of the Infectious Diseases Society of America* 46 (2): 155–64. https://doi.org/10.1086/524891.

Steiner, Benjamin M, David Julian McClements, and Gabriel Davidov-Pardo. 2018. “Encapsulation Systems for Lutein: A Review.” *Trends in Food Science & Technology* 82: 71–81. https://doi.org/https://doi.org/10.1016/j.tifs.2018.10.003.

Suleman, Nadia, Rahul S Kalhapure, Chunderika Mocktar, Sanjeev Rambharose, Moganavelli

Singh, and Thirumala Govender. 2015. “Silver Salts of Carboxylic Acid Terminated Generation 1 Poly (Propyl Ether Imine) (PETIM) Dendron and Dendrimers as Antimicrobial Agents against S. Aureus and MRSA.” *RSC Advances* 5 (44): 34967–78. https://doi.org/10.1039/C5RA03179F.

Suttiponparnit, Komkrit, Jingkun Jiang, Manoranjan Sahu, Sirikalaya Suvachittanont, Tawatchai Charinpanitkul, and Pratim Biswas. 2010. “Role of Surface Area, Primary Particle Size, and Crystal Phase on Titanium Dioxide Nanoparticle Dispersion Properties.” *Nanoscale Res Lett* 6 (1): 27. https://doi.org/10.1007/s11671-010-9772-1.

Talele, Paurnima, Saugata Sahu, and Ashok Kumar Mishra. 2018. “Physicochemical Characterization of Solid Lipid Nanoparticles Comprised of Glycerol Monostearate and Bile Salts.” *Colloids and Surfaces B: Biointerfaces* 172: 517–25. https://doi.org/https://doi.org/10.1016/j.colsurfb.2018.08.067.

Tan, Tai Boon, Nor Shariffa Yussof, Faridah Abas, Hamed Mirhosseini, Imededdine Arbi Nehdi, and Chin Ping Tan. 2016. “Stability Evaluation of Lutein Nanodispersions Prepared via Solvent Displacement Method: The Effect of Emulsifiers with Different Stabilizing Mechanisms.” *Food Chemistry* 205: 155–62. https://doi.org/https://doi.org/10.1016/j.foodchem.2016.03.008.

Tavano, Lorena, Elisabetta Mazzotta, and Rita Muzzalupo. 2018. “Innovative Topical Formulations from Diclofenac Sodium Used as Surfadrug: The Birth of Diclosomes.” *Colloids and Surfaces B: Biointerfaces* 164: 177–84. https://doi.org/https://doi.org/10.1016/j.colsurfb.2018.01.030.

Thomas, Sara E, and Earl H Harrison. 2016. “Mechanisms of Selective Delivery of Xanthophylls to Retinal Pigment Epithelial Cells by Human Lipoproteins.” *Journal of Lipid Research* 57

(10): 1865–78. https://doi.org/10.1194/jlr.M070193.

Tiwari, Gaurav, Ruchi Tiwari, Birendra Sriwastawa, L Bhati, S Pandey, P Pandey, and Saurabh K Bannerjee. 2012. "Drug Delivery Systems: An Updated Review." *International Journal of Pharmaceutical Investigation* 2 (1): 2–11. https://doi.org/10.4103/2230-973X.96920.

Tsaousis, Konstantinos T, David F Chang, Liliana Werner, Jesus Paulo Perez, Jia J Guan, Nicholas Reiter, He J Li, and Nick Mamalis. 2018. "Comparison of Different Types of Phacoemulsification Tips. III. Morphological Changes Induced after Multiple Uses in an Ex Vivo Model." *Journal of Cataract and Refractive Surgery* 44 (1): 91–97. https://doi.org/10.1016/j.jcrs.2017.08.023.

Turk, Ceyda Tuba Sengel, Umut Can Oz, Tugrul Mert Serim, and Canan Hascicek. 2014. "Formulation and Optimization of Nonionic Surfactants Emulsified Nimesulide-Loaded PLGA-Based Nanoparticles by Design of Experiments." *AAPS PharmSciTech* 15 (1): 161–76. https://doi.org/10.1208/s12249-013-0048-9.

USFDA. n.d. "Inactive Ingredient Search for Approved Drug Products." Accessed July 28, 2019. https://www.accessdata.fda.gov/scripts/cder/iig/index.cfm.

Vannucci, R C, and J M Perlman. 1997. "Interventions for Perinatal Hypoxic-Ischemic Encephalopathy." *Pediatrics* 100 (6): 1004–14.

Ventola, C Lee. 2015a. "The Antibiotic Resistance Crisis: Part 1: Causes and Threats." *P & T : A Peer-Reviewed Journal for Formulary Management (2015)* 40 (4): 277–83. https://doi.org/Article.

———. 2015b. "The Antibiotic Resistance Crisis: Part 2: Management Strategies and New Agents." *P & T : A Peer-Reviewed Journal for Formulary Management* 40 (5): 344–52. http://www.pubmedcentral.nih.gov/articlerender.fcgi?artid=4422635&tool=pmcentrez&ren

dertype=abstract.

Verma, Shivani, Ankur Bhardwaj, Mohit Vij, Pawan Bajpai, Nishant Goutam, and Lalit Kumar. 2014. "Oleic Acid Vesicles: A New Approach for Topical Delivery of Antifungal Agent." *Artificial Cells, Nanomedicine, and Biotechnology* 42 (2): 95–101. https://doi.org/10.3109/21691401.2013.794351.

Vishwanathan, Rohini, Matthew J Kuchan, Sarbattama Sen, and Elizabeth J Johnson. 2014. "Lutein and Preterm Infants with Decreased Concentrations of Brain Carotenoids." *Journal of Pediatric Gastroenterology and Nutrition* 59 (5): 659–65. https://doi.org/10.1097/MPG.0000000000000389.

Walton, Jeanette D, David R Kattan, Sharon K Thomas, Barbara A Spengler, Hong-Fen Guo, June L Biedler, Nai-Kong V Cheung, and Robert A Ross. 2004. "Characteristics of Stem Cells from Human Neuroblastoma Cell Lines and in Tumors." *Neoplasia (New York, N.Y.)* 6 (6): 838–45. https://doi.org/10.1593/neo.04310.

Wang, X F, S L Zhang, L Y Zhu, S Y Xie, Z Dong, Y Wang, and W Z Zhou. 2012. "Enhancement of Antibacterial Activity of Tilmicosin against Staphylococcus Aureus by Solid Lipid Nanoparticles in Vitro and in Vivo." *Veterinary Journal (London, England : 1997)* 191 (1): 115–20. https://doi.org/10.1016/j.tvjl.2010.11.019.

Waugh, Christine D, and V A Medical. 2007. "Clotrimazole Targets-Pharmacodynamics," 1–4.

Westesen, K, H Bunjes, and M H J Koch. 1997. "Physicochemical Characterization of Lipid Nanoparticles and Evaluation of Their Drug Loading Capacity and Sustained Release Potential." *Journal of Controlled Release* 48 (2): 223–36. https://doi.org/https://doi.org/10.1016/S0168-3659(97)00046-1.

Wissing, S A, O Kayser, and R H Muller. 2004. "Solid Lipid Nanoparticles for Parenteral Drug

Delivery." *Advanced Drug Delivery Reviews* 56 (9): 1257–72. https://doi.org/10.1016/j.addr.2003.12.002.

Witteveen, Frans. 2018. TOPICAL FLAVOURING COMPOSITIONS COMPRISING OLEIC ACID AND SODIUM OLEATE. US 2018 / 0042289 A1, issued 2018. https://patentimages.storage.googleapis.com/36/03/66/a8e8457f053715/US20180042289A1.pdf.

Wu, D, and W M Pardridge. 1999. "Blood-Brain Barrier Transport of Reduced Folic Acid." *Pharmaceutical Research* 16 (3): 415–19.

Xie, Shuyu, Luyan Zhu, Zhao Dong, Yan Wang, Xiaofang Wang, and WenZhong Zhou. 2011. "Preparation and Evaluation of Ofloxacin-Loaded Palmitic Acid Solid Lipid Nanoparticles." *International Journal of Nanomedicine* 6 (March): 547–55. https://doi.org/10.2147/IJN.S17083.

Zhang, Wenli, Jianping Liu, Suchun Li, Mengyuan Chen, and Huan Liu. 2008. "Preparation and Evaluation of Stealth Tashinone IIA-Loaded Solid Lipid Nanoparticles: Influence of Poloxamer 188 Coating on Phagocytic Uptake." *Journal of Microencapsulation* 25 (3): 203–9. https://doi.org/10.1080/02652040701852181.

Zhang, Xingwang, Huijie Xing, Yue Zhao, and Zhiguo Ma. 2018. "Pharmaceutical Dispersion Techniques for Dissolution and Bioavailability Enhancement of Poorly Water-Soluble Drugs." *Pharmaceutics* . https://doi.org/10.3390/pharmaceutics10030074.

Zhang, Yangqing, Lina Tang, Leilei Sun, Junbo Bao, Cunxian Song, Laiqiang Huang, Kexin Liu, et al. 2010. "A Novel Paclitaxel-Loaded Poly(ε-Caprolactone)/Poloxamer 188 Blend Nanoparticle Overcoming Multidrug Resistance for Cancer Treatment." *Acta Biomaterialia* 6 (6): 2045–52. https://doi.org/https://doi.org/10.1016/j.actbio.2009.11.035.

Zhao, Rongbao, Ndeye Diop-Bove, Michele Visentin, and I David Goldman. 2011. "Mechanisms of Membrane Transport of Folates into Cells and across Epithelia." *Annual Review of Nutrition* 31 (August): 177–201. https://doi.org/10.1146/annurev-nutr-072610-145133.

Vita

Pradeep Kumar Bolla, was born on October 3, 1987 in the city of Warangal, Telangana state, India. He completed his secondary school (2003) in Warangal and intermediate (2005) in Hyderabad, Telangana. He earned his Bachelor's Degree in Pharmacy (2010) from Kakatiya University, Warangal, Telangana, India and Master of Science in Pharmacy (2012) with specialization in Pharmacology and Toxicology from National Institute of Pharmaceutical Education and Research, Hyderabad, Telangana, India. Bolla worked as Project Trainee at National Institute of Nutrition, Hyderabad (2011 – 2012); Scientific Writer at Indegene Life Systems, Bengaluru (2012 – 2014); Medical Writer at ClinTec International, Hyderabad (2014 – 2016) and Oncology Submission Writer at Novartis, Hyderabad, India (2016 – 2017). Thereafter, he joined the doctoral program in Biomedical Engineering at University of Texas at El Paso in Fall 2017 and worked as a Teaching/Research Assistant at the UTEP School of Pharmacy. He also worked as a Formulation and Drug Delivery Intern at High Point University under the supervision of Dr. Jwala Renukuntla.

Bolla is a recipient of Anita Mochen Loya Fellowship (2017 – 2018) and International Student Scholarship (Fall 2019) at UTEP and travel award from the organizers to attend Gordon Research Conference, New Hampshire, USA. He also served as the Secretary of AAPS-UTEP student chapter (2018 – 2019) and President of University Cricket Club (2017 – 2018) at UTEP.

Bolla has published eight technical scientific articles in reputed peer-reviewed formulation research journals, presented >20 posters in international and national conferences. His research expertise is in development and characterization of novel and conventional formulations to improve solubility and permeability of small molecules for drug delivery applications.

Contact Information: bollaniper@gmail.com, pradeepbolla87@gmail.com